


Review

Decaborane: From Alfred Stock and Rocket Fuel Projects to Nowadays [†]

Igor B. Sivaev 

A.N. Nesmeyanov Institute of Organoelement Compounds, Russian Academy of Sciences, 28 Vavilov Str., 119334 Moscow, Russia; sivaev@ineos.ac.ru

[†] Dedicated to Professor John D. Kennedy on his 80th birthday and in recognition of his outstanding contributions to the chemistry of boranes and metallaboranes.

Abstract: The review covers more than a century of decaborane chemistry from the first synthesis by Alfred Stock to the present day. The main attention is paid to the reactions of the substitution of hydrogen atoms by various atoms and groups with the formation of *exo*-polyhedral boron–halogen, boron–oxygen, boron–sulfur, boron–nitrogen, boron–phosphorus, and boron–carbon bonds. Particular attention is paid to the chemistry of *conjuncto*-borane *anti*-[B₁₈H₂₂], whose structure is formed by two decaborane moieties with a common edge, the chemistry of which has been intensively developed in the last decade.

Keywords: decaborane; history; properties; derivatives

1. Introduction

Decaborane [B₁₀H₁₄] plays a central role in the chemistry of polyhedral boron hydrides. Decaborane is an essential boron reagent for the preparation of medium and higher carboranes C₂B_nH_{n+2} (n = 8–10) [1] and the carba-*closo*-decaborate anions [CB₉H₁₀][−] [2]. Until recently, the synthesis of the *closo*-dodecaborate [B₁₂H₁₂]^{2−} [3,4] and the carba-*closo*-dodecaborate [CB₁₁H₁₂][−] [5,6] anions was also based on the use of decaborane, and it is still used for the synthesis of the *closo*-decaborate anion [B₁₀H₁₀]^{2−} [7,8]. In addition, decaborane can be used to prepare boron coatings [9–13], nanoparticles [14], microcrystals [15,16], boron nitride nanosheets [17], and nanotubes [18], as well as various metal boride thin films [19–24]. Recently, a decaborane-based fuel cell power source with a high energy density was developed [25]. The intensive development of the chemistry of decaborane is associated with the 1950s to the early 1960s, when the main types of its transformations were discovered and described. These early studies were reviewed in the 1960s by Hawthorne [26] and Zakharkin et al. [27]. This area was also partly elucidated in *Boron Hydride Chemistry* [28] and *Comprehensive Inorganic Chemistry I* [29]. Recent studies in the field of decaborane chemistry, deepening and expanding the previously described conclusions using modern instrumental methods, were briefly covered in *Comprehensive Inorganic Chemistry III* [30]. Therefore, the purpose of this review is to give the most complete picture of the current state of the chemistry of decaborane and its derivatives.

2. Synthesis, Structure, and General Properties

The formation of this ten-vertex cluster during the pyrolysis of diborane B₂H₆ was first described by Alfred Stock and co-workers more than 100 years ago [31,32]. The best yields of decaborane(14) were obtained by heating diborane to 120 °C for 47 h. The low volatility of decaborane allows it to be easily separated from other volatile boron hydrides while being volatile enough to be easily separated from non-volatile products. Decaborane is a colorless, air-stable, easily subliming, malodorous, crystalline solid that melts at 99.7 °C and boils with decomposition at 213 °C [33]. For a long time, interest in the chemistry of



Citation: Sivaev, I.B. Decaborane: From Alfred Stock and Rocket Fuel Projects to Nowadays. *Molecules* **2023**, *28*, 6287. <https://doi.org/10.3390/molecules28176287>

Academic Editor: M. Concepción Gimeno

Received: 2 August 2023

Revised: 21 August 2023

Accepted: 24 August 2023

Published: 28 August 2023



Copyright: © 2023 by the author. Licensee MDPI, Basel, Switzerland. This article is an open access article distributed under the terms and conditions of the Creative Commons Attribution (CC BY) license (<https://creativecommons.org/licenses/by/4.0/>).

boron hydrides was mainly academic but was supported by the fact that boranes and some related compounds did not comply with the usual rules relating the chemical composition to the classical theory of valence. At the same time, various assumptions were made about the structure of $B_{10}H_{14}$, including linear [34] or naphthalene-like [35] structures.

Practical interest in boron hydrides, and decaborane in particular, arose shortly after World War II, when the United States government launched programs (Projects Hermes, Zip, and HEF (High-Energy Fuels)) [36,37] whose purpose was to develop borane-based aviation and rocket fuels capable of generating much higher energy than conventional kerosene-based fuels [38–40]. As a part of this program, two chemical companies, Callery Chemical Company and Olin-Mathieson Corporation, developed eight pilot and production plants and produced an array of borane-derived energetic products, including methyldecaborane (HEF-4), ethyldecaborane (HEF-3), and ethylacetylenedecaborane (HEF-5), to be tested as additives to propellants and explosives [41]. Almost at the same time, due to the development of various physical research methods, such as single-crystal X-ray diffraction, neutron diffraction, and gas phase electron diffraction, the molecular structure of $[B_{10}H_{14}]$ was determined [42–50]. The decaborane molecule was found to be shaped like a boat built from ten BH-units, with four additional BHB bridges decorating its bow and stern (Figure 1).

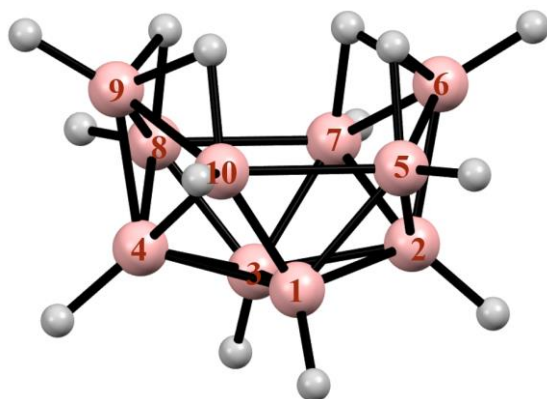


Figure 1. Structure and numbering of atoms in decaborane $B_{10}H_{14}$.

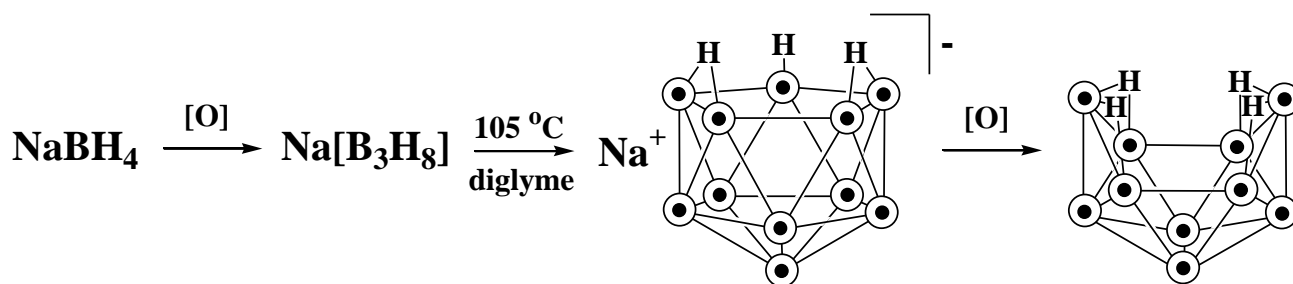
Shortly thereafter, the future Nobel Winner Lipscomb and his collaborators developed bond counting rules and topological principles that made it possible to describe bonding in boron hydrides. According to the topological formalism, the binding in the decaborane molecule can be described by a combination of four 3c-2e B-H-B bonds, six closed or fractional closed 3c-2e B-B-B bonds, and two 2c-2e B-B bonds [51–53]. Some time later, molecular orbital theory in the form of the extended Hückel theory was originated and applied to decaborane to provide an alternative to this topological approach [54–56]. Subsequently, both the logical basis and the parameters for these molecular orbitals were greatly improved using the more rigorous molecular self-consistent field (SCF) method [57,58]. More recently, the electronic structure of decaborane has been described in terms of the Bader's theory "Atoms in Molecules" (AIM) [59].

A powerful tool for determining the structure of polyhedral boron hydrides is NMR spectroscopy, the practical birth of which coincided with a wave of interest in the chemistry of boron hydrides. Therefore, it is not surprising that decaborane was one of the first molecules to be investigated using NMR spectroscopy [60–62]. The subsequent development of the instrumental base and methods of NMR spectroscopy caused repeated studies [63–70]. The decaborane molecule has also been characterized by IR [59,71,72], Raman [59], electron [73–75], NQR [76,77], photoelectron [78], and electron energy loss [79] spectroscopy. The ionization potentials of decaborane and ^{11}B -enriched decaborane were determined to be 11.0 eV [80] and 10.26 eV [81], respectively. The dipole moment of decaborane was determined by measuring the dielectric constants of benzene, cyclohexane,

and carbon disulfide solutions and varies from 3.17 D in carbon disulfide to 3.62 D in benzene [82]. The magnetic susceptibility of decaborane is $-116 \pm 1.5 \times 10^{-6}$ emu mol $^{-1}$ [82]. The heat of formation of decaborane was determined to be -66.1 kJ/mol [83]. The heat capacity of decaborane has been measured, and the derived thermodynamic functions have been calculated [84,85]. The heats of melting and vaporization [85], as well as the vapor pressure of decaborane [85,86], were also determined. Pressure-induced room temperature transformations of decaborane up to 131 GPa were studied using in situ optical spectroscopy techniques [87].

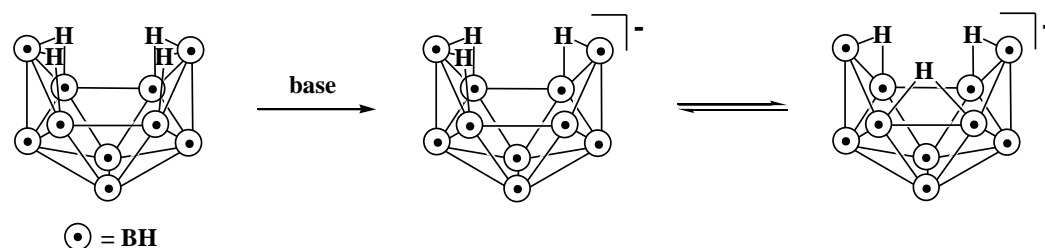
The industrial production of boron hydrides, which involved more than 2000 people, was accompanied by various accidents, which led to the discovery of the high toxicity of decaborane and its derivatives [88–92]. With decaborane, intoxication, headaches, tremors, impaired coordination, confusion, anxiety, photophobia, and other symptoms are observed. Moreover, intoxication can occur from relatively small amounts of decaborane. Decaborane can be detected by its odor at or near its maximum acceptable concentration, but there is considerable olfactory fatigue. Repeated exposure to decaborane can cause severe damage to the nervous system [93]. The effects of decaborane on various animals have also been studied [93–111]. A number of studies were directed to study the mechanism of decaborane action on living organisms [112–130].

The production of decaborane, established in the 1950s, was based on the pyrolytic conversion of diborane proposed by Alfred Stock [33]. At the same time, attempts were made to find an alternative to this dangerous process, among which the use of the CW CO₂ laser is worth mentioning [131]. Almost at the same time, a convenient and effective method was proposed, which is based on the oxidation of sodium tetrahydroborate NaBH₄ to the octahydrotriborate anion [B₃H₈] $^{-}$, followed by its pyrolysis in diglyme at 105 °C to the tetradecahydro-*nido*-undecaborate anion [B₁₁H₁₄] $^{-}$ [132]. The subsequent mild oxidation of [B₁₁H₁₄] $^{-}$ gives decaborane [B₁₀H₁₄] (Scheme 1) [133–136]. Decaborane can also be obtained by the cage-opening of the *closo*-decaborate anion [B₁₀H₁₀] $^{2-}$ on protonation with strong acids such as sulfuric acid [137].



Scheme 1. Synthesis of decaborane(14) from sodium tetrahydroborate NaBH₄.

Decaborane(14) has an acidic character [138] and can be deprotonated with strong bases, such as sodium hydride [139], tetraalkylammonium hydroxides [140], diethylamine [140], triethylamine [140,141], methylenetriphenylphosphorane [141,142], or a Proton Sponge (PS) [143,144] to give the corresponding salts of the tridecahydro-*nido*-decaborate [B₁₀H₁₃] $^{-}$ anion (Scheme 2). The pK_a value of decaborane(14) in aqueous ethanol was found to vary from 2.41 to 3.21 depending on the water content [145].



Scheme 2. Preparation of the $[\text{B}_{10}\text{H}_{13}]^-$ anion and its tautomeric forms.

The $(\text{Et}_3\text{NH})[\text{B}_{10}\text{H}_{13}]$ and $(\text{Et}_4\text{N})[\text{B}_{10}\text{H}_{13}]$ salts obtained by the deprotonation of decaborane with Et_3N and $(\text{Et}_4\text{N})\text{OH}$, respectively, have been found to trigger the hypergolic reactivity of some polar aprotic organic solvents, such as tetrahydrofuran and ethyl acetate [146].

The solid state structures of $(\text{Et}_3\text{NH})[\text{B}_{10}\text{H}_{13}]$ [147], $(\text{BnNMe}_3)[\text{B}_{10}\text{H}_{13}]$ [148], and $(\text{HPS})[\text{B}_{10}\text{H}_{13}]$ [144] were determined by single-crystal X-ray diffraction. The solid state structure of the $[\text{B}_{10}\text{H}_{13}]^-$ anion (Figure 2) can be derived from the structure of $\text{B}_{10}\text{H}_{14}$ by $\mu\text{-H}(9,10)$ deprotonation.

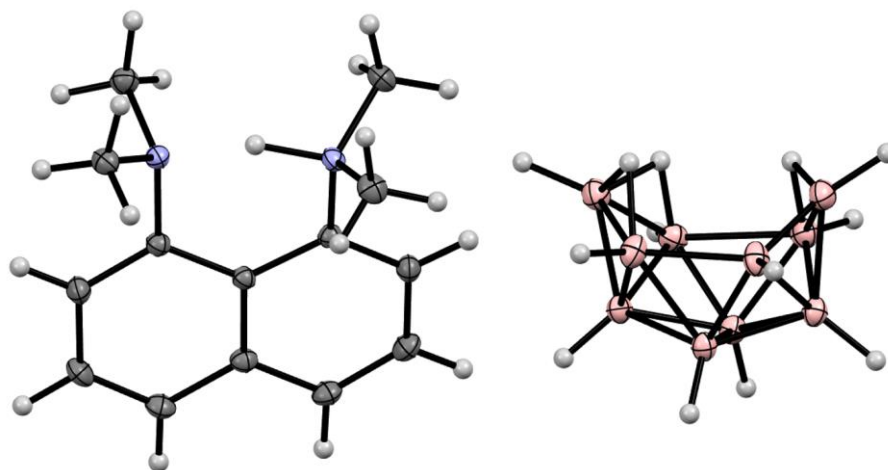
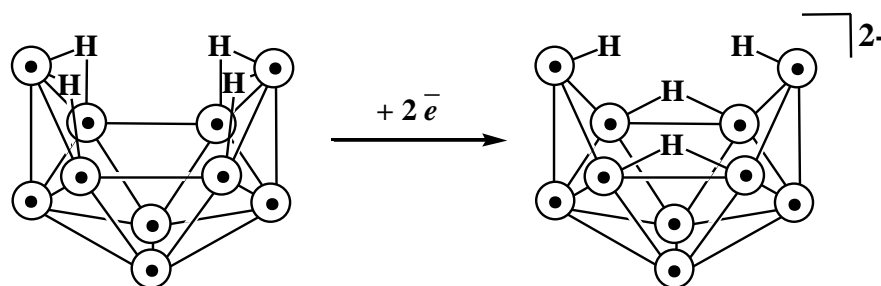


Figure 2. Solid state structures of the $(\text{HPS})^+$ cation (left) and of the $[\text{nido-B}_{10}\text{H}_{13}]^-$ anion (right) in the crystal structure of $(\text{HPS})[\text{B}_{10}\text{H}_{13}]$.

In the solution, the $[\text{B}_{10}\text{H}_{13}]^-$ anion exists as a mixture of symmetrical and unsymmetrical H -tautomers with different arrangements of bridging hydrogens (Figure 2) [143,149], with an interconversion ΔG^\ddagger value of less than 7 kcal/mol [144].

Strong bases such as sodium hydride in ether solvents are able to remove two protons from decaborane(14) to form the $[\text{B}_{10}\text{H}_{12}]^{2-}$ dianion [140,150,151]. The latter is unstable in solution and transforms into other decaborates and their derivatives [151]. According to quantum chemical calculations, the $[\text{B}_{10}\text{H}_{12}]^{2-}$ anion has the C_2 -symmetric structure with $\mu\text{-B}(5)\text{HB}(6)$ and $\mu\text{-B}(8)\text{HB}(9)$ bridging hydrogens [152].

The reduction of decaborane(14) with KBH_4 in water results in the formation of the $[\text{arachno-B}_{10}\text{H}_{14}]^{2-}$ anion with a boron cage geometry near the same as that of the starting $[\text{nido-B}_{10}\text{H}_{14}]$ (Scheme 3), which was isolated by precipitation from an aqueous solution in the form of rubidium, cesium, or tetramethylammonium salts [153,154]. The structure of the $[\text{B}_{10}\text{H}_{14}]^{2-}$ anion was proposed using ^{11}B NMR spectroscopy [155]. The solid state structure of $(\text{Me}_4\text{N})_2[\text{B}_{10}\text{H}_{14}]$ was determined by single-crystal X-ray diffraction [154]. It was supposed that the reaction proceeds by hydride transfer with the formation of the $[\text{B}_{10}\text{H}_{15}]^-$ anion. The latter is unstable in the solution and loses hydrogen to form $[\text{nido-B}_{10}\text{H}_{13}]^-$ [156,157].



Scheme 3. Preparation of the $[\text{arachno-B}_{10}\text{H}_{14}]^{2-}$ anion.

It should be borne in mind that decaborane itself has pronounced reducing properties. Due to this, the possibility of its use as a reducing agent in organic synthesis was studied. In particular, decaborane can be used for the reduction of acetals to ethers [158], the reductive esterification of aromatic aldehydes [159,160], and the reductive amination of acetals with aromatic amines [161]. Decaborane can also be used for chemoselective reduction aldehydes and ketones [162–164], the dehalogenation of α -halocarbonyl compounds [165], and the hydrogenation of alkenes or alkynes [166].

The bridging hydrogens in decaborane(14) were found to exchange rapidly for deuterium atoms with D_2O in 1,4-dioxane or acetonitrile to give $[\mu_4\text{-B}_{10}\text{H}_{10}\text{D}_4]$ [72,167,168]. The use of DCl in 1,4-dioxane makes it possible to obtain the decadeuterated decaborane $[\mu_4\text{-5,6,7,8,9,10-B}_{10}\text{H}_4\text{D}_{10}]$ [169]. The treatment of decaborane(14) with DCl in a carbon disulfide solution and in the presence of AlCl_3 results in the tetradeuterated decaborane $[1,2,3,4\text{-B}_{10}\text{H}_{10}\text{D}_4]$ [169,170]. If the reaction is carried out under heating in sealed ampoule, the product is the octadeuterated decaborane $[1,2,3,4,5,7,8,10\text{-B}_{10}\text{H}_6\text{D}_8]$ [72]. The tetradeuterated decaborane $[5,7,8,10\text{-B}_{10}\text{H}_{10}\text{D}_4]$ was obtained by the reaction of $[1,2,3,4,5,7,8,10\text{-B}_{10}\text{H}_6\text{D}_8]$ with HCl in a carbon disulfide solution and in the presence of AlCl_3 [72]. The octadeuterated decaborane $[\mu_4\text{-1,2,3,4-B}_{10}\text{H}_6\text{D}_8]$ was prepared by the reaction of $[1,2,3,4\text{-B}_{10}\text{H}_{10}\text{D}_4]$ with D_2O in acetonitrile [72], whereas the dodecadeuterated decaborane $[\mu_4\text{-1,2,3,4,5,7,8,10-B}_{10}\text{H}_2\text{D}_{12}]$ was obtained by heating $[\mu_4\text{-B}_{10}\text{H}_{10}\text{D}_4]$ with DCl in carbon disulfide in sealed ampoule in the presence of AlCl_3 [72]. Deuterated aromatic solvents can also act as a source of deuterium. For example, heating decaborane(14) in benzene- d_6 in the presence of AlCl_3 under reflux leads to the tetradeuterated decaborane $[1,2,3,4\text{-B}_{10}\text{H}_{10}\text{D}_4]$, while the reaction of decaborane(14) with AlCl_3 in toluene- d_8 at 5°C results in the dideuterated decaborane $[2,4\text{-B}_{10}\text{H}_{12}\text{D}_2]$ [171]. The reaction of $[1,2,3,4\text{-B}_{10}\text{H}_{10}\text{D}_4]$ with AlCl_3 in benzene leads to $[1,3\text{-B}_{10}\text{H}_{12}\text{D}_2]$ [172].

3. Halogen Derivatives

Stock first reported the preparation of halogen derivatives of decaborane(14) by the direct reaction of decaborane with halogens in a sealed tube [33]. These reactions were re-investigated in the 1960s. It was found that the reaction of decaborane(14) with 1 equiv. iodine at $110\text{--}120^\circ\text{C}$ leads to the formation of a mixture of 1- and 2-iodo derivatives of decaborane in a ratio of $\sim 1:2$ [173,174]. The resulting mixture of isomers can be separated by fractional crystallization from low-boiling alkanes (pentane, hexane, heptane) [173] or chromatographically [175]. The assignment of the substitution position was made based on the ^{11}B NMR spectra [174,176,177]; however, the 1-isomer was initially erroneously assigned as the 5-isomer [173,178]. The subsequent reaction of 2-iododecaborane with iodine at 110°C results in a mixture of the 1,2- and 2,4-diiodo derivatives $[1,2\text{-I}_2\text{-B}_{10}\text{H}_{12}]$ and $[2,4\text{-I}_2\text{-B}_{10}\text{H}_{12}]$ in a nearly equal ratio, while the similar reaction of 1-iododecaborane produces mainly $[1,2\text{-I}_2\text{-B}_{10}\text{H}_{12}]$. The reaction of decaborane(14) with an excess of iodine was found to give a mixture of $[1,2\text{-I}_2\text{-B}_{10}\text{H}_{12}]$ and $[2,4\text{-I}_2\text{-B}_{10}\text{H}_{12}]$ in a ratio of $\sim 1:2$ [173]. The reaction of decaborane(14) with iodine or iodine chloride in carbon disulfide in the presence of AlCl_3 was found to give a mixture of the 1- and 2-iodo derivatives of decaborane in the same ratio of $\sim 1:2$ [179]. Later, the 1- and 2-iodo derivatives of decaborane were synthesized by the reaction of decaborane(14) with iodine chloride in refluxing dichloromethane in the

presence of AlCl_3 and reliably characterized by NMR spectroscopy [180]. The solid state structures of [1-I- $\text{B}_{10}\text{H}_{13}$] [181], [2-I- $\text{B}_{10}\text{H}_{13}$] (Figure 3) [180], and [2,4-I₂- $\text{B}_{10}\text{H}_{12}$] [182] were determined by single-crystal X-ray diffraction.

The 5- and 6-iodo derivatives of decaborane were prepared in an indirect way. The treatment of [*arachno*-6,9-(Me_2S)₂- $\text{B}_{10}\text{H}_{12}$] with anhydrous HI in benzene under reflux conditions results in a mixture of the 5- and 6-iodo derivatives of decaborane [5-I- $\text{B}_{10}\text{H}_{13}$] and [6-I- $\text{B}_{10}\text{H}_{13}$] [174], which was separated by fraction crystallization from hexane [174] or chromatographically [175]. The reaction of [*arachno*-6,9-(Et_2S)₂- $\text{B}_{10}\text{H}_{12}$] with anhydrous HI in benzene at room temperature was found to give the 5-iodo derivative [5-I- $\text{B}_{10}\text{H}_{13}$] [183–185]. The reaction of $(\text{NH}_4)_2[\text{closo-}\text{B}_{10}\text{H}_{10}]$ with anhydrous HCl in a mixture of AlI_3 and 1-butyl-3-methylimidazolium iodide (bmimI) at 70 °C proceeds with the boron cage opening and results in the 6-iodo derivative of decaborane [6-I- $\text{B}_{10}\text{H}_{13}$] [186]. The 6-iodo derivative isomerizes to the 5-iodo derivative [5-I- $\text{B}_{10}\text{H}_{13}$] in the presence of a catalytic amount of triethylamine in toluene at 60 °C. It is assumed that the isomerization occurs through the transformation of [6-I- $\text{B}_{10}\text{H}_{13}$] into the [6-I- $\text{B}_{10}\text{H}_{13}$][−] anion, followed by its isomerization [187]. The 6-iodo derivative [6-I- $\text{B}_{10}\text{H}_{13}$] was also found to undergo photochemical isomerization to [5-I- $\text{B}_{10}\text{H}_{13}$] under UV-irradiation in a solution [187]. The solid state structures of [5-I- $\text{B}_{10}\text{H}_{13}$] [187] and [6-I- $\text{B}_{10}\text{H}_{13}$] [186] were determined by single-crystal X-ray diffraction (Figure 4). The 6-iodo derivative [6-I- $\text{B}_{10}\text{H}_{13}$] was also obtained by the reaction of $(\text{NH}_4)_2[\text{closo-}\text{B}_{10}\text{H}_{10}]$ with AlI_3 , followed by the hydrolysis of the resulting intermediate [188].

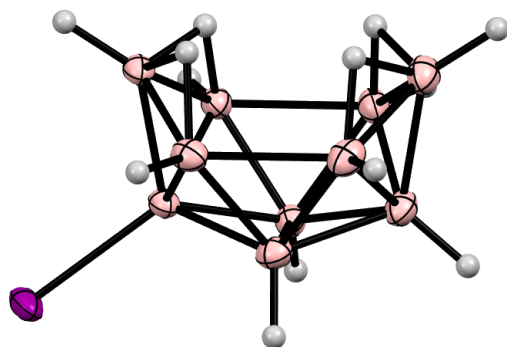


Figure 3. Solid state structure of the 2-iodo derivative of decaborane [2-I- $\text{B}_{10}\text{H}_{13}$].

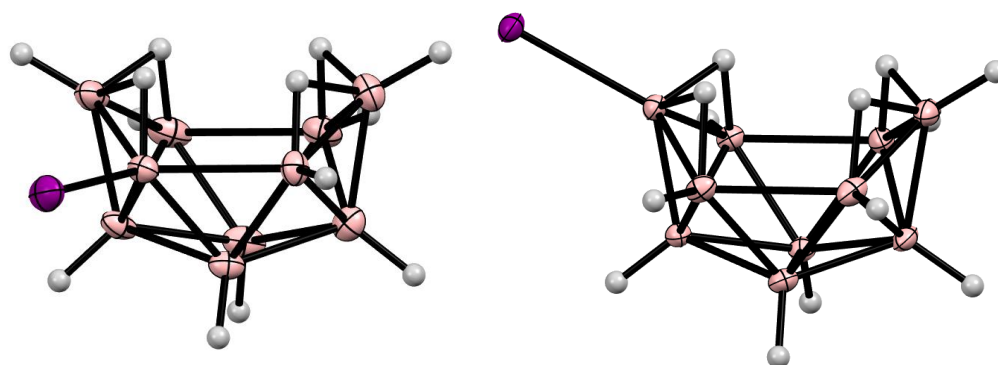


Figure 4. Solid state structures of [5-I- $\text{B}_{10}\text{H}_{13}$] (left) and [6-I- $\text{B}_{10}\text{H}_{13}$] (right).

The reactions of decaborane(14) with bromine in dichloromethane in the presence of AlCl_3 [189] or AlBr_3 [190], or in carbon disulfide in the presence of AlCl_3 [174], lead to the formation of a mixture of 1- and 2-bromo derivatives of decaborane [1-Br- $\text{B}_{10}\text{H}_{13}$] and [2-Br- $\text{B}_{10}\text{H}_{13}$], which can be separated by fractional crystallization from hexane [173,189,190] or chromatographically [175].

The 5- and 6-bromo derivatives of decaborane were also prepared in an indirect way. The treatment of [*arachno*-6,9-(Me_2S)₂- $\text{B}_{10}\text{H}_{12}$] with anhydrous HBr in benzene under reflux conditions results in a mixture of the 5- and 6-bromo derivatives of decaborane [5-Br-

$B_{10}H_{13}$] and [6-Br- $B_{10}H_{13}$] in a ratio of ~1:4, which was separated by fraction crystallization from hexane [174] or chromatographically [175,190]. The reactions of [*arachno*-6,9-(R_2S) $_2$ - $B_{10}H_{12}$] ($R = Me, Et$) with anhydrous HBr in benzene at room temperature were found to give the 5-bromo derivative [5-Br- $B_{10}H_{13}$] [183–185]. The reaction of $(NH_4)_2[*closo*- $B_{10}H_{10}$] with anhydrous HBr in a mixture of $AlBr_3$ and 1-butyl-3-methylimidazolium bromide (bmimBr) at 70 °C proceeds with the boron cage opening and results in the 6-bromo derivative of decaborane [6-Br- $B_{10}H_{13}$] [186]. The 6-bromo derivative isomerizes to the 5-bromo derivative [5-Br- $B_{10}H_{13}$] in the presence of a catalytic amount of triethylamine in toluene at 60 °C [187]. The solid state structures of [5-Br- $B_{10}H_{13}$] [187] and [6-Br- $B_{10}H_{13}$] [186] were determined by single-crystal X-ray diffraction (Figure 5). The 6-bromo derivative [6-Br- $B_{10}H_{13}$] was also obtained by the reaction of $(NH_4)_2[*closo*- $B_{10}H_{10}$] with $AlBr_3$, followed by the hydrolysis of the resulting intermediate [188].$$

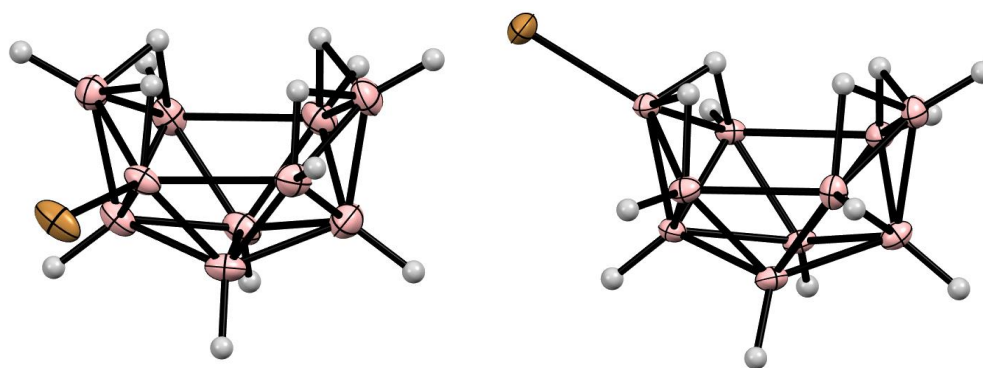


Figure 5. Solid state structures of [5-Br- $B_{10}H_{13}$] (left) and [6-Br- $B_{10}H_{13}$] (right).

The reaction of dimethylstannaundecaborane [*nido*- $Me_2SnB_{10}H_{12}$] with bromine in carbon disulfide leads to the oxidative removal of tin with the formation of the 5,10-dibromo derivative of decaborane [5,10-Br $_2$ - $B_{10}H_{12}$] (Figure 6) [191].

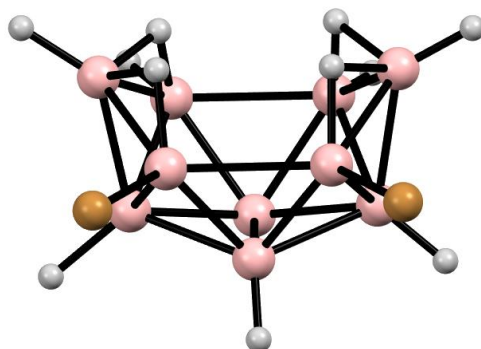


Figure 6. Solid state structure of the 5,10-dibromo derivative of decaborane [5,10-Br $_2$ - $B_{10}H_{12}$].

The reaction of decaborane(14) with chlorine in dichloromethane in the presence of $AlCl_3$ results in a mixture of the 1- and 2-chloro derivatives of decaborane [1-Cl- $B_{10}H_{13}$] and [2-Cl- $B_{10}H_{13}$] [174,189]. Unexpectedly, a mixture of the 1- and 2-chloro derivatives of decaborane was obtained in the reaction of decaborane(14) with 1,1-difluoroethane in carbon disulfide in the presence of $AlCl_3$ [192]. The isomers were separated by fractional crystallization from pentane or hexane [174,189,192] or chromatographically [175], and the substitution position was assigned using ^{11}B NMR spectroscopy [174,193].

Similar to the corresponding iodo and bromo derivatives, the 5- and 6-chloro derivatives of decaborane were prepared in an indirect way. The treatment of [*arachno*-6,9-(Me_2S) $_2$ - $B_{10}H_{12}$] with anhydrous HCl in benzene under reflux conditions results mainly in the 6-chloro derivative of decaborane [6-Cl- $B_{10}H_{13}$] with some amount of the 5-chloro isomer [174]. The reactions of [*arachno*-6,9-(Et_2S) $_2$ - $B_{10}H_{12}$] with anhydrous HCl or $HgCl_2$

in benzene at room temperature were also found to give the 6-chloro derivative $[6\text{-Cl-B}_{10}\text{H}_{13}]$ [183–185]. The reaction of $(\text{NH}_4)_2[\text{closo-B}_{10}\text{H}_{10}]$ with anhydrous HCl in a mixture of AlCl_3 and 1-butyl-3-methylimidazolium chloride (bmimCl) at 70°C proceeds with the boron cage opening and results in the 6-chloro derivative of decaborane $[6\text{-Cl-B}_{10}\text{H}_{13}]$ [186]. The 6-chloro derivative of decaborane can also be prepared by the reactions of $(\text{NH}_4)_2[\text{closo-B}_{10}\text{H}_{10}]$ with triflic acid in dichloromethane, respectively [186]. The 6-chloro derivative isomerizes to the 5-chloro derivative $[5\text{-Cl-B}_{10}\text{H}_{13}]$ in the presence of a catalytic amount of triethylamine in toluene at 60°C [187]. It was assumed that the isomerization occurs through the transformation of $[6\text{-Cl-B}_{10}\text{H}_{13}]$ into the $[6\text{-Cl-B}_{10}\text{H}_{13}]^-$ anion, followed by its isomerization. The solid state structures of $[6\text{-Cl-B}_{10}\text{H}_{13}]$, $(\text{HPS})[6\text{-Cl-B}_{10}\text{H}_{12}]$, and $(\text{HPS})[5\text{-Cl-B}_{10}\text{H}_{12}]$ were determined by single-crystal X-ray diffraction (Figure 7) [186,187]. The B-H-B bridge deprotonation at the site adjacent to the halogenated boron atoms was revealed [187].

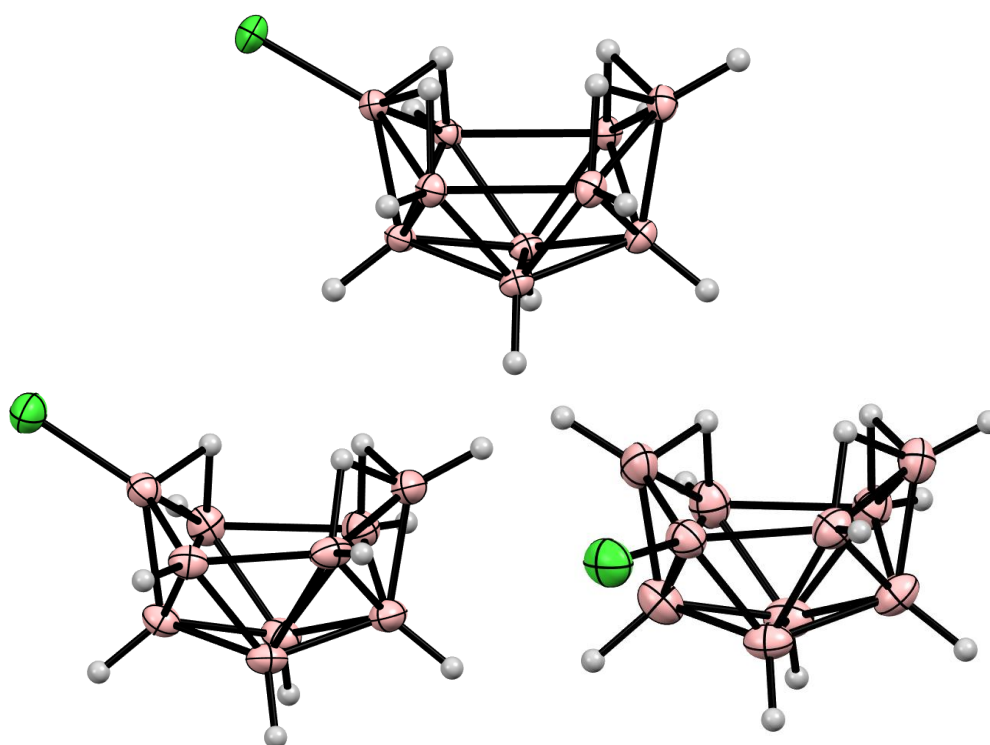


Figure 7. Solid state structures of $[6\text{-Cl-B}_{10}\text{H}_{13}]$ (top) as well as the $[6\text{-Cl-B}_{10}\text{H}_{12}]^-$ (bottom left) and $[5\text{-Cl-B}_{10}\text{H}_{12}]^-$ (bottom right) anions in the crystal structures of the corresponding protonated Proton Sponge salts.

The 6-chloro derivative $[6\text{-Cl-B}_{10}\text{H}_{13}]$ was also obtained by the reaction of $(\text{NH}_4)_2[\text{closo-B}_{10}\text{H}_{10}]$ or $(\text{Et}_4\text{N})_2[\text{closo-B}_{10}\text{H}_{10}]$ with AlCl_3 , followed by the hydrolysis of the resulting intermediate [188,194,195].

The 6-fluoro derivative of decaborane $[6\text{-F-B}_{10}\text{H}_{13}]$ was first obtained by the reaction of $[\text{arachno-6,9-(Et}_2\text{S)}_2\text{-B}_{10}\text{H}_{12}]$ with anhydrous HF in benzene at room temperature [183–185]. Later, the 6-fluoro derivative was prepared by the reaction of $(\text{NH}_4)_2[\text{closo-B}_{10}\text{H}_{10}]$ with triflic acid in 1-fluoropentane [186]. The solid state structure of $[6\text{-F-B}_{10}\text{H}_{13}]$ was determined by single-crystal X-ray diffraction (Figure 8) [186].

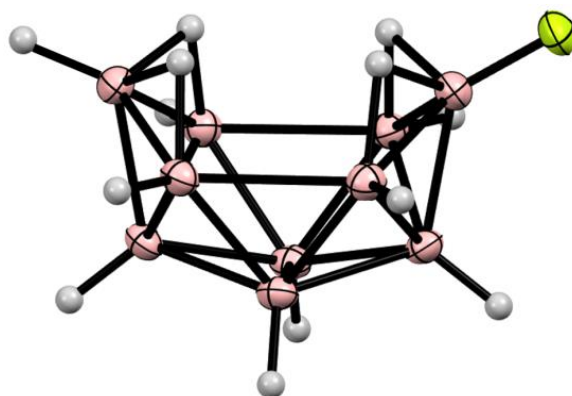


Figure 8. Solid state structure of the 6-fluoro derivative of decaborane [6-F-B₁₀H₁₃].

4. Derivatives with a B-O Bond

Due to the lack of electrophilic reagents for the introduction of oxygen substituents, the corresponding decaborane derivatives with substituents localized in the “bottom” of the decaborane basket have not yet been obtained. Alkoxy derivatives of decaborane [5-RO-B₁₀H₁₃] (R = Me, Et, Pr, Bu) were first obtained in low (13–20%) yields by trying to iodinate Na[B₁₀H₁₃] in the corresponding esters [196]. The phenoxy derivative [5-PhO-B₁₀H₁₃] was obtained in the same way, using anisole as a solvent [196]. The substitution position was determined using ¹¹B NMR spectroscopy [197]. It was assumed that their formation proceeds through the formation of oxonium derivatives of *arachno*-decaborane [R₂O-B₁₀H₁₃]⁺, followed by the elimination of one alkyl group [26]. The reaction of Na[B₁₀H₁₃] with SnCl₄ in diethyl ether leads to a mixture of 6- and 5-alkoxy derivatives of decaborane [6-EtO-B₁₀H₁₃] and [5-EtO-B₁₀H₁₃] in a ratio varying from 85:15 to 70:30 depending on the reaction temperature. The isomers were separated using column chromatography on silica [198]. It should be noted that the direct reactions of decaborane(14) with alcohols and phenols ROH leads to its complete degradation to the corresponding trialkyl- or triarylborates (RO)₃B [199]. The trimethylsiloxy derivative [6-Me₃SiO-B₁₀H₁₃] was obtained in a low yield (5–20%) from the reactions of Na[B₁₀H₁₃] and Na₂[B₁₀H₁₂] with Me₃SiCl in diethyl ether [198]. The report on the preparation of a trimethylsilyl derivative [Me₃Si-B₁₀H₁₃] under similar conditions [200] should apparently be considered erroneous.

The reactions of 5-bromo derivative [5-Br-B₁₀H₁₃] with alcohols ROH in the presence of NaHCO₃ in dichloromethane lead to 6-alkoxy derivatives [6-RO-B₁₀H₁₃] (R = Me, Et, *t*-Bu, *c*-Hx, CH₂CH₂SH, CH₂CH₂I, CH₂CH₂OCH₂CH₂Cl, (CH₂)₃C≡CH, CH(CH₂CH=CH₂)₂), while the reactions of 6-bromo derivative [6-Br-B₁₀H₁₃] with alcohols ROH in the presence of NaHCO₃ in dichloromethane lead to 5-alkoxy derivatives [5-RO-B₁₀H₁₃] (R = Me, *t*-Bu, *c*-Hx, CH₂CH₂SH, CH₂CH₂I, CH₂CH₂N(CO)₂C₂H₄, CH₂CH₂OCH₂CH₂Cl, (CH₂)₃C≡CH, CH₂C≡CCH₃, CH(CH₂CH=CH₂)₂). The reactions of [5-Br-B₁₀H₁₃] and [6-Br-B₁₀H₁₃] with 1,4-cyclohexyldiol lead to the compounds [μ-6,6′-(OC₆H₁₀O)-(B₁₀H₁₃)₂] and [μ-5,5′-(OC₆H₁₀O)-(B₁₀H₁₃)₂], respectively. The reactions of alcohols with [6-Br-B₁₀H₁₃] proceed quickly at room temperature, while those with [5-Br-B₁₀H₁₃] require heating (70 °C) to achieve completion. The reaction of [6-Br-B₁₀H₁₃] with ethanol was largely complete after 12 h at room temperature, but the reactions with 2-iodoethanol (~20 h), 2-bromoethanol (~40 h), 2-chloroethanol (~100 h), and 2-fluoroethanol (~125 h) all took increasingly longer times. The reactions with chloro- and iodo-derivatives of decaborane were found to proceed in a similar way; however, the reaction rate decreases in the halogen series I~Br > Cl [198]. The solid state structures of [5-MeO-B₁₀H₁₃] (Figure 9), [6-*t*-BuO-B₁₀H₁₃] (Figure 9), [5-ClCH₂CH₂OCH₂CH₂O-B₁₀H₁₃], [6-ClCH₂CH₂OCH₂CH₂O-B₁₀H₁₃], [5-MeC≡CCH₂O-B₁₀H₁₃], and [μ-6,6′-(OC₆H₁₀O)-(B₁₀H₁₃)₂] (Figure 9) were determined by single-crystal X-ray diffraction [201].

The 6-triflate derivative of decaborane [6-TfO-B₁₀H₁₃] was prepared by the reaction of Cs₂[*closo*-B₁₀H₁₀] with neat triflic acid at an ambient temperature [202,203]. In contrast, the

reaction of $(\text{NH}_4)_2[\text{closo-B}_{10}\text{H}_{10}]$ with triflic acid in 1-butyl-3-methylimidazolium triflate at 60 °C results in the 5-triflate derivative of decaborane $[\text{5-TfO-B}_{10}\text{H}_{13}]$ [204]. It was found that the reaction proceeds through the formation of the 6-triflate derivative, which, upon heating, isomerizes into the 5-triflate derivative. In the presence of a catalytic amount of triethylamine, the isomerization of $[\text{6-TfO-B}_{10}\text{H}_{13}]$ to $[\text{5-TfO-B}_{10}\text{H}_{13}]$ proceeds even at room temperature [204]. The reactions of $[\text{5-TfO-B}_{10}\text{H}_{13}]$ with methanol and 4-methoxyphenol in 1,2-dichloroethane at 70 °C result in the corresponding ethers $[\text{6-RO-B}_{10}\text{H}_{13}]$ ($\text{R} = \text{Me}, \text{C}_6\text{H}_4\text{-4-OMe}$) [204]. The solid state structures of $[\text{6-TfO-B}_{10}\text{H}_{13}]$ [202] and $[\text{5-TfO-B}_{10}\text{H}_{13}]$ [204] were determined by single-crystal X-ray diffraction (Figure 10).

The reactions of $\text{Na}_2[\text{closo-B}_{10}\text{H}_{10}]$ with alcohols ROH ($\text{R} = \text{Me}, \text{Et}, i\text{-Pr}, \text{Bu}, \text{Ph}$) in hexane in the presence of trimethylsilyl triflate lead to the corresponding 6-alkoxy derivatives of decaborane $[\text{6-RO-B}_{10}\text{H}_{13}]$ [205]. The reaction with water under the same conditions results in the 6-trimethylsiloxy derivative $[\text{6-Me}_3\text{SiO-B}_{10}\text{H}_{13}]$ [205].

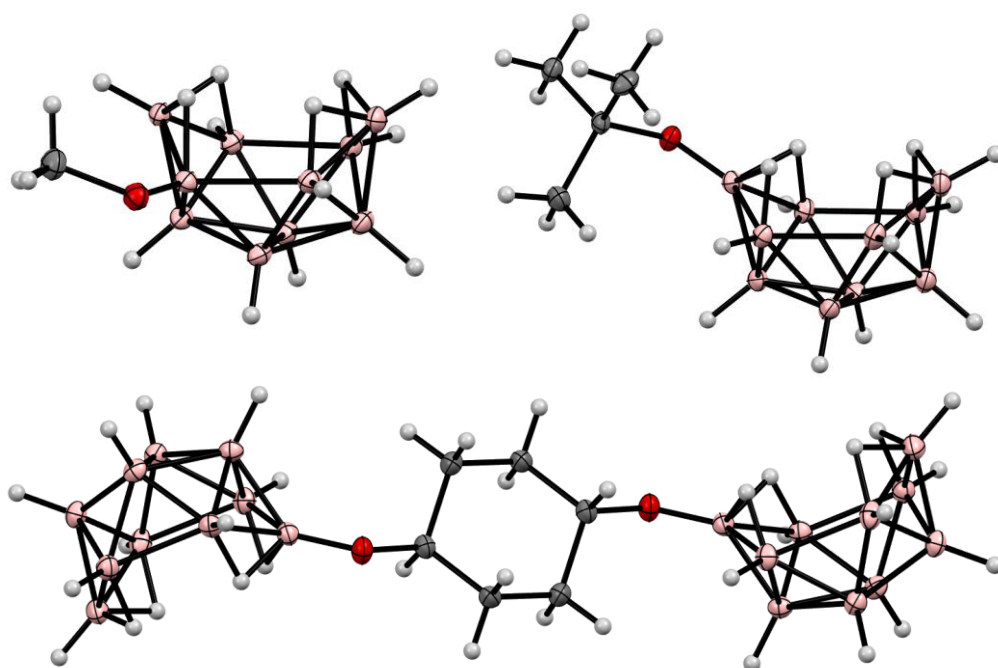


Figure 9. Solid state structures of $[\text{5-MeO-B}_{10}\text{H}_{13}]$ (top left), $[\text{6-}t\text{-BuO-B}_{10}\text{H}_{13}]$ (top right), and $[\mu\text{-6,6'-(OC}_6\text{H}_{10}\text{O)-(B}_{10}\text{H}_{13})_2]$ (bottom).

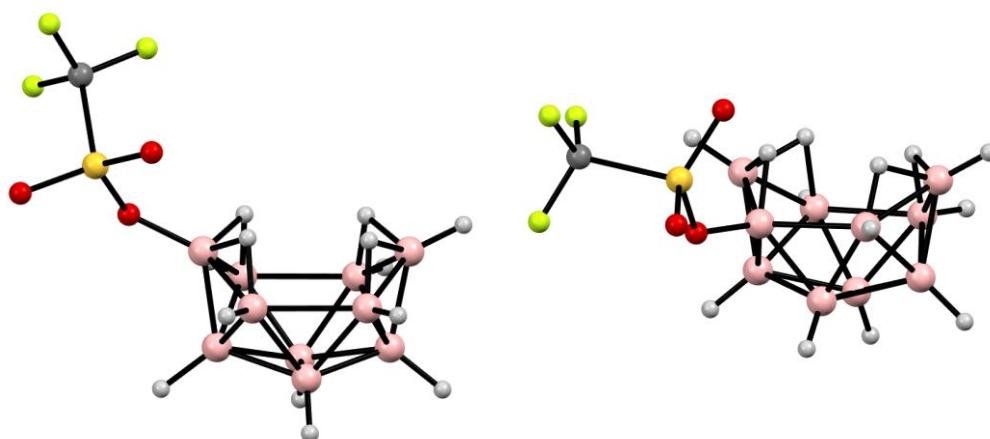


Figure 10. Solid state structures of $[\text{6-TfO-B}_{10}\text{H}_{13}]$ (left) and $[\text{5-TfO-B}_{10}\text{H}_{13}]$ (right).

In a similar way, the reaction of $(\text{NH}_4)_2[\text{closo-B}_{10}\text{H}_{10}]$ with sulfuric acid produces the 6-hydroxy derivative of decaborane $[\text{6-HO-B}_{10}\text{H}_{13}]$ [206]. The 6-hydroxy derivative was

also obtained as a by-product of the reaction of [*arachno*-6,9-(Me₂S)₂-B₁₀H₁₂] with sulfuric acid in benzene [207].

The 6-acetoxy derivative of *nido*-decaborane [6-AcO-B₁₀H₁₃] was obtained by the reaction of [*arachno*-6,9-(Me₂S)₂-B₁₀H₁₂] with mercury acetate [208]. The 6-acetoxy derivative of the *arachno*-decaborate anion [*arachno*-6-AcO-B₁₀H₁₃]^{2−} was obtained by the reaction of decaborane with 1-ethyl-3-methylimidazolium acetate (C₂mim)(OAc). The solid state structure of (C₂mim)₂[6-AcO-B₁₀H₁₃] was determined by single-crystal X-ray diffraction (Figure 11) [209].

The bis(decaboranyl) ether [μ-6,6'-O-(B₁₀H₁₃)₂] was prepared by the reaction of [*arachno*-6,9-(R₂S)₂-B₁₀H₁₂] (R = Me, Et) with sulfuric acid in benzene [210,211]. Its structure was determined by ¹¹B NMR spectroscopy [183,211] and supported by single-crystal X-ray diffraction [212]. The bis(decaboranyl) ether [μ-6,6'-O-(B₁₀H₁₃)₂] was also obtained by the dehydration of (H₃O)₂[*closo*-B₁₀H₁₀] [213].

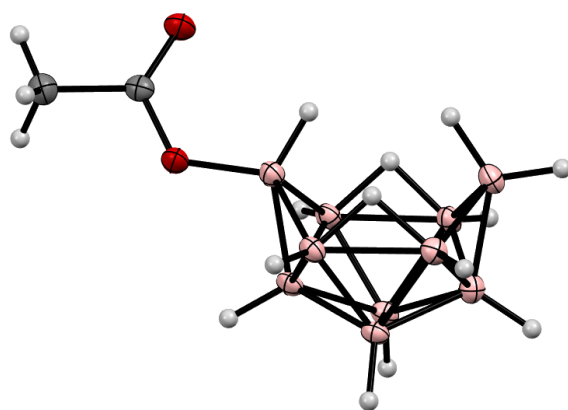


Figure 11. Structure of the [6-*arachno*-AcO-B₁₀H₁₃]^{2−} anion in the crystal structure of (C₂mim)₂[6-AcO-B₁₀H₁₃].

The preparation of decaborane derivatives with amides [*arachno*-6,9-(MeRN(R')CO)₂-B₁₀H₁₂] (R = H, R' = H, Me; R = Me, R' = H, Me), triphenylphosphine oxide [*arachno*-6,9-(Ph₃PO)₂-B₁₀H₁₂], and dimethylsulfoxide [*arachno*-6,9-(Me₂SO)₂-B₁₀H₁₂] has also been reported [214–217].

5. Derivatives with a B-S Bond

The reaction of decaborane(14) with sulfur in the presence of AlCl₃ at 120 °C results in a mixture of the mercapto derivatives [1-HS-B₁₀H₁₃], [2-HS-B₁₀H₁₃], and [1,2-(HS)₂-B₁₀H₁₂] [218,219]. The solid state structures of these mercapto derivatives were determined by single-crystal X-ray diffraction (Figure 12) [219].

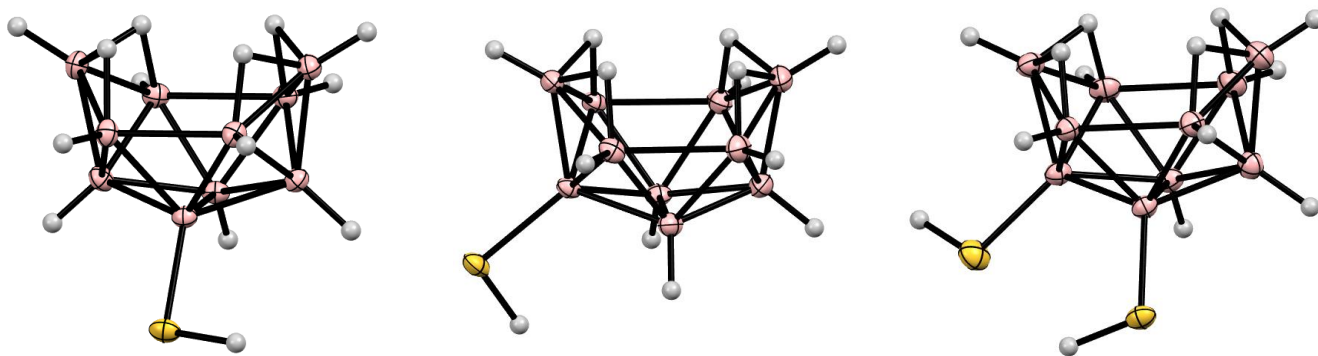


Figure 12. Solid state structures of the mercapto derivatives of decaborane [1-HS-B₁₀H₁₃] (left), [2-HS-B₁₀H₁₃] (middle), and [1,2-(HS)₂-B₁₀H₁₂] (right).

The reactions of $\text{Na}_2[\text{closo-B}_{10}\text{H}_{10}]$ with thiols RSH ($\text{R} = i\text{-Pr}, i\text{-Bu}, c\text{-Hx}, \text{C}_6\text{H}_4\text{-}p\text{-Me}, \text{C}_6\text{H}_4\text{-}p\text{-F}$) in hexane in the presence of trimethylsilyl triflate led to the corresponding 6-alkyl- and 6-arylsulfides $[\text{6-RS-B}_{10}\text{H}_{13}]$ [205]. It should be noted that the direct reactions of decaborane(14) with alkyl thiols RS lead to its complete degradation to the corresponding trialkylthioborates $(\text{RS})_3\text{B}$ [220].

Due to its use in the synthesis of carboranes, the 6,9-bis(dimethylsulfonium) derivative of the *arachno*-decaborate anion $[\text{arachno-6,9-(Me}_2\text{S)}_2\text{-B}_{10}\text{H}_{12}]$, which is formed by refluxing decaborane with dimethyl sulfide in ether or benzene, is the most known decaborane derivative with a B-S bond [214,221,222]. The solid state structure of $[\text{arachno-6,9-(Me}_2\text{S)}_2\text{-B}_{10}\text{H}_{12}]$ was determined by single-crystal X-ray diffraction [223]. The 6,9-bis(dimethylsulfonium) derivative was studied by X-ray and X-ray photoelectron spectroscopy [224–226], and its diamagnetic susceptibility was determined [227]. The Me_2S substituents in $[\text{arachno-6,9-(Me}_2\text{S)}_2\text{-B}_{10}\text{H}_{12}]$ can be easily replaced by stronger Lewis bases [214,228]. A series of other bis(dialkylsulfonium) derivatives ($[\text{arachno-6,9-(RR'S)}_2\text{-B}_{10}\text{H}_{12}]$ ($\text{R} = \text{R}' = \text{Et}, \text{Pr}$; $\text{RR}' = (\text{CH}_2)_4, (\text{CH}_2\text{CH}_2)_2\text{S}, (\text{CH}_2\text{CH}_2)_2\text{O}$) have been prepared in a similar manner [215,220,228,229].

The bis(diethylsulfonium) derivative $[\text{arachno-6,9-(Et}_2\text{S)}_2\text{-B}_{10}\text{H}_{12}]$ can also be obtained by the reaction of $(\text{NH}_4)_2[\text{closo-B}_{10}\text{H}_{10}]$ with anhydrous hydrogen chloride in diethylsulfide [230]. This approach has been extended to other salts of the *closo*-decaborate anion and other strong acids, including $(\text{H}_3\text{O})_2[\text{closo-B}_{10}\text{H}_{10}]$ [231,232].

The reactions of 2-halogen derivatives of decaborane $[\text{2-X-B}_{10}\text{H}_{13}]$ ($\text{X} = \text{Cl}, \text{Br}, \text{I}$) with dimethylsulfide Me_2S give the corresponding 2-halogen-6,9-bis(dimethylsulfonium) derivatives $[\text{arachno-2-X-6,9-(Me}_2\text{S)}_2\text{-B}_{10}\text{H}_{11}]$ [233,234]. In a similar way, the reactions of 5-halogen derivatives of decaborane $[\text{5-X-B}_{10}\text{H}_{13}]$ ($\text{X} = \text{F}, \text{Br}, \text{I}$) with dialkylsulfides R_2S ($\text{R} = \text{Me}, \text{Et}$) result in the corresponding 5-halogen-6,9-bis(dialkylsulfonium) derivatives $[\text{arachno-5-X-6,9-(R}_2\text{S)}_2\text{-B}_{10}\text{H}_{11}]$, while the reactions of the 6-chloro derivative proceed with the halogen displacement, giving $[\text{arachno-6,9-(R}_2\text{S)}_2\text{-B}_{10}\text{H}_{12}]$ [185]. The solid state structure of $[\text{5-Br-6,9-(R}_2\text{S)}_2\text{-B}_{10}\text{H}_{11}]$ was determined by single-crystal X-ray diffraction [235]. The reactions of 2,4-dichloro- and 1,2,4-trichloro derivatives of decaborane $[\text{nido-2,4-Cl}_2\text{-B}_{10}\text{H}_{12}]$ and $[\text{nido-1,2,4-Cl}_3\text{-B}_{10}\text{H}_{11}]$ with dimethylsulfide were found to proceed with the boron cage rearrangement, resulting in $[\text{arachno-1,7-Cl}_2\text{-6,9-(Me}_2\text{S)}_2\text{-B}_{10}\text{H}_{10}]$ and $[\text{arachno-1,3,7-Cl}_3\text{-6,9-(Me}_2\text{S)}_2\text{-B}_{10}\text{H}_9]$, respectively [236]. The solid state structures of $[\text{1,7-Cl}_2\text{-6,9-(Me}_2\text{S)}_2\text{-B}_{10}\text{H}_{10}]$ and $[\text{1,3,7-Cl}_3\text{-6,9-(Me}_2\text{S)}_2\text{-B}_{10}\text{H}_9]$ were determined by single-crystal X-ray diffraction [236].

The reaction of the 5-triflate derivative of decaborane $[\text{5-TfO-B}_{10}\text{H}_{13}]$ with dimethylsulfide in toluene results in the 5-triflate-6,9-bis(dialkylsulfonium) derivative $[\text{arachno-5-TfO-6,9-B}_{10}\text{H}_{11}(\text{SMe}_2)_2]$, while the similar reaction of the 5-triflate derivative $[\text{6-TfO-B}_{10}\text{H}_{13}]$ proceeds with the substitution of the triflate group, giving $[\text{arachno-6,9-B}_{10}\text{H}_{12}(\text{SMe}_2)_2]$ [204]. The solid state structure of $[\text{5-TfO-6,9-(Me}_2\text{S)}_2\text{-B}_{10}\text{H}_{11}]$ was determined by single-crystal X-ray diffraction [204].

The 5-dimethylsulfonium derivative of decaborane $[\text{nido-5-Me}_2\text{S-B}_{10}\text{H}_{12}]$ was obtained by heating $[\text{arachno-6,9-(Me}_2\text{S)}_2\text{-B}_{10}\text{H}_{12}]$ in toluene or mesitylene, and its solid state structure was determined by single-crystal X-ray diffraction (Figure 13) [215,222,237,238]. It was found that the B-H-B bridge deprotonation occurs at the site adjacent to the substituted boron atom, and thus, the structure of $[\text{5-Me}_2\text{S-B}_{10}\text{H}_{12}]$ is similar to the structure of the $[\text{6-Cl-B}_{10}\text{H}_{12}]^-$ anion [187].

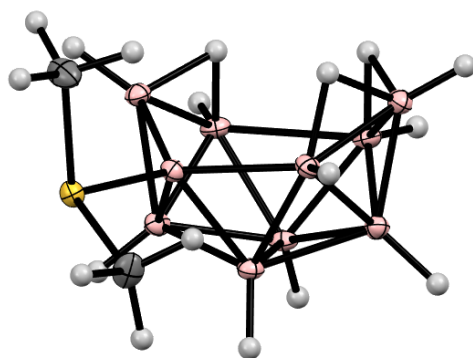


Figure 13. Solid state structure of [nido-5-Me₂S-B₁₀H₁₂].

The preparation of the bis(dimethylthioformamide) [*arachno*-6,9-(Me₂N(H)CS)₂-B₁₀H₁₂] [215] and the bis(di(alkyl/aryl)thiourea) [*arachno*-6,9-((RHN)₂CS)₂-B₁₀H₁₂] (R = Et, Ph) [217,239] derivatives has also been reported.

6. Derivatives with a B-N Bond

Heating decaborane(14) in acetonitrile under reflux proceeds with hydrogen elimination, resulting in the 6,9-bis(acetonitrilium) derivative of the *arachno*-decaborate anion [*arachno*-6,9-(MeC≡N)₂-B₁₀H₁₂] [240], which was the first structurally characterized decaborane derivative [217,241–243] (Figure 14). The 6,9-bis(acetonitrilium) derivative was studied by X-ray photoelectron spectroscopy [226], and its diamagnetic susceptibility was determined [227]. The 6,9-bis(propionitrilium) and 6,9-bis(benzonitrilium) derivatives [*arachno*-6,9-(RC≡N)₂-B₁₀H₁₂] (R = Et, Ph) were prepared in a similar way from decaborane(14) and propionitrile [244] or benzonitrile [217], respectively. The reaction of the 6,9-bis(acetonitrilium) derivative with diethylcyanamide in diethyl ether results in [*arachno*-6,9-(Et₂NC≡N)₂-B₁₀H₁₂] [214,245]. The reaction of the 2-bromo derivative of decaborane [2-Br-B₁₀H₁₃] gives [*arachno*-6,9-(MeC≡N)₂-2-Br-B₁₀H₁₁] [233].

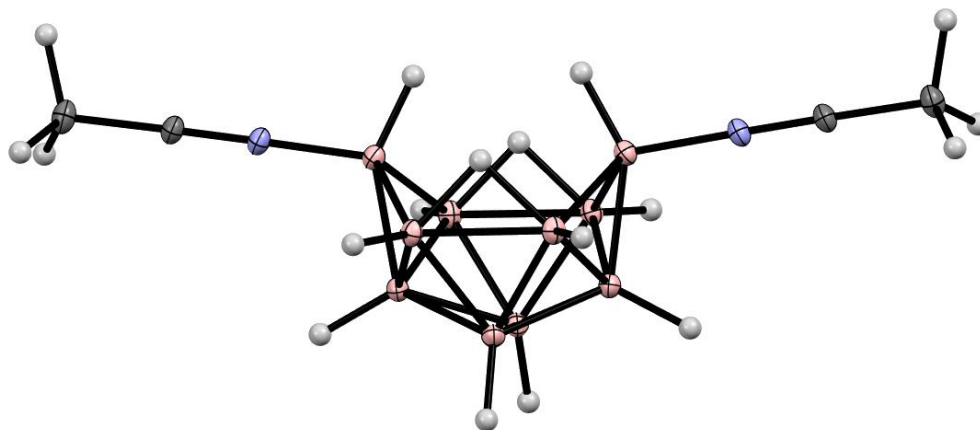


Figure 14. Solid state structure of [*arachno*-6,9-(MeC≡N)₂-B₁₀H₁₂].

The 6,9-bis(acetonitrilium) derivative [*arachno*-6,9-(MeC≡N)₂-B₁₀H₁₂] reacts with *N*-nucleophiles (primary and secondary amines and hydrazine), giving the corresponding amidines [*arachno*-6,9-(RR′N(Me)C=HN)₂-B₁₀H₁₂] (R = H, R′ = Et, Pr, Bu, Ph, NH₂, NHMe; R = R′ = Et, Pr, Bu) [246–248]. The solid state structures of the amidines [6,9-(Bu₂N(Me)C=HN)₂-B₁₀H₁₂] and [6,9-(PhHN(Me)C=HN)₂-B₁₀H₁₂]·Et₂O were determined by single-crystal X-ray diffraction (Figure 15) [248]. It should be noted that the reactions with primary amines produce mainly the *ZE* isomers, whereas the reactions with secondary amines result only in the *EE* isomers.

The reaction of the 6,9-bis(acetonitrilium) derivative with methanol results in the formation of the corresponding imidate [*arachno*-6,9-(MeO(Me)C=HN)₂-B₁₀H₁₂] [248]. Nowa-

days, the addition of nucleophiles to the activated triple $\text{-C}\equiv\text{N-}$ bond of nitrilium derivatives of various polyhedral boron hydrides has become a widely used method for their modification [249–258].

The reactions of the 6,9-bis(acetonitrilium) derivative with tertiary amines in refluxing benzene or toluene lead to the corresponding 6,9-bis(trialkylammonium) derivatives [*arachno*-6,9-(R_3N) $_2$ - $\text{B}_{10}\text{H}_{12}$] ($\text{R} = \text{Me, Et}$) [214,245]. The 6,9-bis(ammonium) derivative [*arachno*-6,9-(H_3N) $_2$ - $\text{B}_{10}\text{H}_{12}$] was prepared by the reaction of decaborane(14) with ammonia in benzene or toluene [259,260]. The solid state structures of [6,9-(H_3N) $_2$ - $\text{B}_{10}\text{H}_{12}$] (Figure 16) [243,261], [6,9-(Me_3N) $_2$ - $\text{B}_{10}\text{H}_{12}$] [262], and [6,9-(Et_3N) $_2$ - $\text{B}_{10}\text{H}_{12}$] [263] were determined by single-crystal X-ray diffraction. [6,9-(H_3N) $_2$ - $\text{B}_{10}\text{H}_{12}$] and [6,9-(Et_3N) $_2$ - $\text{B}_{10}\text{H}_{12}$] were studied by X-ray photoelectron and X-ray fluorescence spectroscopy [225,226,264]. The diamagnetic susceptibilities of [6,9-(Me_3N) $_2$ - $\text{B}_{10}\text{H}_{12}$] and [6,9-(Et_3N) $_2$ - $\text{B}_{10}\text{H}_{12}$] were determined [227]. The thermal decomposition of the 6,9-bis(ammonium) derivative [*arachno*-6,9-(H_3N) $_2$ - $\text{B}_{10}\text{H}_{12}$] was studied [260,265,266].

The reaction of decaborane(14) with diethylamine in cyclohexane results in the diethylammonium derivative of the *arachno*-decaborate anion (Et_2NH_2)[*arachno*-6- $\text{Et}_2\text{HN-B}_{10}\text{H}_{13}$] [267]. Similar alkylammonium derivatives (Me_4N)[*arachno*-6- $\text{RR}'\text{R}''\text{N-B}_{10}\text{H}_{13}$] ($\text{R} = \text{Et, R}' = \text{R}'' = \text{H}$; $\text{R} = \text{R}' = \text{Et, R}'' = \text{H}$; $\text{R} = \text{R}' = \text{R}'' = \text{Et}$; $\text{RR}' = (\text{CH}_2)_5, \text{R}'' = \text{H}$) were prepared by the reactions of $\text{Na}[\text{B}_{10}\text{H}_{13}]$ with the corresponding amines, followed by precipitation with $(\text{Me}_4\text{N})\text{Cl}$ [267]. Heating (Et_2NH_2)[*arachno*-6- $\text{Et}_2\text{HN-B}_{10}\text{H}_{13}$] in THF under reflux gives the 6,9-bis(diethylammonium) derivative [*arachno*-6,9-(Et_2HN) $_2$ - $\text{B}_{10}\text{H}_{12}$], whereas the similar reaction in acetonitrile leads to [*arachno*-6- $\text{Et}_2\text{HN-9-Et}_2\text{N}(\text{Me})\text{C}\equiv\text{HN-B}_{10}\text{H}_{12}$] [267]. The reactions of $\text{Na}[\text{arachno-6-Et}_2\text{HN-B}_{10}\text{H}_{13}]$ with acetonitrile and dimethylsulfide in the presence of dry HCl result in [*arachno*-6- $\text{Et}_2\text{NH-9-MeC}\equiv\text{N-B}_{10}\text{H}_{12}$] and [*arachno*-6- $\text{Et}_2\text{NH-9-Me}_2\text{S-B}_{10}\text{H}_{12}$], respectively [267]. In a similar way, the reaction of (Me_4N)[*arachno*-6- $\text{Et}_3\text{N-B}_{10}\text{H}_{13}$] with acetonitrile leads to [*arachno*-6- $\text{Et}_3\text{N-9-MeC}\equiv\text{N-B}_{10}\text{H}_{12}$] [221]. The reactions of $\text{Na}[\text{arachno-6-Et}_2\text{HN-B}_{10}\text{H}_{13}]$ with amines in THF produce the corresponding 6,9-bis(alkylammonium) derivatives [*arachno*-6- $\text{Et}_2\text{NH-9-RR}'\text{R}''\text{N-B}_{10}\text{H}_{12}$] ($\text{R} = \text{Et, R}' = \text{R}'' = \text{H}$; $\text{R} = \text{R}' = \text{Et, R}'' = \text{H}$; $\text{R} = \text{R}' = \text{R}'' = \text{Me}$) [267].

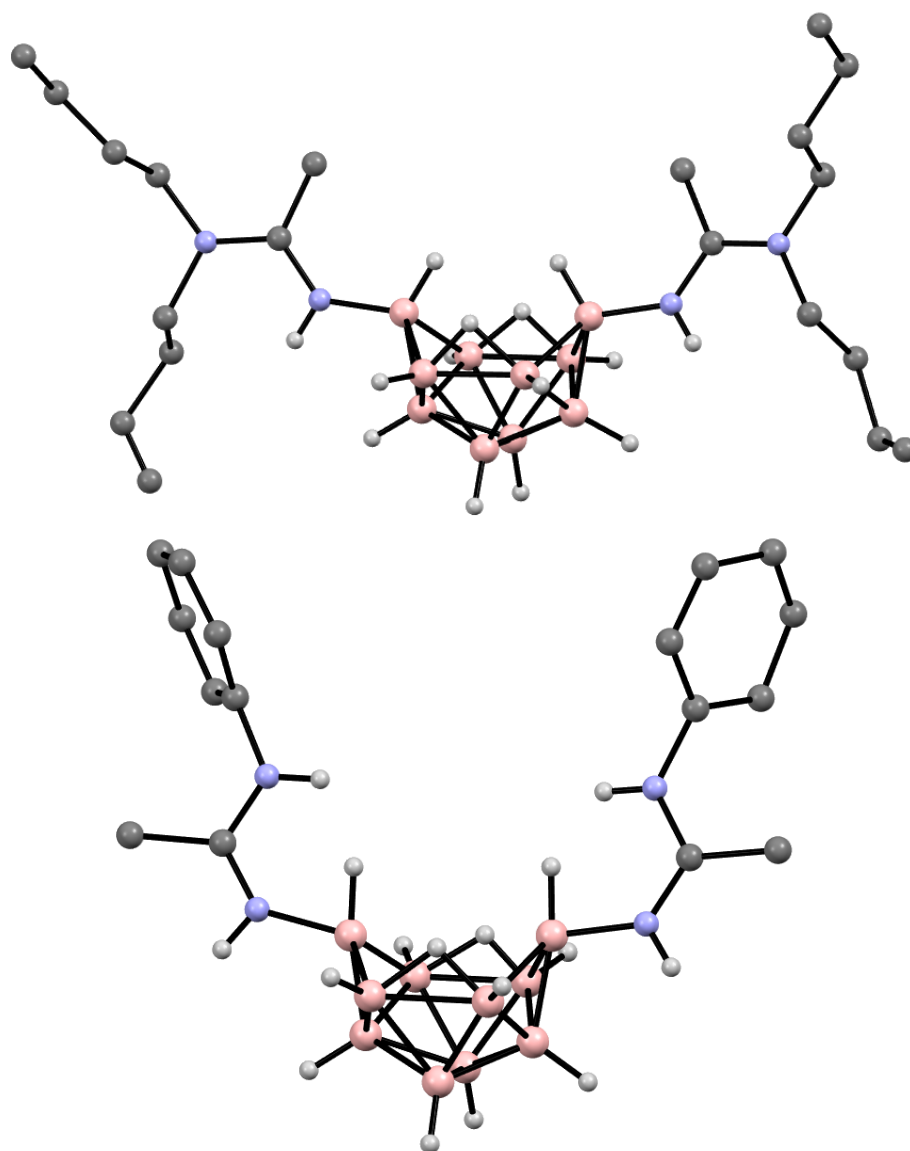


Figure 15. Solid state structures of the decaborane-based amidines $[6,9-(\text{Bu}_2\text{N}(\text{Me})\text{C}=\text{HN})_2\text{-B}_{10}\text{H}_{12}]$ (**top**) and $[6,9-(\text{PhHN}(\text{Me})\text{C}=\text{HN})_2\text{-B}_{10}\text{H}_{12}]$ (**bottom**).

The reactions of decaborane(14) with pyridines, quinolines, and isoquinoline lead to the corresponding $[\text{arachno-}6,9\text{-L}_2\text{-B}_{10}\text{H}_{12}]$ (L = pyridine, 2-methylpyridine, 3-methylpyridine, 4-methylpyridine, 2-ethynylpyridine, 2-cyanopyridine, quinoline, 2-methylquinoline, 8-methylquinoline, isoquinoline) derivatives (Scheme 4) [214,236,268,269]. A more convenient way to prepare 6,9-bis(pyridinium) derivatives is the nucleophilic substitution of the dialkylsulfide groups in $[\text{arachno-}6,9\text{-(R}_2\text{S)}_2\text{-B}_{10}\text{H}_{12}]$ (R = Me, Et). In this way, the $[\text{arachno-}6,9\text{-L}_2\text{-B}_{10}\text{H}_{12}]$ (L = pyridine, 2-methylpyridine, 3-methylpyridine, 4-methylpyridine, 2,3-dimethylpyridine, 2,4-dimethylpyridine, 2,5-dimethylpyridine, 2,6-dimethylpyridine, 3,4-dimethylpyridine, 2-methyl-5-ethylpyridine, 2-phenylpyridine, 4-benzylpyridine, 4-styrylpyridine, 2-methoxypyridine, 4-methoxypyridine, 3-chloropyridine, 4-chloropyridine, 2-bromopyridine, 4-bromopyridine, 3,5-dibromopyridine, 3-cyanopyridine, 4-cyanopyridine, 4-acetylpyridine, quinoline) derivatives were synthesized (Scheme 4) [229,270–272].

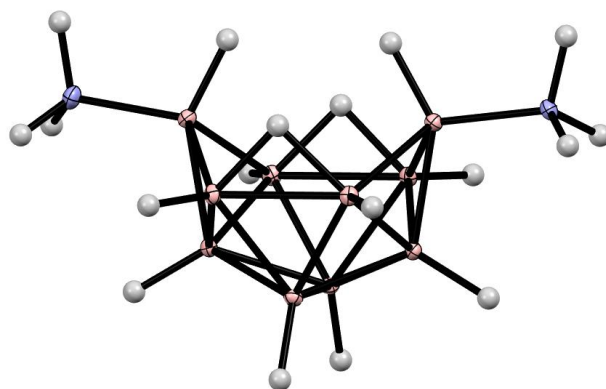
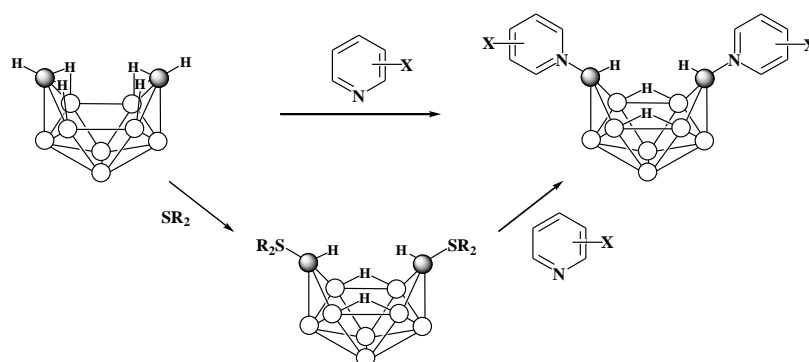


Figure 16. Solid state structure of $[arachno-6,9-(H_3N)_2-B_{10}H_{12}]$.



Scheme 4. Synthesis of 6,9-bis(pyridinium) derivatives $[6,9-L_2-B_{10}H_{12}]$.

All compounds of this series are brightly colored from yellow to red, which is the reason for the interest in their study by UV and luminescent spectroscopy [229,271–273]. The 6,9-bis(pyridinium) derivative $[6,9-Py_2-B_{10}H_{12}]$ was studied by X-ray photoelectron and X-ray fluorescence spectroscopy [225,226] and, its diamagnetic susceptibility was determined [227]. The thermal decomposition of the 6,9-bis(pyridinium) and 6,9-bis(quinolinium) derivatives was studied [274]. The solid state structures of $[6,9-Py_2-B_{10}H_{12}]$ [275], $[6,9-(HC\equiv C-o-C_5H_4N)_2-B_{10}H_{12}]$ [269], and $[6,9-(N\equiv C-o-C_5H_4N)_2-B_{10}H_{12}] \cdot CH_2Cl_2$ [269] were determined by single-crystal X-ray diffraction (Figure 17).

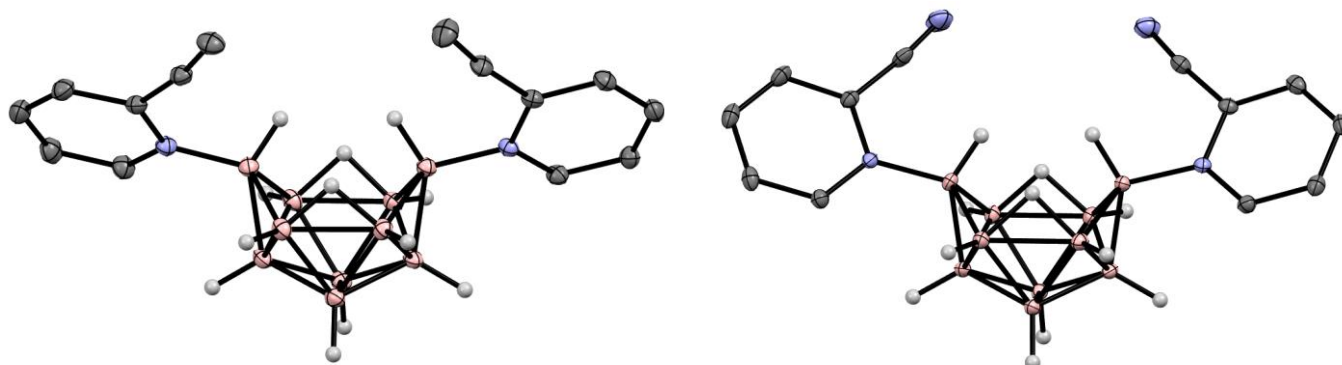
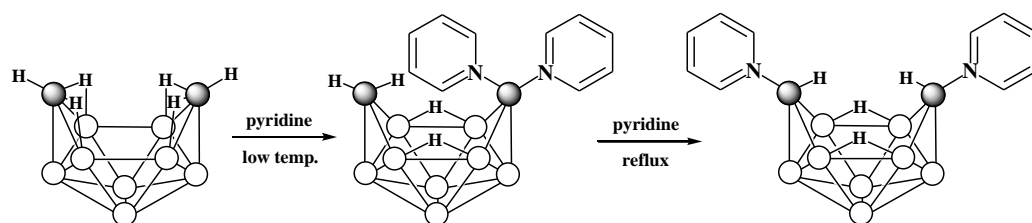


Figure 17. Solid state structures of $[arachno-6,9-(HC\equiv C-o-C_5H_4N)_2-B_{10}H_{12}]$ (left) and $[arachno-6,9-(N\equiv C-o-C_5H_4N)_2-B_{10}H_{12}]$ (right). Hydrogen atoms of organic substituents are omitted for clarity.

It should be noted that the reaction of decaborane(14) with pyridine at low temperatures was found to form the 6,6-bis(pyridinium) derivative $[arachno-6,6-Py_2-B_{10}H_{12}]$, which, upon refluxing in dry degassed pyridine, converts into the more stable 6,9-isomer (Scheme 5) [268].



Scheme 5. Synthesis of [arachno-6,6-Py₂-B₁₀H₁₂] and its transformation to [arachno-6,9-Py₂-B₁₀H₁₂].

The reaction of [6,9-(Me₂S)₂-B₁₀H₁₂] with pyrazine in dichloromethane gives the pyrazine-bridged derivative [μ-6,6'-pyrazine-(9-Me₂S-B₁₀H₁₂)₂], whereas the reaction with 4,4'-bipyridine leads to the product of the substitution of the Me₂S groups with azaheterocycle [6,9-(NC₅H₄C₅H₄N)₂-B₁₀H₁₂] (Figure 18) [276].

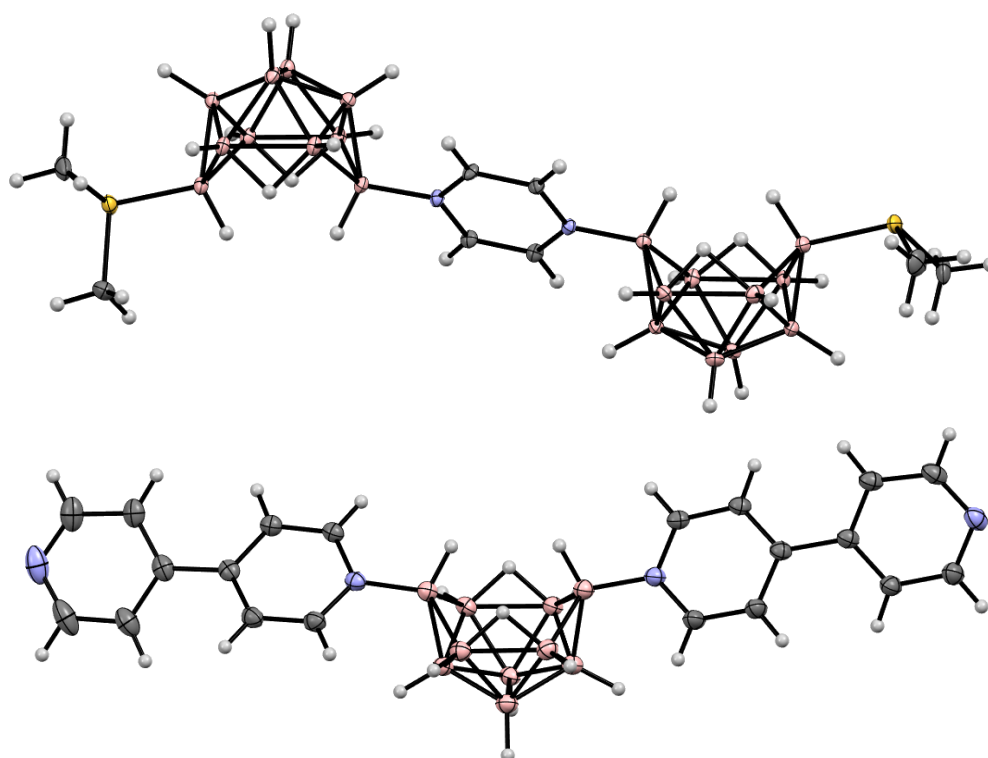
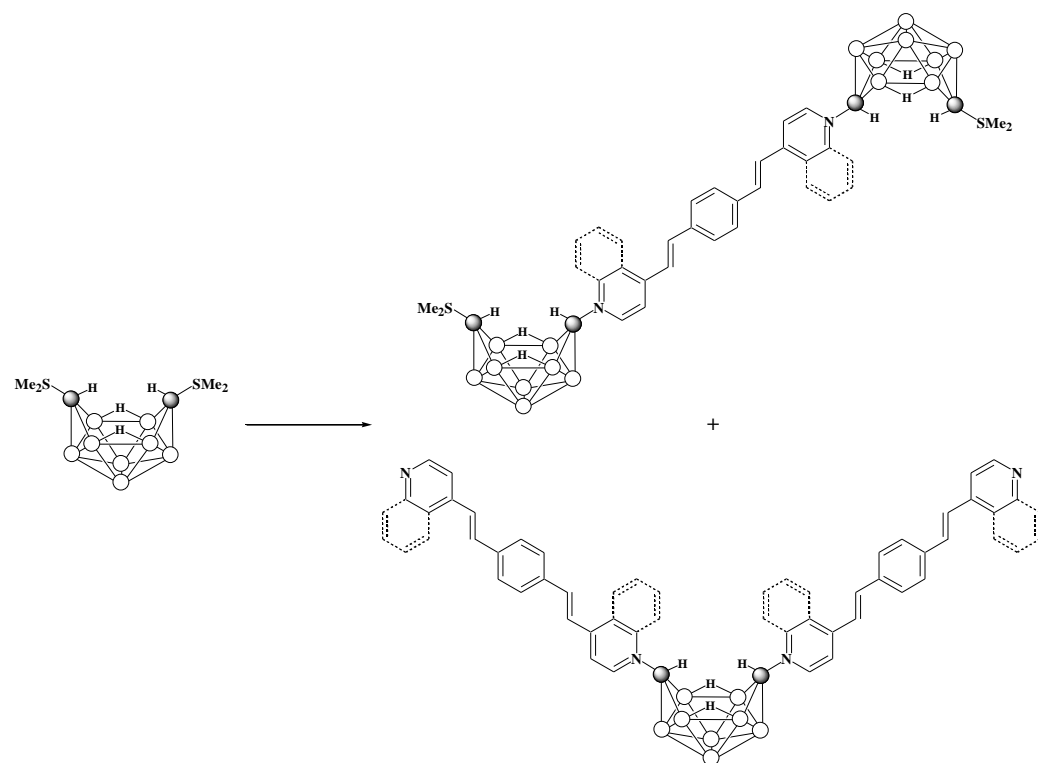


Figure 18. Solid state structures of [μ-6,6'-pyrazine-(9-Me₂S-B₁₀H₁₂)₂] (top) and [6,9-(NC₅H₄C₅H₄N)₂-B₁₀H₁₂] (bottom).

The similar reactions of [6,9-(Me₂S)₂-B₁₀H₁₂] with 1,4-bis[β-(4-pyridyl)vinyl]benzene and 1,4-bis[β-(4-quinolyl)vinyl]benzene were found to produce mixtures of the corresponding bridged and terminal substituted derivatives (Scheme 6) [277].

The reactions of Na[arachno-6-Et₂HN-B₁₀H₁₃] and (Me₄N)[arachno-6-Et₃N-B₁₀H₁₃] with pyridine in THF produce the corresponding 6-alkylammonium-9-pyridinium derivatives [arachno-6-Et₂RN-9-Py-B₁₀H₁₂] (R = H, Et) [267,278].

The reactions of decaborane(14) with imidazoles in refluxing benzene result in the corresponding 6,9-bis(imidazolium) derivatives [arachno-6,9-(RIm)₂-Me₂S-B₁₀H₁₂] (R = H, Me, Et, Bu) (Figure 19). The hypergolic properties of the 6,9-bis(imidazolium) derivatives prepared were studied [279].



Scheme 6. Reactions of [arachno-6,9-(Me₂S)₂-B₁₀H₁₂] with 1,4-bis[β-(4-pyridyl)vinyl]benzene and 1,4-bis[β-(4-quinolyl)vinyl]benzene.

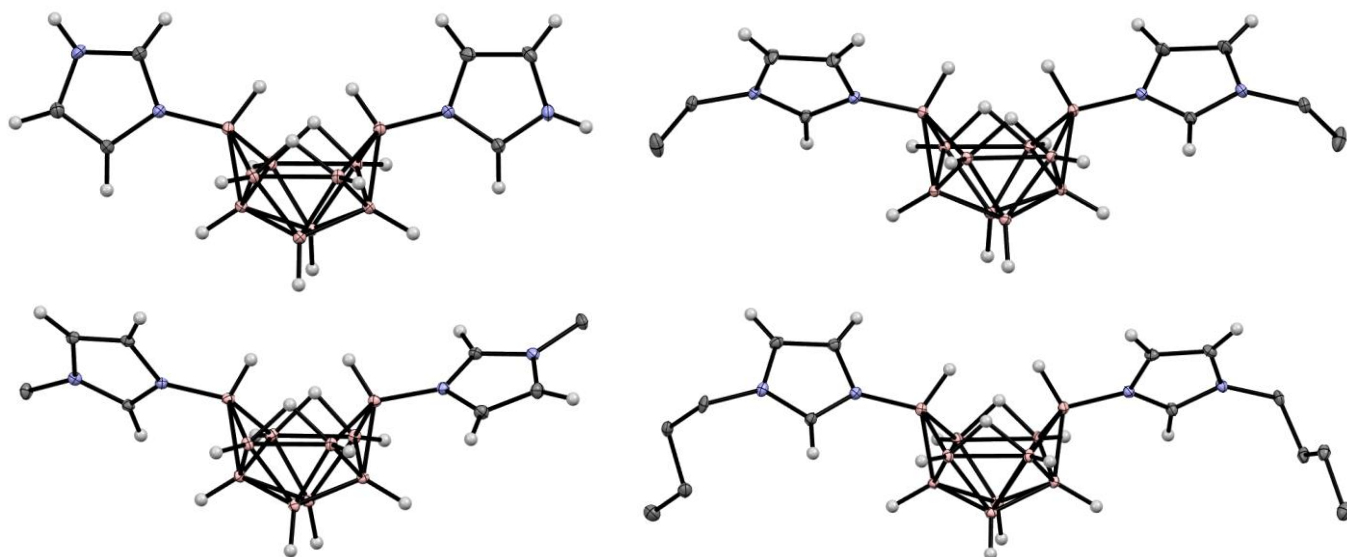


Figure 19. Solid state structures of [6,9-(HIm)₂-Me₂S-B₁₀H₁₂] (**top left**), [6,9-(MeIm)₂-Me₂S-B₁₀H₁₂] (**top right**), [6,9-(EtIm)₂-Me₂S-B₁₀H₁₂] (**bottom left**), and [6,9-(BuIm)₂-Me₂S-B₁₀H₁₂] (**top right**). Hydrogen atoms of alkyl groups are omitted for clarity.

The reactions of decaborane(14) with 2-isopropyl- and 2-methyl-5-(2-chloroethyl) tetrazoles in benzene result in the corresponding 6,9-bis(tetrazolium) derivatives [arachno-6,9-L₂-Me₂S-B₁₀H₁₂] [280].

The 6-isothiocyanato derivative [6-SCN-B₁₀H₁₃] was prepared by the reaction of [6,9-(R₂S)₂-B₁₀H₁₂] (R = Me, Et) with mercury isothiocyanate [208]. Alternatively, the 6-isothiocyanato derivative can be prepared by the reaction of decaborane(14) with NaSCN

in 1,2-dimethoxyethane in the presence of dry HCl [281]. The solid state structure of [6-SCN-B₁₀H₁₃] was determined by single-crystal X-ray diffraction (Figure 20) [281].

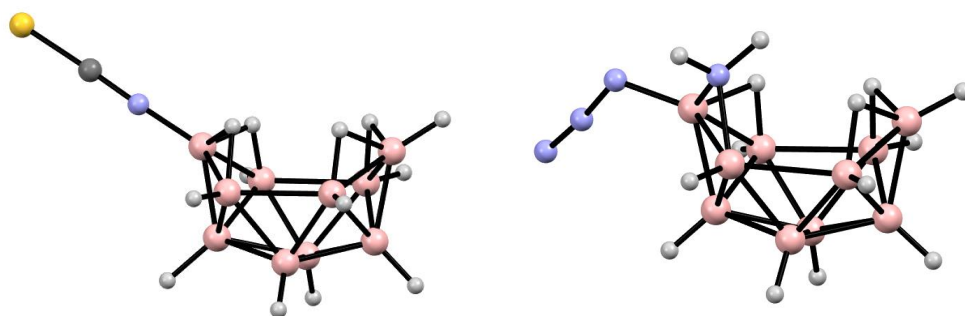


Figure 20. Solid state structures of [6-SCN-B₁₀H₁₃] (left) and [6-N₃-μ-5,6-NH₂-B₁₀H₁₁] (right).

The reaction of [6,9-(Me₂S)₂-B₁₀H₁₂] with excess HN₃ in toluene results in the 6-azido-μ-5,6-amino derivative [6-N₃-μ-5,6-NH₂-B₁₀H₁₁], the structure of which was determined by single-crystal X-ray diffraction (Figure 20) [282].

7. Derivatives with a B-P Bond

The reaction of decaborane(14) with triphenylphosphine in diethyl ether under reflux results in the 6,9-bis(triphenylphosphonium) derivative of the *arachno*-decaborate anion [arachno-6,9-(Ph₃P)₂-B₁₀H₁₂]; the same product can be prepared by the reaction of [6,9-(MeC≡N)₂-B₁₀H₁₂] with triphenylphosphine in hot acetonitrile [214,245,283]. The solid state structure of [arachno-6,9-(Ph₃P)₂-B₁₀H₁₂]·2DMF·H₂O was determined by single-crystal X-ray diffraction [284]. The 6,9-bis(triphenylphosphonium) derivative was also studied by X-ray emission and X-ray photoelectron spectroscopy [279,280], and its diamagnetic susceptibility was determined [227]. The reaction of [6,9-(Me₂S)₂-2-Br-B₁₀H₁₁] with triphenylphosphine in benzene results in the corresponding 6,9-bis(triphenylphosphonium) derivative [6,9-(Ph₃P)₂-2-Br-B₁₀H₁₁] [233].

The reaction of decaborane(14) with PhMe₂P at low temperatures (~200 K) gives a mixture of *exo,exo*- and *exo,endo*-isomers of [6,9-(PhMe₂P)₂-arachno-B₁₀H₁₂], which were separated chromatographically [285,286]. The structure of both isomers was confirmed by single-crystal X-ray diffraction (Figure 21) [286].

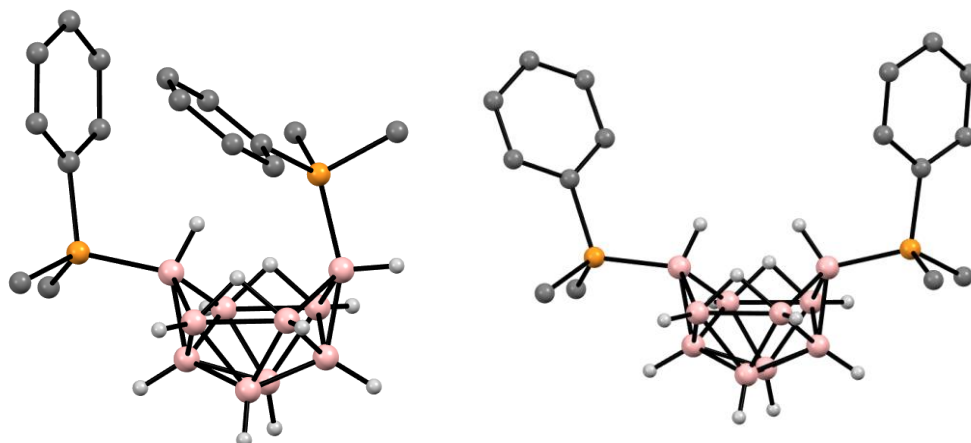


Figure 21. Solid state structures of *exo,endo*-[6,9-(PhMe₂P)₂-arachno-B₁₀H₁₂] (left) and *exo,exo*-[6,9-(PhMe₂P)₂-arachno-B₁₀H₁₂] (right). Hydrogen atoms of organic substituents are omitted for clarity.

Under similar conditions, the reaction of the 2,4-dichloro derivatives of decaborane with PhMe₂P solely produces the *exo,endo*-isomer of [6,9-(PhMe₂P)₂-2,4-Cl₂-arachno-B₁₀H₁₀], while the reaction of 2-bromo leads to mixtures of *exo,exo*- and *exo,endo*-isomers and [6,9-

(PhMe₂P)₂-2-Br-*arachno*-B₁₀H₁₁]. It is interesting to note that in the reaction of the 2-bromo derivative, it is precisely the 6,9-*exo,endo*-isomer that is formed, without any traces of the 9,6-*exo,endo*-isomer. The solid state structure of the *exo,endo*-isomer [6,9-(PhMe₂P)₂-2-Br-*arachno*-B₁₀H₁₂] was determined by single-crystal X-ray diffraction (Figure 22) [286].

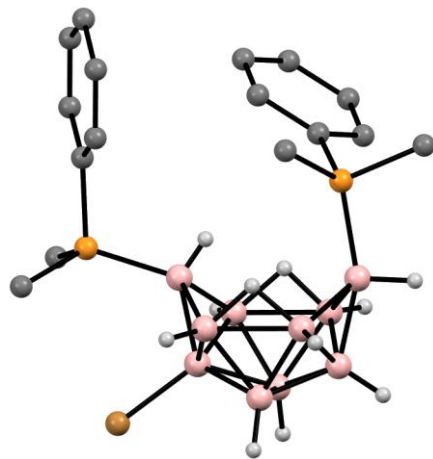


Figure 22. Solid state structure of *exo,endo*-[6,9-(PhMe₂P)₂-2-Br-*arachno*-B₁₀H₁₂]. Hydrogen atoms of organic substituents are omitted for clarity.

The reaction of decaborane(14) with triethylphosphine in benzene results in the 6,9-bis(triethylphosphonium) derivative [*arachno*-6,9-(Et₃P)₂-B₁₀H₁₂] [287], whereas the 6,9-bis(diphenylphosphonium) and 6,9-bis(phenylphosphonium) derivatives [*arachno*-6,9-(Ph₂HP)₂-B₁₀H₁₂] and [*arachno*-6,9-(PhH₂P)₂-B₁₀H₁₂] were prepared by the reactions of the corresponding phosphines with [*arachno*-6,9-(Et₂S)₂-B₁₀H₁₂] [217].

The phosphite, phosphinite, and thiophosphite derivatives of the *arachno*-decaborate anion [*arachno*-6,9-(R₂R'P)₂-B₁₀H₁₂] (R = R' = OMe, OEt, OPh; R = Ph, R' = OEt; R = OBu, R' = Ph; R = R' = SEt) were prepared by the direct reactions of decaborane(14) with the corresponding phosphorus compounds or via substitution of the Me₂S and MeCN groups in [*arachno*-6,9-(Me₂S)₂-B₁₀H₁₂] and [*arachno*-6,9-(MeC≡N)₂-B₁₀H₁₂], respectively [217,288–290].

The reaction of decaborane(14) with diphenylchlorophosphine in diethyl ether gives the 6,9-bis(chlorodiphenylphosphonium) derivative [*arachno*-6,9-(ClPh₂P)₂-B₁₀H₁₂], which, upon the treatment with dimethylamine in alcohols, lead to the corresponding phosphonites [6,9-(ROPh₂P)₂-B₁₀H₁₂] (R = Me, Et, CH₂CH₂OH) [290]. The reaction of [6,9-(ClPh₂P)₂-B₁₀H₁₂] with dimethylamine in aqueous solution water results in the bis(dimethylammonium) salt of the corresponding acid (Me₂NH₂)₂[6,9-(OPh₂P)₂-B₁₀H₁₂] [290]. The 6,9-bis-(hydroxy diphenylphosphonium) derivative [6,9-(HOPh₂P)₂-B₁₀H₁₂] was prepared by the reaction of [6,9-(ClPh₂P)₂-B₁₀H₁₂] with water in acetone [290].

The 6,9-bis(chlorodiphenylphosphonium) derivative reacts with ammonia, hydrazine, primary aliphatic amines, and ethylenimine in alcohols to form the corresponding 6,9-bis(aminodiphenylphosphonium) derivatives [6,9-(R'RNPh₂P)₂-B₁₀H₁₂] (R = H, R' = NH₂, Me, Bu; R = R' = CH₂CH₂) [290]. The reactions of decaborane(14) or [*arachno*-6,9-(R₂S)₂-B₁₀H₁₂] (R = Me, Et) with dimethylaminophosphines in refluxing benzene lead to the corresponding 6,9-bis(dimethylaminophosphonium) derivatives [6,9-(RR'(Me₂N)P)₂-B₁₀H₁₂] (R = R' = NMe₂; R = NMe₂, R' = Ph, Cl; R = R' = Ph; R = Ph, R' = Cl; RR' = OCH₂CH₂O) [217].

The reaction of [6,9-(ClPh₂P)₂-B₁₀H₁₂] with NaN₃ in ethanol results in the 6,9-bis-(azidodiphenylphosphonium) derivative [6,9-(N₃Ph₂P)₂-B₁₀H₁₂] [290], which, upon the treatment with triphenylphosphine in refluxing benzene, gives the 6,9-bis(triphenylphosphineiminodiphenyl phosphonium) derivative [6,9-(Ph₃P=NPh₂P)₂-B₁₀H₁₂] [291].

The bifunctional derivatives [6,9-(XPh₂P)₂-B₁₀H₁₂] (X = Cl, OH, N₃) were used for the synthesis of decaborane-based polymers [291,292]. The chemistry of decaborane-based polymers is considered in detail in the review [293]. The formation of decaborane-based

polymers along with a small amount of [6,9-(dppf)₂-B₁₀H₁₂] has also been reported in the reaction of decaborane(14) with 1,1'-bis(diphenylphosphino)ferrocene (dppf) [294].

The reaction of Na[B₁₀H₁₃] with tributylphosphine in acetonitrile in the presence of dry HCl leads to [*arachno*-6-Bu₃P-9-MeC≡N-B₁₀H₁₂] [221]. The reaction of Na[B₁₀H₁₃] with diphenylchlorophosphine in diethyl ether leads to the diphenylphosphine derivative [*nido*-μ-5,6-Ph₂P-B₁₀H₁₃] [295], whose structure was determined by single-crystal X-ray diffraction [296]. The same compound was reported to be formed in the reaction of the so-called “Grignard derivative” [B₁₀H₁₃MgI] formed by the treatment of decaborane(14) with MeMgI, with diphenylchlorophosphine in diethyl ether [297]. The diphenylphosphine derivative [*nido*-μ-5,6-Ph₂P-B₁₀H₁₃] is easily deprotonated with triethylamine or sodium hydroxide to form the corresponding salts [295,297]. The solid state structure of the triphenylmethylphosponium salt (Ph₃PMe)[*arachno*-μ-6,9-Ph₂P-B₁₀H₁₂] was determined by single-crystal X-ray diffraction (Figure 23) [298].

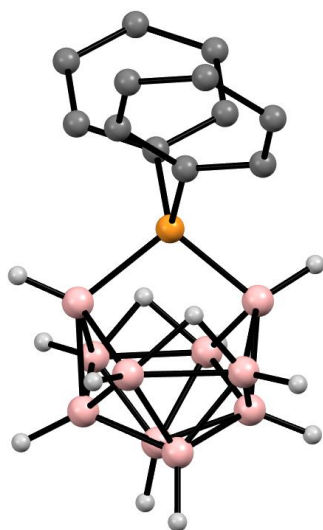


Figure 23. Solid state structure of the [*arachno*-μ-6,9-Ph₂P-B₁₀H₁₂][−] anion. Hydrogen atoms of organic substituents are omitted for clarity.

It should be noted that the reactions of [6,9-(MeC≡N)₂-B₁₀H₁₂] with low-coordinated phosphorus compounds, such as phosphalkynes RC≡P (R = *t*-Bu, Ad), do not lead to substitution of hydrogens but to the incorporation of phosphorus into the decaborane basket with the formation of 11-vertex phosphoboranes [*nido*-RC(H)=PB₁₀H₁₃] [299,300].

8. Derivatives with a B-As Bond

The 6,9-bis(trialkyl/arylarsonium) derivatives [6,9-(R₃As)₂-B₁₀H₁₂] (R = Et, Ph) were prepared by the reactions of decaborane(14) or [6,9-(MeC≡N)₂-B₁₀H₁₂] with the corresponding arsines in benzene or toluene [287]. The reaction of decaborane(14) with triethoxyarsine in benzene leads to [6,9-((EtO)₃As)₂-B₁₀H₁₂] [289].

9. Derivatives with a B-C Bond

Decaborane derivatives with a B-C bond are probably the most studied area of decaborane chemistry. Like the halogenation of decaborane, the direct alkylation reactions result in the substitution of hydrogen atoms at “the bottom” of the decaborane basket. The reaction of decaborane(14) with methyl bromide in carbon disulfide in the presence of AlCl₃ at 80 °C gives a mixture of the 2-methyl [2-Me-B₁₀H₁₃], 1,2- and 3,4-dimethyl [1,2-Me₂-B₁₀H₁₂] and [2,4-Me₂-B₁₀H₁₂], 1,2,3- and 1,2,4-trimethyl [1,2,3-Me₃-B₁₀H₁₁] and [1,2,4-Me₃-B₁₀H₁₁], 1,2,3,4- and 1,2,3,5(or 8)-tetramethyl [1,2,3,4-Me₄-B₁₀H₁₀], and [1,2,3,5(or 8)-Me₄-B₁₀H₁₀] derivatives, which were chromatographically separated [301]. The methylation of decaborane(14) was also studied using methyl chloride [302,303].

The reaction of decaborane(14) with neat methyl iodide in the presence of AlCl_3 at room temperature gives the 1,2,3,4-tetramethyl derivative $[1,2,3,4\text{-Me}_4\text{-B}_{10}\text{H}_{10}]$, whereas the reaction at 120°C leads to the octasubstituted product $[1\text{-I-}2,3,4,5,6,7,8\text{-Me}_7\text{-B}_{10}\text{H}_6]$. The similar octasubstituted derivative $[1\text{-TfO-}2,3,4,5,6,7,8\text{-Me}_7\text{-B}_{10}\text{H}_6]$ was obtained by the reaction of decaborane(14) with TfOMe in the presence of a catalytic amount of triflic acid at 120°C . The solid state structures of $[1\text{-I-}2,3,4,5,6,7,8\text{-Me}_7\text{-B}_{10}\text{H}_6]$ and $[1\text{-TfO-}2,3,4,5,6,7,8\text{-Me}_7\text{-B}_{10}\text{H}_6]$ were determined by single-crystal X-ray diffraction (Figure 24) [304]. The methyl derivatives prepared can be easily deprotonated with a Proton Sponge to give the corresponding salts [304].

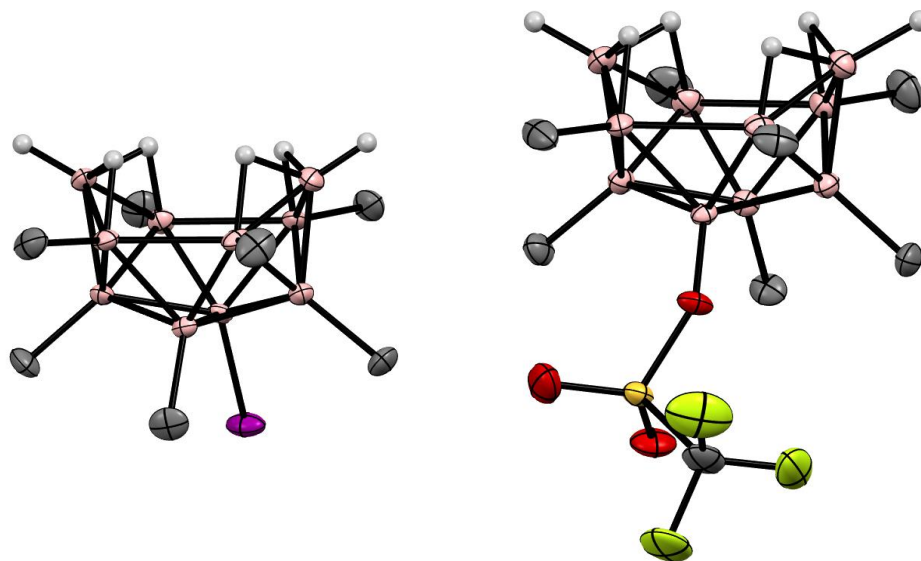


Figure 24. Solid state structures of $[1\text{-I-}2,3,4,5,6,7,8\text{-Me}_7\text{-B}_{10}\text{H}_6]$ (left) and $[1\text{-TfO-}2,3,4,5,6,7,8\text{-Me}_7\text{-B}_{10}\text{H}_6]$ (right). Hydrogen atoms of methyl groups are omitted for clarity.

The reaction of decaborane(14) with ethyl bromide in carbon disulfide in the presence of AlCl_3 under reflux gives a mixture of mono-, di-, and triethyl derivatives [305]. The monoethyl derivative of decaborane was prepared by the reaction of decaborane(14) with neat ethyl bromide in the presence of AlCl_3 [306]. The solid state structure of the 1-ethyl derivative of decaborane $[1\text{-Et-B}_{10}\text{H}_{13}]$ was determined by single-crystal X-ray diffraction [307].

The reaction of decaborane(14) with MeLi in benzene followed by treatment with HCl has been reported to give a mixture of the 6-methyl-, 6,5(or 8)- and 6,9-dimethyl derivatives of decaborane [308]. The reaction with EtLi in benzene gives the 6-ethyl derivative $[6\text{-Et-B}_{10}\text{H}_{13}]$ [308]. The reaction of decaborane(14) with MeMgI has been shown to proceed by two routes. The major reaction yields the so-called “Grignard derivative” $[\text{B}_{10}\text{H}_{13}\text{MgI}]$ and methane, and the minor reaction produces the 6-methyl derivative of decaborane. The reaction of the “Grignard derivative” with dimethyl sulfate produces a mixture of the 5- and 6-methyl derivatives of decaborane [309]. In a similar way, the reaction of decaborane(14) with EtMgI produces the “Grignard derivative” as the main product and the 6-ethyl derivative of decaborane as a by-product. The reaction of the “Grignard derivative” with $[\text{Et}_3\text{O}]\text{BF}_4$ or diethyl sulfate gives the 5-ethyl derivative of decaborane $[5\text{-Et-B}_{10}\text{H}_{13}]$ [309]. A series of alkyl derivatives $[\text{R-B}_{10}\text{H}_{13}]$ (R = butyl, amyl, hexyl, cyclohexyl, heptyl, octyl) was prepared by the reactions of the “Grignard derivative” with the corresponding alkyl fluorides [310]. The 6-benzyl derivative of decaborane $[6\text{-Bn-B}_{10}\text{H}_{13}]$ can be prepared by the reaction of the “Grignard derivative” with benzyl chloride or $\text{Na}[\text{B}_{10}\text{H}_{13}]$ with benzyl bromide [309,311,312].

Later, these reactions were re-examined, and it was shown that the first stage of the reaction of decaborane(14) with the alkyllithium reagents RLi is deprotonation of

decaborane with the formation of $\text{Li}[\text{B}_{10}\text{H}_{13}]$. The reaction with the second equivalent of RLi produces $\text{Li}_2[\text{arachno-6-R-B}_{10}\text{H}_{13}]$, which, when treated with HCl , gives $\text{Li}[\text{arachno-6-R-B}_{10}\text{H}_{14}]$ and then $[\text{nido-6-R-B}_{10}\text{H}_{13}]$ ($\text{R} = \text{Me}$, $n\text{-Bu}$, $t\text{-Bu}$). The use of pre-prepared salts of the $[\text{B}_{10}\text{H}_{13}]^-$ anion makes it possible to reduce the formation of by-products [237,313].

Another approach to the 6-alkyl derivatives of decaborane includes the reactions of $[\text{arachno-6,9-(Me}_2\text{S)}_2\text{-B}_{10}\text{H}_{12}]$ with alkenes in dichloromethane, resulting in $[\text{nido-6-R-8-Me}_2\text{S-B}_{10}\text{H}_{11}]$ ($\text{R} = \text{cyclohexyl}$, cyclohexenyl , hexyl , octyl , $2,3\text{-dimethyl-1-butyl}$, $2,3\text{-dimethyl-2-butyl}$, 2-methyl-2-butyl , $(1R)\text{-}(+)\text{-}\alpha\text{-pinene}$, and $(1S)\text{-}(-)\text{-}\beta\text{-pinene}$), which can be reduced using Superhydride $\text{Li}[\text{Et}_3\text{BH}]$ in THF to $[\text{6-R-B}_{10}\text{H}_{12}]^-$ and then protonated with $\text{HCl}/\text{Et}_2\text{O}$ to $[\text{6-R-B}_{10}\text{H}_{13}]$ [222,237,313–315]. From the point of view of organic chemistry, these reactions can be considered as the hydroboration reactions. The solid state structures of $[\text{6-Chx-8-Me}_2\text{S-B}_{10}\text{H}_{11}]$ [316], $[\text{6-Thx-8-Me}_2\text{S-B}_{10}\text{H}_{11}]$ [237] (Figure 25), and $[\text{6-Thx-B}_{10}\text{H}_{13}]$ [237] (Figure 26) were determined by single-crystal X-ray diffraction.

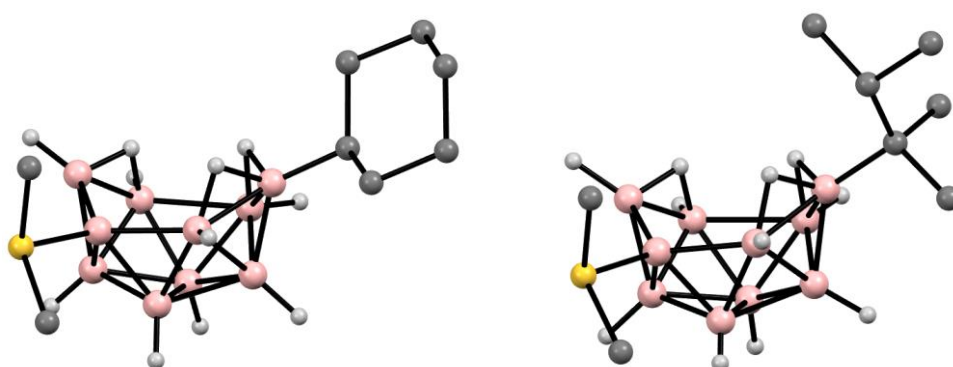


Figure 25. Solid state structures of $[\text{6-Chx-8-Me}_2\text{S-B}_{10}\text{H}_{11}]$ (left) and $[\text{6-Thx-8-Me}_2\text{S-B}_{10}\text{H}_{11}]$ (right). Hydrogen atoms of organic substituents are omitted for clarity.

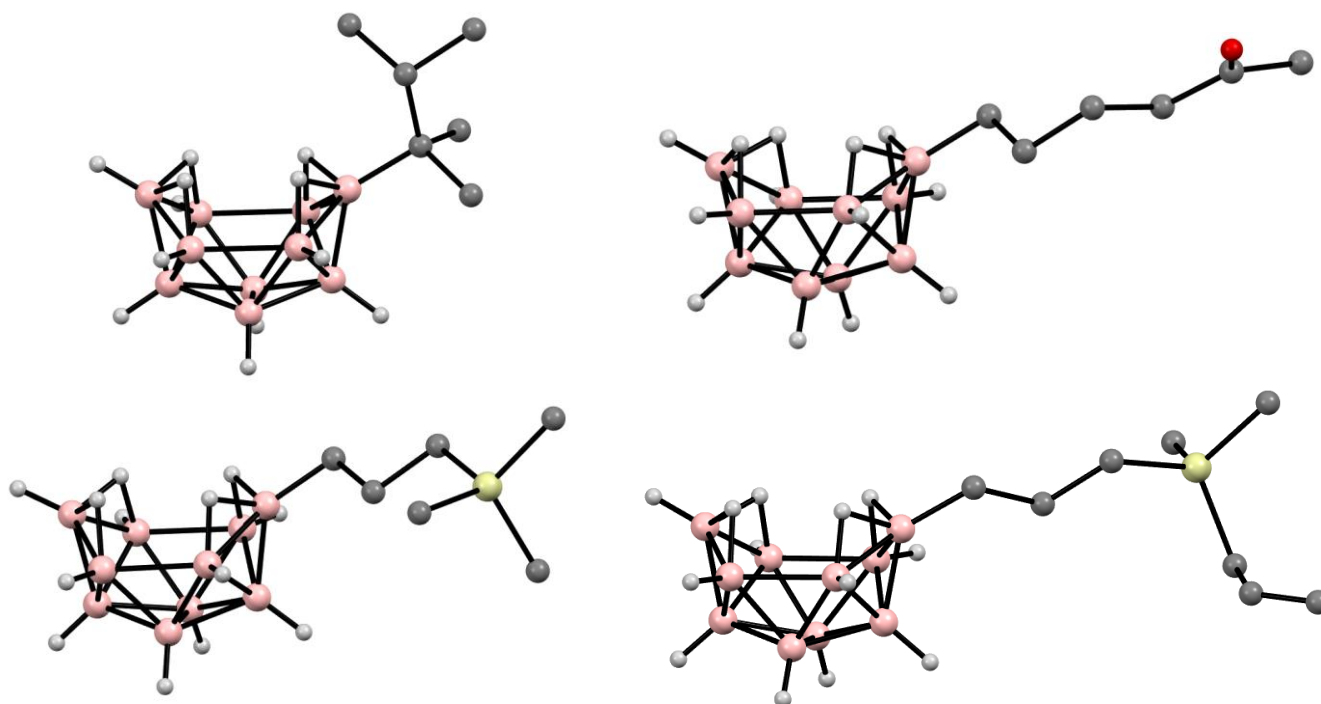


Figure 26. Solid state structures of $[\text{6-Thx-B}_{10}\text{H}_{13}]$ (top left), $[\text{6-MeC(O)CH}_2\text{CH}_2\text{CH}_2\text{CH}_2\text{-B}_{10}\text{H}_{13}]$ (top right), $[\text{6-Me}_3\text{SiCH}_2\text{CH}_2\text{CH}_2\text{-B}_{10}\text{H}_{13}]$ (bottom left), and $[\text{6-H}_2\text{C=CHCH}_2\text{SiMe}_2\text{CH}_2\text{CH}_2\text{CH}_2\text{-B}_{10}\text{H}_{13}]$ (bottom right). Hydrogen atoms of organic substituents are omitted for clarity.

Another convenient method for the synthesis of 6-alkyl derivatives of decaborane is based on the use of ionic liquids as a solvent. The reactions of decaborane(14) with terminal alkenes in biphasic ionic-liquid/toluene mixtures lead to the corresponding 6-alkyl derivatives [6-R-B₁₀H₁₃] (R = C₆H₁₃, C₈H₁₇, C₁₆H₃₃, CH(*i*-Pr)CH₂CHMe₂, (CH₂)₂C₆H₅, (CH₂)₃C₆H₅, (CH₂)₆Br, (CH₂)₄CH=CH₂, (CH₂)₆CH=CH₂, (CH₂)₃OC₃H₇, (CH₂)₃SiMe₃, (CH₂)₄COMe, (CH₂)₆OAc, (CH₂)₃OBn, (CH₂)₃OH, and (CH₂)₃Bpin, norbornenyl) [317–320]. The best results were observed for reactions with [bmim]X (1-butyl-3-methylimidazolium, X = Cl[−] or BF₄[−]) and bmpyX (1-butyl-4-methylpyridinium, X = Cl[−] or BF₄[−]). The reaction mechanism includes the ionic-liquid-promoted formation of the [B₁₀H₁₃][−] anion, its addition to the alkene to form the [6-R-B₁₀H₁₂][−] anion, and, finally, the protonation of the last one to form the final product [6-R-B₁₀H₁₃] [314]. The solid state structures of [6-Me₃Si(CH₂)₃-B₁₀H₁₃] and [6-MeC(O)(CH₂)₄-B₁₀H₁₃] were determined by single-crystal X-ray diffraction (Figure 26) [318]. The 6-cyclohexyl derivative of decaborane [*nido*-6-C₆H₁₁-B₁₀H₁₃] was obtained in a low yield from the reaction of Cs₂[*closo*-B₁₀H₁₀] with triflic acid in cyclohexane (Figure 27) [202,203]. In a similar way, the 6-hexyl derivative [*nido*-6-C₆H₁₃-B₁₀H₁₃] was isolated from the reaction of (NH₄)₂[*closo*-B₁₀H₁₀] with concentrated nitric acid in hexane [321].

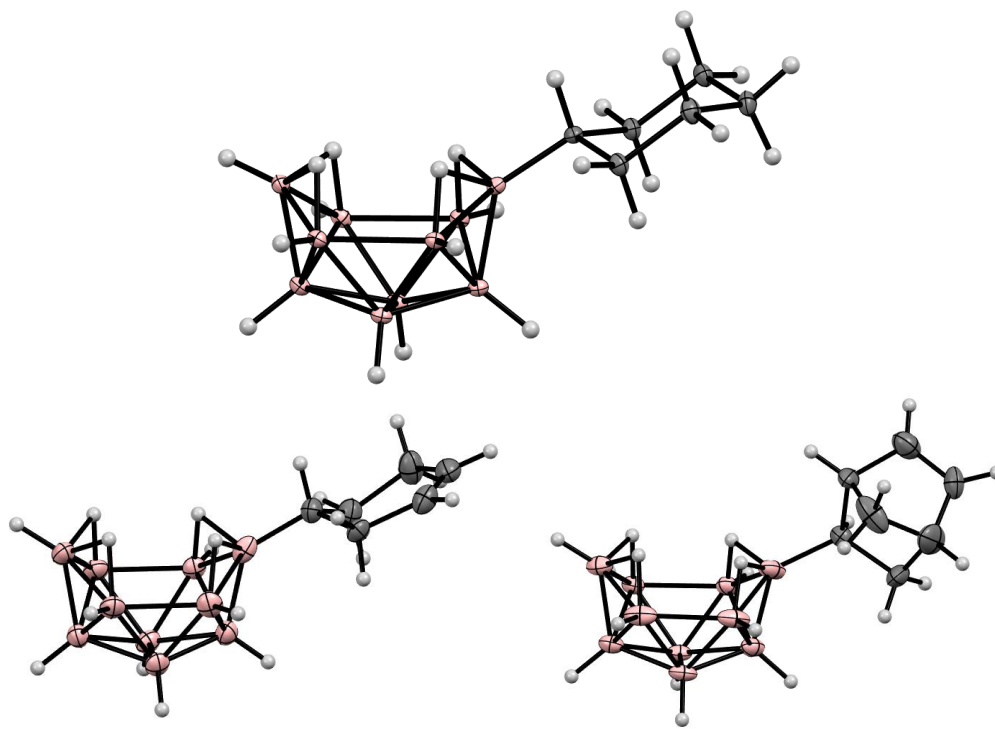


Figure 27. Solid state structures of [*nido*-6-C₆H₁₁-B₁₀H₁₃] (**top**), [6-(4'-cyclohexenyl)-B₁₀H₁₃] (**bottom left**) and [6-(5'-norbornenyl)-B₁₀H₁₃] (**bottom right**).

The Cp₂Ti(CO)₂-catalyzed reactions of decaborane(14) with terminal alkenes have been found to result in the high-yield formation of 6-alkyl derivatives of decaborane [6-R-B₁₀H₁₃] (R = C₆H₁₃, C₈H₁₇, (CH₂)₃SiMe₃) [322,323]. The reactions of decaborane(14) with equimolar amounts of bifunctional alkenes such as diallyldimethylsilane, 1,5-hexadiene, 1,4-cyclohexadiene, 1,5-cyclooctadiene, and 2,5-norbornadiene produce the corresponding decaborane derivatives with a double bond in the substituent [6-R-B₁₀H₁₃] (R = (CH₂)₃SiMe₂CH₂CH=CH₂, (CH₂)₄CH=CH₂, 4-cyclohexenyl, 5-cyclooctenyl, 5-norbornenyl) [322–325]. The solid state structures of [6-H₂C=CHCH₂SiMe₂(CH₂)₃-B₁₀H₁₃] (Figure 26) [322], [6-(4'-cyclohexenyl)-B₁₀H₁₃] (Figure 27) [325], and [6-(5'-norbornenyl)-B₁₀H₁₃] (Figure 27) [324] were determined by single-crystal X-ray diffraction.

The reactions of multifunctional alkenes with an excess amount of decaborane(14) produce the saturated linked-cage compounds with two ([μ-6,6'-Me₂Si-(6-(CH₂)₃-B₁₀H₁₃)₂], [μ-6,6'-(CH₂)₆-(B₁₀H₁₃)₂], [μ-6,6'-(1'',5''-cyclooctyl)-(B₁₀H₁₃)₂], and [μ-6,6'-(2'',5''-norbornyl)-

($\text{B}_{10}\text{H}_{13}$)₂) or four ($[\mu^4\text{-}6,6',6'',6'''\text{-Si-(6-(CH}_2)_3\text{-B}_{10}\text{H}_{13})_4]$) decaborane units [322,323,325]. The solid state structures of $[\mu\text{-}6,6'\text{-(CH}_2)_6\text{-(B}_{10}\text{H}_{13})_2]$, $[\mu\text{-}6,6'\text{-(2'',5''-norbornyl)-(B}_{10}\text{H}_{13})_2]$, and $[\mu^4\text{-}6,6',6'',6'''\text{-Si-(6-(CH}_2)_3\text{-B}_{10}\text{H}_{13})_4]$ were determined by single-crystal X-ray diffraction (Figure 28) [322,323,325].

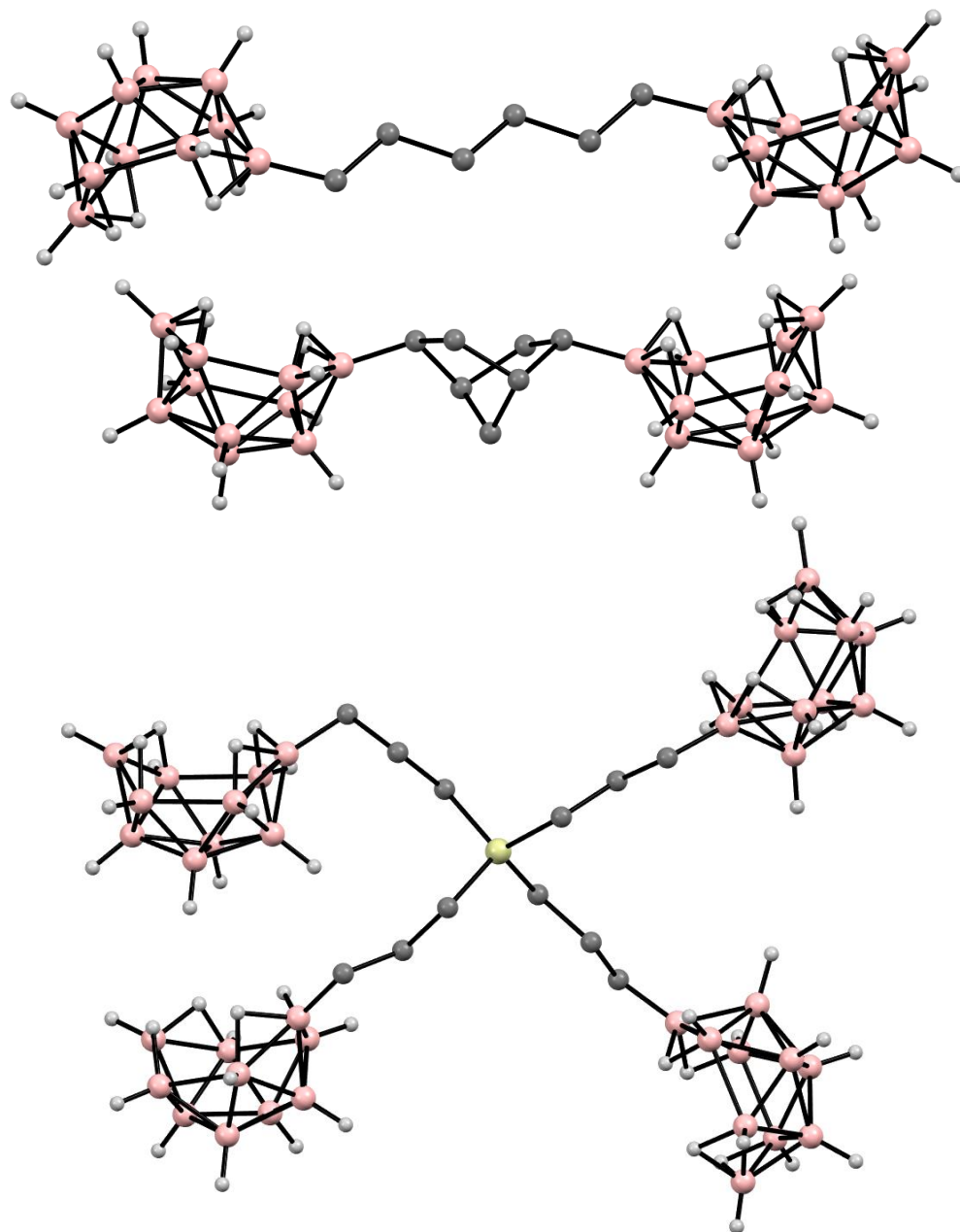


Figure 28. Solid state structures of $[\mu\text{-}6,6'\text{-(CH}_2)_6\text{-(B}_{10}\text{H}_{13})_2]$ (**top**), $[\mu\text{-}6,6'\text{-(2'',5''-norbornyl)-(B}_{10}\text{H}_{13})_2]$ (**middle**), and $[\mu^4\text{-}6,6',6'',6'''\text{-Si-(6-(CH}_2)_3\text{-B}_{10}\text{H}_{13})_4]$ (**bottom**). Hydrogen atoms of organic substituents are omitted for clarity.

The derivatives with the two decaborane units $[\mu\text{-}6,6'\text{-(1'',5''-cyclooctyl)-(B}_{10}\text{H}_{13})_2]$ and $[\mu\text{-}6,6'\text{-(2'',5''-norbornyl)-(B}_{10}\text{H}_{13})_2]$ can also be prepared by the titanium-catalyzed reactions of decaborane(14) with $[6\text{-(5'-cyclooctenyl)-B}_{10}\text{H}_{13}]$ and $[6\text{-(5'-norbornenyl)-B}_{10}\text{H}_{13}]$, respectively [325].

The 6-alkyl derivatives of decaborane with substituents containing double bonds in the side chain (hexenyl, norbornenyl, etc.) are used for the synthesis of decaborane-based polymers and boron-containing ceramics [319,324–332].

The reactions of decaborane(14) with terminal alkenes in the presence of catalytic amounts of PtBr_2 or H_2PtCl_6 lead to the 6,9-dialkyl derivatives *nido*-[6,9- $\text{R}_2\text{-B}_{10}\text{H}_{12}$] ($\text{R} = \text{C}_2\text{H}_5, \text{C}_3\text{H}_7, \text{C}_4\text{H}_9, \text{C}_5\text{H}_{11}$) [333]. The reactions of [5-TfO- $\text{B}_{10}\text{H}_{13}$] and [5-I- $\text{B}_{10}\text{H}_{13}$] with 1-pentene in the presence of a catalytic amount of PtBr_2 at 55 °C lead to the corresponding 6,9-dialkyl derivatives [6,9-(C_5H_{11}) $_2$ -5-TfO- $\text{B}_{10}\text{H}_{11}$] and [6,9-(C_5H_{11}) $_2$ -5-I- $\text{B}_{10}\text{H}_{11}$] [204]. The solid state structure of [6,9-(C_5H_{11}) $_2$ -5-I- $\text{B}_{10}\text{H}_{11}$] was determined by single-crystal X-ray diffraction (Figure 29) [204].

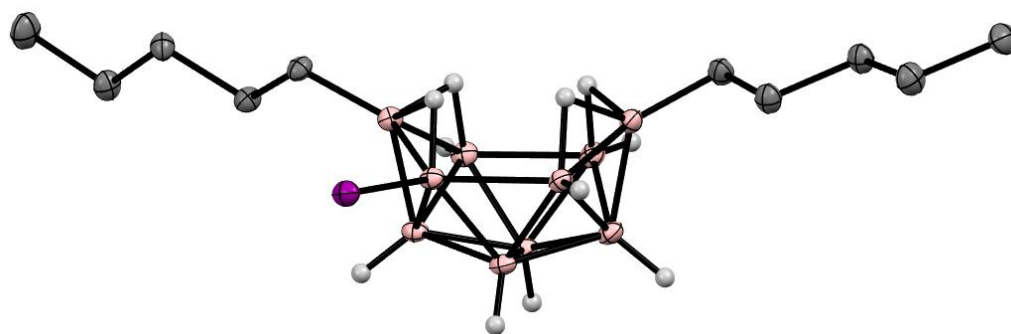


Figure 29. Solid state structure of [6,9-(C_5H_{11}) $_2$ -5-I- $\text{B}_{10}\text{H}_{11}$]. Hydrogen atoms of organic substituents are omitted for clarity.

The reactions of decaborane(14) with terminal alkynes in toluene in the presence of $[\text{Cp}^*\text{IrCl}_2]_2$ or $[(p\text{-cymene})\text{RuCl}_2]_2$ as catalysts lead to the corresponding 6,9-di(β -alkenyl) derivatives of decaborane [6,9-((*E*)- $\text{RCH}=\text{CH}$) $_2$ - $\text{B}_{10}\text{H}_{12}$] ($\text{R} = \text{H}, \text{C}_6\text{H}_{13}, \text{C}_6\text{H}_5, (\text{CH}_2)_2\text{Br}, (\text{CH}_2)_3\text{Cl}, \text{SiMe}_3$) [334,335]. The solid state structures of [6,9-((*E*)- $\text{Br}(\text{CH}_2)_2\text{CH}=\text{CH}$) $_2$ - $\text{B}_{10}\text{H}_{12}$] and [6,9-((*E*)- $\text{Me}_3\text{SiCH}=\text{CH}$) $_2$ - $\text{B}_{10}\text{H}_{12}$] were determined by single-crystal X-ray diffraction (Figure 30) [334,335].

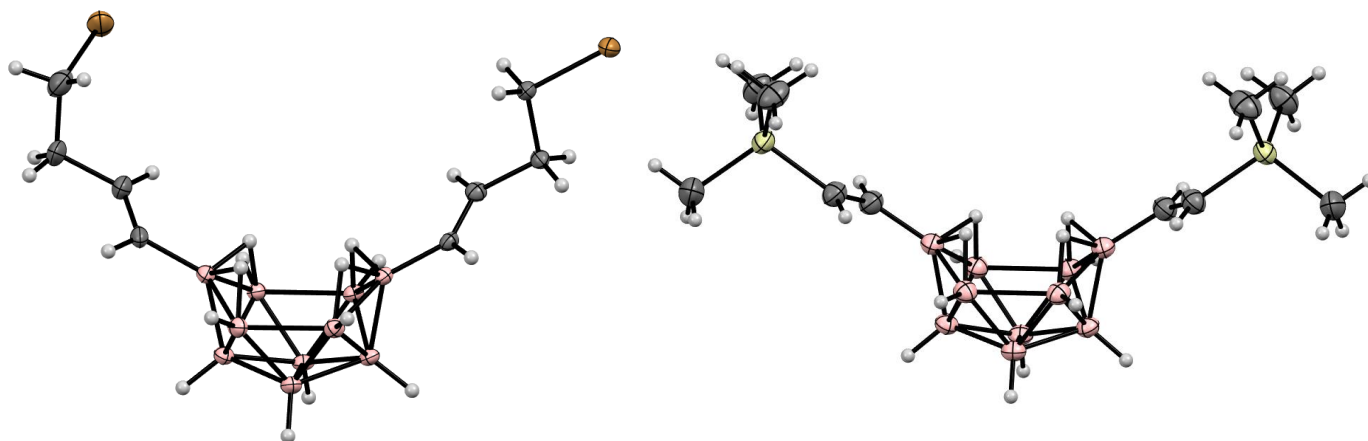


Figure 30. Solid state structures of [6,9-((*E*)- $\text{Br}(\text{CH}_2)_2\text{CH}=\text{CH}$) $_2$ - $\text{B}_{10}\text{H}_{12}$] (left) and [6,9-((*E*)- $\text{Me}_3\text{SiCH}=\text{CH}$) $_2$ - $\text{B}_{10}\text{H}_{12}$] (right).

In contrast to $[(p\text{-cymene})\text{RuCl}_2]_2$, the reactions of decaborane(14) with terminal alkynes in the presence of $[(p\text{-cymene})\text{RuI}_2]_2$ result in the 6,9-di(α -alkenyl) derivatives [6,9-($\text{R}(\text{H}_2\text{C}=\text{C})_2$ - $\text{B}_{10}\text{H}_{12}$] ($\text{R} = \text{C}_6\text{H}_{13}, \text{CH}_2\text{-}i\text{-C}_6\text{H}_{11}, (\text{CH}_2)_2\text{Br}, (\text{CH}_2)_3\text{Cl}$) [334,335]. The solid state structure of [6,9-(*c*- $\text{C}_6\text{H}_{11}\text{CH}_2(\text{H}_2\text{C}=\text{C})_2$ - $\text{B}_{10}\text{H}_{12}$] was determined by single-crystal X-ray diffraction (Figure 31) [334,335].

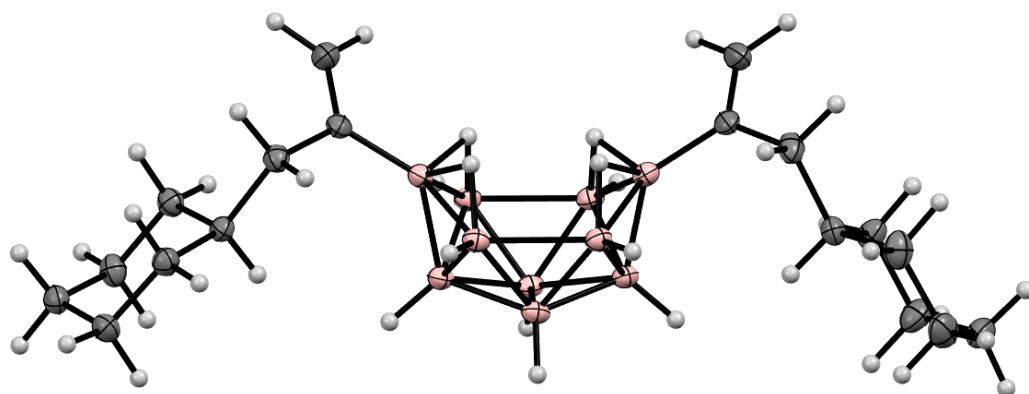


Figure 31. Solid state structure of [6,9-(*c*-C₆H₁₁CH₂(H₂C=C)₂)-B₁₀H₁₂]. Hydrogen atoms of organic substituents are omitted for clarity.

In a similar way, the reactions of 6-alkyldecaboranes [6-R-B₁₀H₁₃] with terminal alkynes in the presence of [Cp*IrCl₂]₂ give asymmetrically substituted 6-alkyl-9-alkenyl-derivatives [6-R-9-((*E*)-R'CH=CH)₂-B₁₀H₁₂] (R = (CH₂)₃SiMe₃, R' = H, C₆H₅, C₆H₄-*m*-CH≡CH; CH₂CH=CH₂; R = C₅H₁₁, R' = H). The solid state structure of [6-Me₃Si(CH₂)₃-9-(*E*)-*m*-HC≡CC₆H₄CH=CH-B₁₀H₁₂] was determined by single-crystal X-ray diffraction (Figure 32) [334,335].

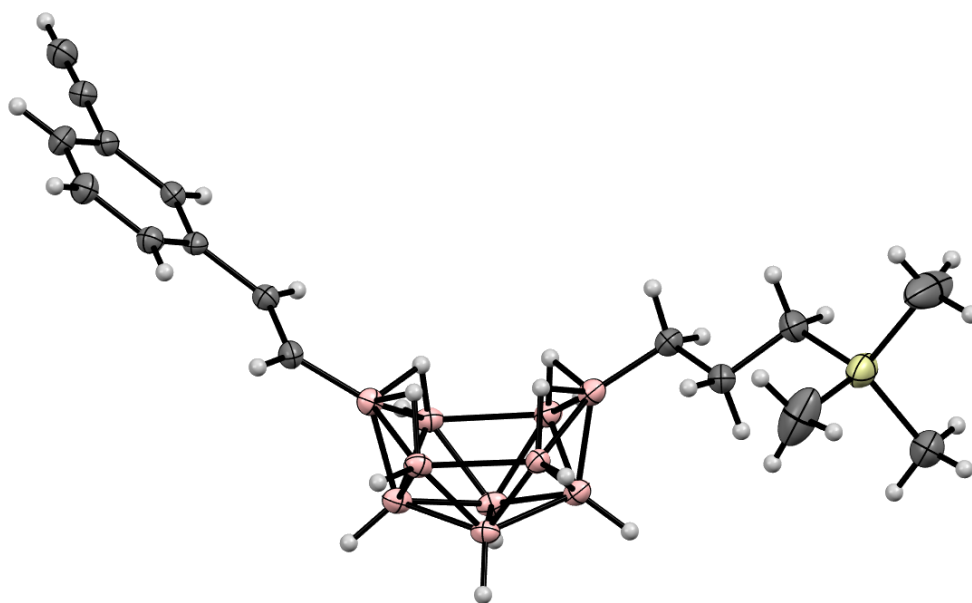


Figure 32. Solid state structure of [6-Me₃Si(CH₂)₃-9-(*E*)-*m*-HC≡CC₆H₄CH=CH-B₁₀H₁₂].

While [Cp*IrCl₂]₂ proved to be inactive for inducing the hydroboration of simple olefins, such as 1-pentene, by either decaborane or the 6-alkyl-decaboranes, it was found to catalyze the hydroboration of 6-alkyl-9-vinyldecaboranes [6-R-9-CH₂=CH-B₁₀H₁₂] (R = C₅H₁₁, (CH₂)₃SiMe₃) by 6-alkyl-decaboranes [6-R-B₁₀H₁₃] (R = C₅H₁₁, (CH₂)₃SiMe₃) to yield linked-cage products [9,9'-μ-CH₂CH₂-(6-R-B₁₀H₁₂)₂] (R = C₅H₁₁, (CH₂)₃SiMe₃) (Figure 33) [335].

The vinyl derivative [6-Me₃Si(CH₂)₃-9-CH₂=CH)₂-B₁₀H₁₂] was found to readily undergo both homo- and cross-metathesis reactions in the presence of Grubbs' II catalyst, giving the corresponding products [9,9'-μ-CH=CH-(6-Me₃Si(CH₂)₃-B₁₀H₁₂)₂] (Figure 34) and [6-Me₃Si(CH₂)₃-9-RCH=CH-B₁₀H₁₂] (R = C₃H₇, (CH₂)₄Br, CH₂SiMe₃) [335].

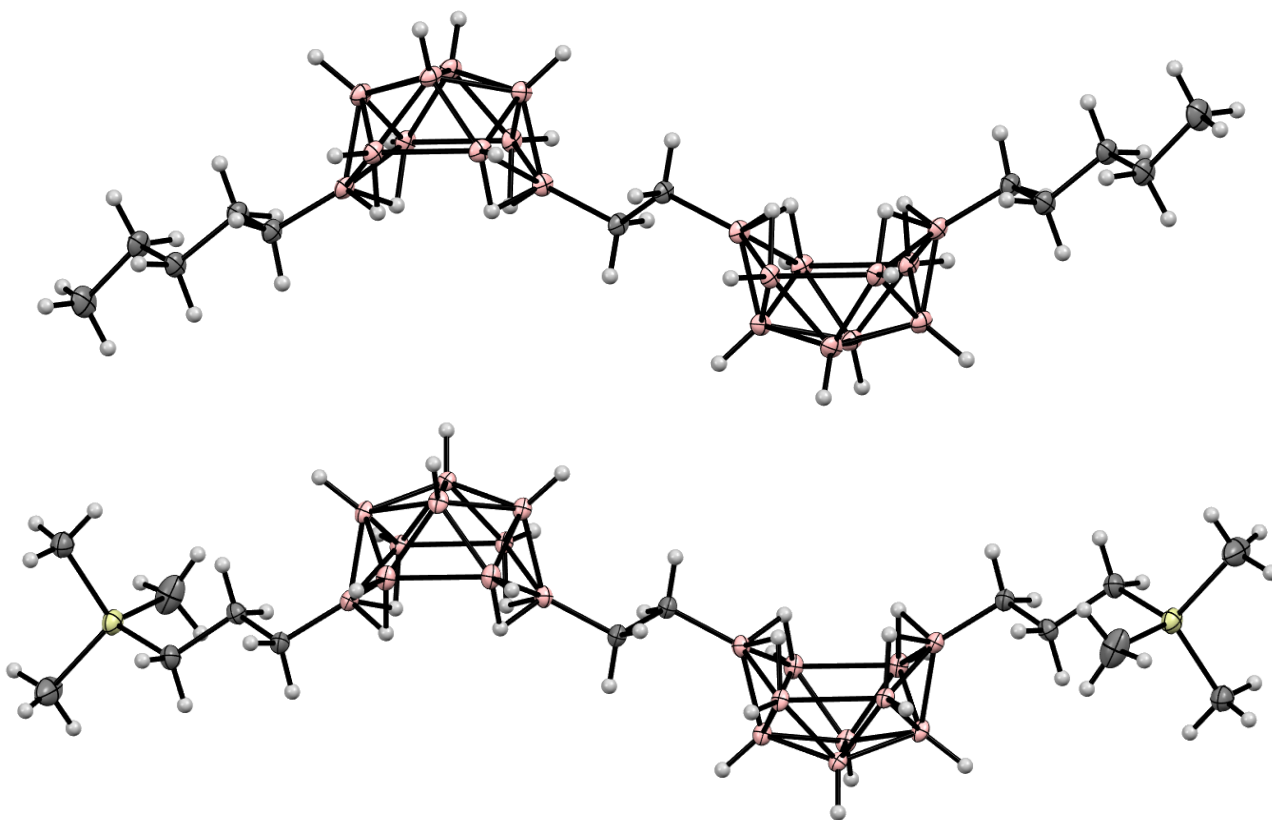


Figure 33. Solid state structures of $[9,9'\text{-}\mu\text{-CH}_2\text{CH}_2\text{-(6-C}_5\text{H}_{11}\text{-B}_{10}\text{H}_{12})_2]$ (**top**) and $[9,9'\text{-}\mu\text{-CH}_2\text{CH}_2\text{-(6-Me}_3\text{Si(CH}_2)_3\text{-B}_{10}\text{H}_{12})_2]$ (**bottom**).

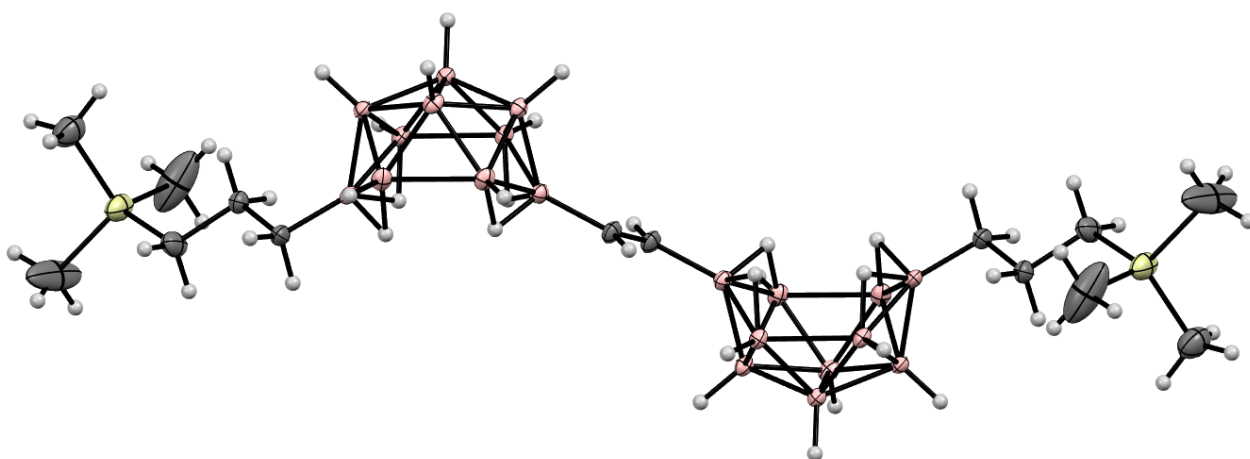


Figure 34. Solid state structure of $[9,9'\text{-}\mu\text{-CH=CH-(6-Me}_3\text{Si(CH}_2)_3\text{-B}_{10}\text{H}_{12})_2]$.

Heating $[\text{arachno-6,9-(Me}_2\text{S)}_2\text{-B}_{10}\text{H}_{12}]$ with silylated acetylenes $\text{Me}_3\text{SiC}\equiv\text{CR}$ ($\text{R} = \text{Me, Bu, SiMe}_3$) leads to the corresponding trimethylsilyl alkenyl derivatives $[\text{nido-6-Me}_3\text{Si(R)C=CH-5-Me}_2\text{S-B}_{10}\text{H}_{11}]$ [336,337]. The solid state structures of $[\text{6-Me}_3\text{Si(Me)C=CH-5-Me}_2\text{S-B}_{10}\text{H}_{11}]$ [336], $[\text{6-Me}_3\text{Si(Bu)C=CH-5-Me}_2\text{S-B}_{10}\text{H}_{11}]$ [337], and $[\text{6-(Me}_3\text{Si)}_2\text{C=CH-5-Me}_2\text{S-B}_{10}\text{H}_{11}]$ [337] were determined by single-crystal X-ray diffraction (Figure 35).

The reaction of $[\text{6,9-(Me}_2\text{S)}_2\text{-B}_{10}\text{H}_{12}]$ with the phosphalkyne $t\text{-BuC}\equiv\text{P}$ in refluxing benzene leads to $[\mu\text{-6(C),6'(C),5'(P)-C(t-Bu)PH-(nido-8-Me}_2\text{S-B}_{10}\text{H}_{11})(nido\text{-B}_{10}\text{H}_{12})]$, in which two decaborane units are linked by the C(t-Bu)PH -bridge (Figure 36) [338].

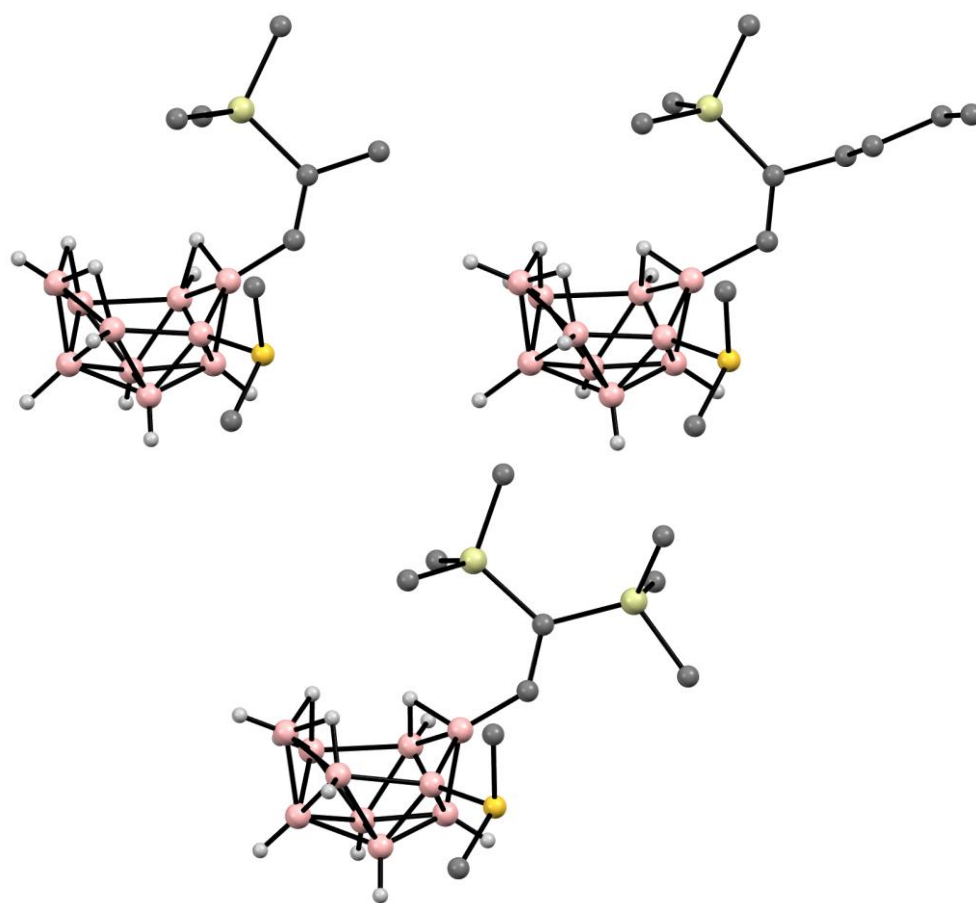


Figure 35. Solid state structures of [6-Me₃Si(Me)C=CH-5-Me₂S-B₁₀H₁₁] (**top left**), [6-Me₃Si(Bu)C=CH-5-Me₂S-B₁₀H₁₁] (**top right**), and [6-(Me₃Si)₂C=CH-5-Me₂S-B₁₀H₁₁] (**bottom**). Hydrogen atoms of organic substituents are omitted for clarity.

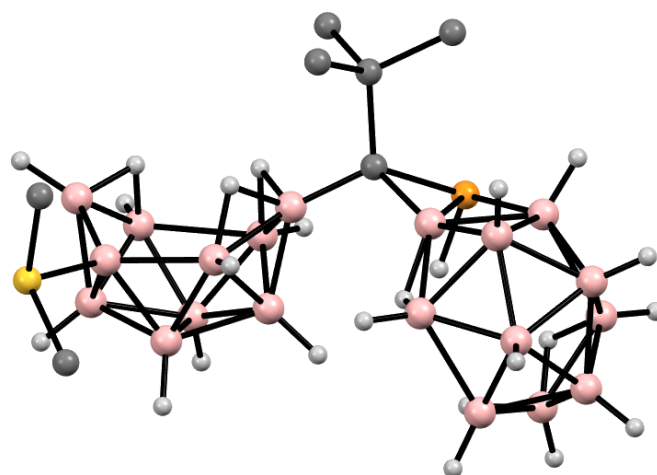


Figure 36. Solid state structure of [μ -6(C),6'(C),5'(P)-C(*t*-Bu)PH-(*nido*-8-Me₂S-B₁₀H₁₁)(*nido*-B₁₀H₁₂)]]. Hydrogen atoms of organic substituents are omitted for clarity.

The derivatives [μ -(*exo*-6(C),*endo*-6(N)-CH=CH-*o*-C₅H₄N)-9(N)-HC≡C-*o*-C₅H₄N-*arachno*-B₁₀H₁₁] (Figure 34) [265] and [μ -(*exo*-6(C),*endo*-6(N)-(closo-1',2'-C₂B₁₀H₁₀-2'-)-*o*-C₅H₄N)- μ -(*exo*-8(C),*exo*-9(N)-CH₂CH₂-*o*-C₅H₄N)-*arachno*-B₁₀H₁₀] (Figure 37) [339] were isolated in minor amounts as products of the intramolecular hydroboration of [*arachno*-6,9-(HC≡C-*o*-C₅H₄N)₂-B₁₀H₁₂] during its thermolysis in 1,2-dichloroethane. In the latter compound, the formation of the *ortho*-carborane fragment occurs as a result

of the reaction of the acetylene group of the substituent with the second molecule of the decaborane derivative.

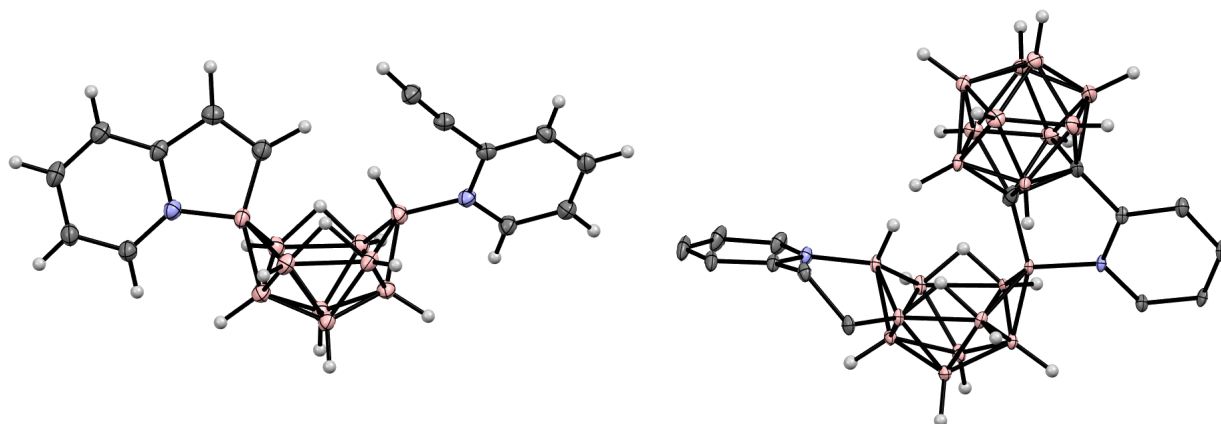


Figure 37. Solid state structures of $[\mu-(exo-6(C),endo-6(N)-CH=CH-o-C_5H_4N)-9(N)-HC\equiv C-o-C_5H_4N-arachno-B_{10}H_{11}]$ (left) and $[\mu-(exo-6(C),endo-6(N)-(closo-1',2'-C_2B_{10}H_{10}-2')-o-C_5H_4N)-\mu-(exo-8(C),exo-9(N)-CH_2CH_2-o-C_5H_4N)-arachno-B_{10}H_{10}]$ (right). Hydrogen atoms of organic substituents in the left structure are omitted for clarity.

The reactions of $Cs_2[closo-B_{10}H_{10}]$ with triflic acid or $(NH_4)_2[closo-B_{10}H_{10}]$ with sulfuric acid in the presence of aromatic hydrocarbons produce the corresponding 6-aryl derivatives of decaborane [*nido*-6-Ar- $B_{10}H_{13}$] (Ar = Ph, C_6H_4-4-Me , $C_6H_3-3,5-Me_2$, $C_6H_2-2,4,6-Me_3$, $C_6H_2-2,4,6-iPr_3$, C_6H_4Cl , $C_6H_4CF_3$) [202,203,321,340]. The solid state structures of [6-Ph- $B_{10}H_{13}$], [6-*p*-Tol- $B_{10}H_{13}$], and [6-(2',4',6'-*i*Pr₃- C_6H_2 - $B_{10}H_{13}$)] were determined by single-crystal X-ray diffraction (Figure 38) [202,203,340].

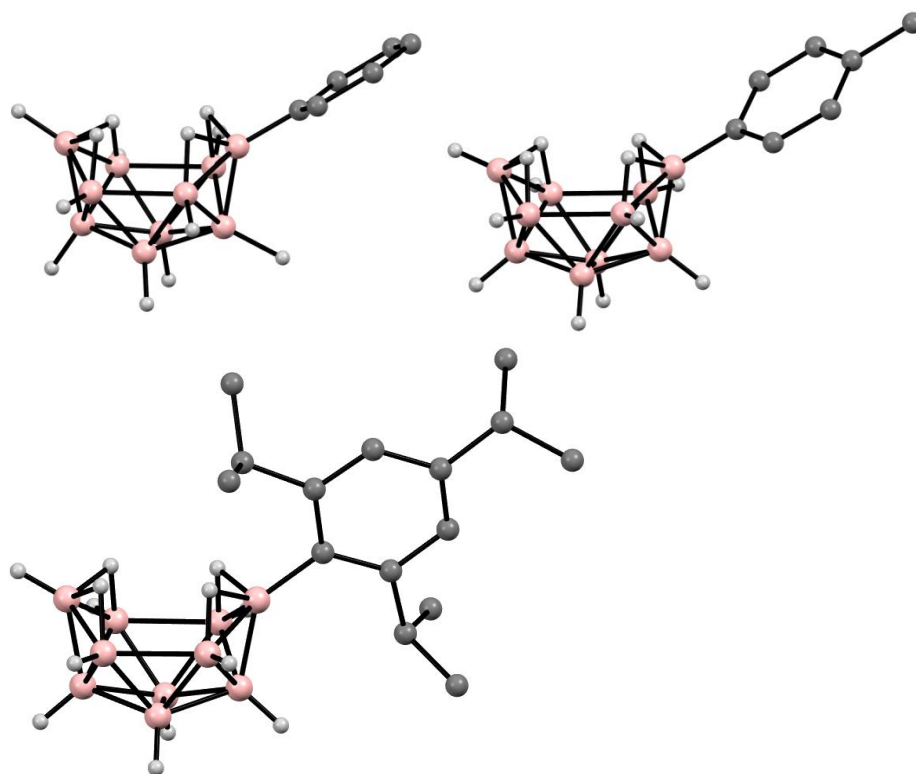


Figure 38. Solid state structures of [6-Ph- $B_{10}H_{13}$] (top left), [6-*p*-Tol- $B_{10}H_{13}$] (top right), and [6-(2',4',6'-*i*Pr₃- C_6H_2 - $B_{10}H_{13}$)] (bottom). Hydrogen atoms of organic substituents are omitted for clarity.

The 6-phenyl derivative [6-Ph-B₁₀H₁₃] was also obtained by the reaction of decaborane(14) with PhLi, followed by the treatment with HCl in Et₂O [237] as well as by the solid state pyrolysis of [nido-Ph₂SnB₁₀H₁₂] at 95 °C [198].

The pyrolysis of decaborane(14) in benzene at 200 °C gives the 5-phenyl derivative [5-Ph-B₁₀H₁₃] as the main product together with some amounts of the 6-isomer and 5,8-diphenyl derivative [5,8-Ph₂-B₁₀H₁₂] [341]. The solid state structures of [5-Ph-B₁₀H₁₃] and [5,8-Ph₂-B₁₀H₁₂] were determined by single-crystal X-ray diffraction (Figure 39) [341].

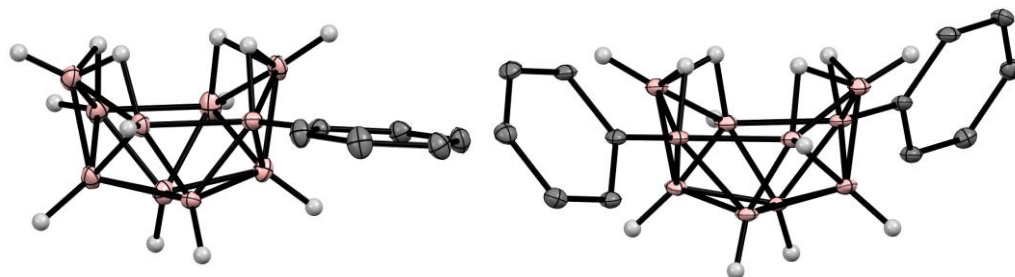


Figure 39. Solid state structures of [5-Ph-B₁₀H₁₃] (**left**) and [5,8-Ph₂-B₁₀H₁₂] (**right**). Hydrogen atoms of organic substituents are omitted for clarity.

The pyrolysis of decaborane(14) in toluene at 250 °C affords the novel microporous polymer named “activated borane”, in which the decaborane clusters are interconnected by toluene moieties. Activated borane displays a high surface area of 774 m² g^{−1}, a thermal stability up to 1000 °C (under Ar), and a sorption capacity to emerging pollutants exceeding the capacity of commercial activated carbon [342].

Heating (HPS)[B₁₀H₁₃] in acetonitrile under reflux results in the formation of the bridged imino derivative (HPS)[*arachno*-μ-6(C),9(*N*)-MeC=NH-B₁₀H₁₂] (Figure 40) [343].

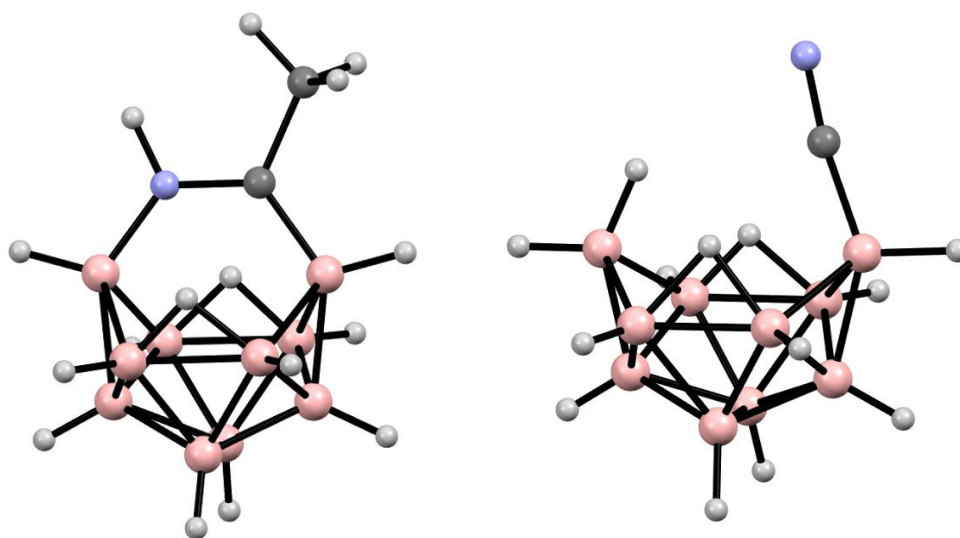


Figure 40. Solid state structures of the [*arachno*-μ-6(C),9(*N*)-MeC=NH-B₁₀H₁₂][−] (**left**) and [*arachno*-endo-6-N≡C-B₁₀H₁₂]^{2−} (**right**) anions.

The reaction of decaborane(14) with sodium cyanide in water followed by the addition of CsCl gives Cs₂[*arachno*-endo-6-N≡C-B₁₀H₁₃] [215]. The solid state structure of the trimethylphenylammonium salt (Me₃NPh)₂[endo-6-N≡C-B₁₀H₁₃] (Figure 40) [344] and lead complex {(Bipy)₂Pb[endo-6-N≡C-B₁₀H₁₃]} [345] were determined by single-crystal X-ray diffraction.

The reactions of decaborane(14) with sodium cyanide and dimethylsulfide or tetrahydrothiophene lead to the corresponding Na[*arachno*-6-N≡C-9-RR'S-B₁₀H₁₂] (R = R' = Me,

$RR' = (CH_2)_4$). $Na[6-N\equiv C-9-Me_2S-B_{10}H_{12}]$ can also be prepared by the reaction of $[6,9-(Me_2S)_2-B_{10}H_{12}]$ with sodium cyanide in dimethylsulfide [215].

10. Derivatives with an *exo*-Polyhedral B-B Bond

Decaborane derivatives with an *exo*-polyhedral B-B bond are rare, since the reaction of decaborane(14) with boron hydrides usually leads to the completion of the polyhedral backbone with the formation of tetradecahydro-*nido*-undecaborate $[B_{11}H_{14}]^-$ [346] and dodecahydro-*closo*-dodecaborate $[B_{12}H_{12}]^{2-}$ [3] anions and their derivatives.

The reactions of decaborane(14) with sterically hindered (alkyl/arylimino)(2,2,6,6-tetramethylpiperidino)boranes lead to the corresponding 6-substituted aminoborane derivatives [*nido*-6-(RNH)(C₅H₆Me₄NH)B-B₁₀H₁₃] (R = *t*-Bu, C₆H₃-2,6-*i*Pr₂) (Figure 41) [347].

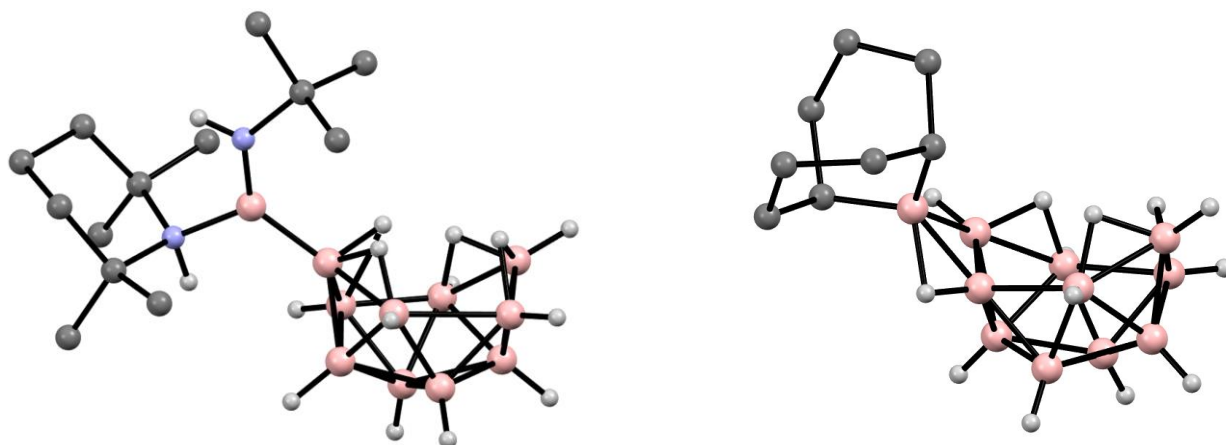


Figure 41. Solid state structures of [*nido*-6-(*t*-BuNH)(C₅H₆Me₄NH)B-B₁₀H₁₃] (**left**) and [μ -5,6-(9-BBN)-B₁₀H₁₃] (**right**). Hydrogen atoms of alkyl groups are omitted for clarity.

The reaction of $Na[B_{10}H_{13}]$ with 9-bora[3.3.1]bicyclononane (9-Br-BBN) in dichloromethane results in the formation of [μ -5,6-(9-BBN)-B₁₀H₁₃], where the 9-BBN group appears in the role of an asymmetric bridge between the B(5) and B(6) positions of the decaborane basket (Figure 41). It is noteworthy that upon the deprotonation of [μ -5,6-(9-BBN)-B₁₀H₁₃] with a Proton Sponge in dichloromethane, the 9-BBN bridging group migrates from the B(6) atom to the B(10) atom, which leads to the formation of an 11-vertex *nido*-structure (HPS)[μ -7,7-CH(CH₂CH₂CH₂)₂CH-B₁₁H₁₂], being a formal derivative of the $[B_{11}H_{14}]^-$ anion [348].

Decaborane derivatives with an *exo*-polyhedral B-B bond also include isomeric *conjuncto*-decaboranes $[B_{10}H_{13}]_2$, which consist of two *nido*-B₁₀ units linked by a direct B-B bond. These compounds were first identified as trace impurities in technical decaborane (14) [349]. In principle, there can be 11 different geometric isomers of *conjuncto*-decaborane $[B_{10}H_{13}]_2$, 4 of which are in the form of enantiomeric pairs. Therefore, various routes (photolysis [350,351], pyrolysis [350,351], γ -irradiation [352], high-energy electron bombardment [351], silent electrical discharge [353]) for synthesizing these compounds have been developed. All of them, as a rule, lead to the formation of mixtures with different isomeric compositions. The solid state structures of the 1,1'- [353], 1,2'- [354], 1,5'- [352], 1,6'- [238], 2,2'- [355,356], and 2,6'- [356] isomers have been determined by single-crystal X-ray diffraction, whereas the 2,5'- [351], 5,5'- [351], and 6,6'- [357] isomers have been characterized by NMR spectroscopy.

The asymmetric derivatives [*arachno*-1-(6'-*nido*-B₁₀H₁₃)-6,9-(Me₂S)₂-B₁₀H₁₁] and [*nido*-4-(2'-*nido*-B₁₀H₁₃)-5-Me₂S-B₁₀H₁₁] (Figure 42) were isolated from the reaction of $[1,5'-(nido-B_{10}H_{13})_2]$ with dimethylsulfide under reflux [238]. The first compound was also obtained by the thermolysis of [*arachno*-6,9-(Me₂S)₂-B₁₀H₁₂] in refluxing toluene [238].

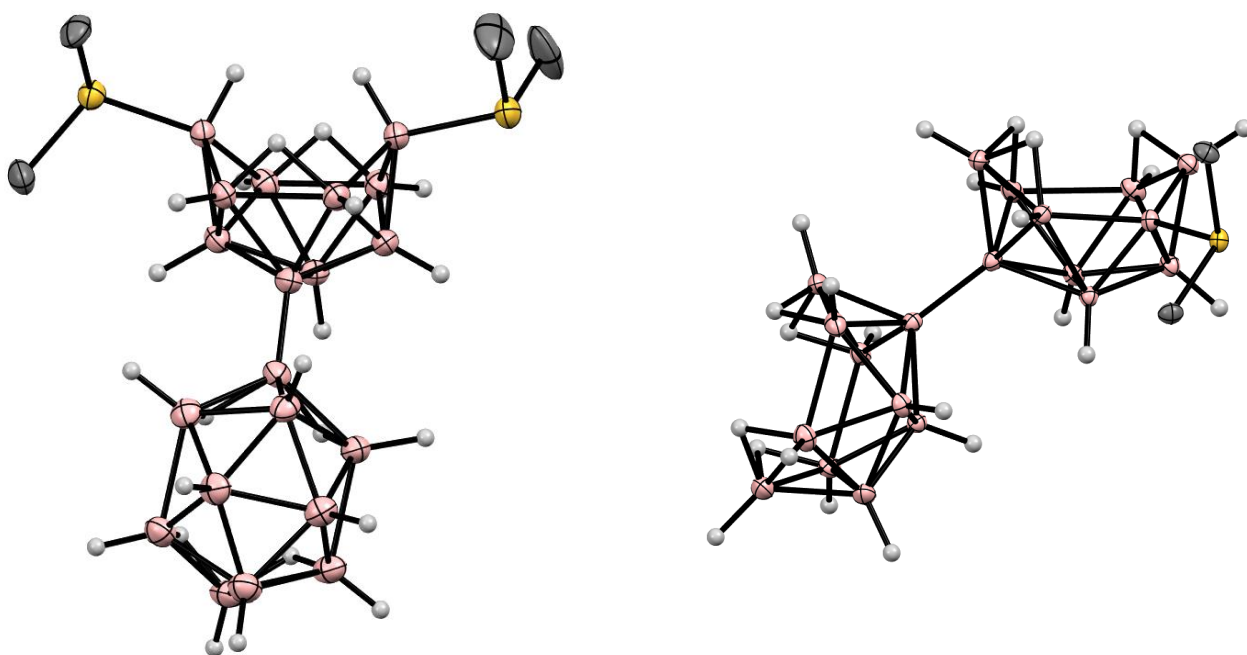


Figure 42. Solid state structures of [arachno-1-(6'-nido-B₁₀H₁₃)-6,9-(Me₂S)₂-B₁₀H₁₁] (**left**) and [nido-4-(2'-nido-B₁₀H₁₃)-5-Me₂S-B₁₀H₁₁] (**right**). Hydrogen atoms of alkyl groups are omitted for clarity.

The isomeric tridecaboranyl species [arachno-1,5-(6'-nido-B₁₀H₁₃)₂-6,9-(Me₂S)₂-B₁₀H₁₀] (Figure 43) and [arachno-1,3-(6'-nido-B₁₀H₁₃)₂-6,9-(Me₂S)₂-B₁₀H₁₀] were isolated from the products of the thermolysis of [arachno-6,9-(Me₂S)₂-B₁₀H₁₂] in refluxing benzene [238,358].



Figure 43. Solid state structure of [arachno-1,5-(6'-nido-B₁₀H₁₃)₂-6,9-(Me₂S)₂-B₁₀H₁₀]. Hydrogen atoms of organic substituents are omitted for clarity.

Here, it is also worth mentioning an unusual structure, in which two hydrogen atoms at positions 5 and 6 of the decaborane basket are replaced by pentaborane moieties—5-

(*nido*-pentaboran-2-yl)-6-(*nido*-pentaboran-1-yl)-*nido*-decaborane, formed as a result of the long-term storage (23 years) of a sealed, under-vacuum pentaborane(9) sample under ambient lighting and temperature conditions (Figure 44) [339].

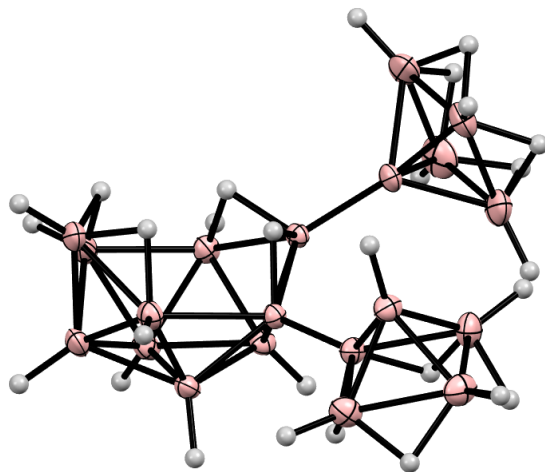


Figure 44. Structure of 5-(*nido*-pentaboran-2-yl)-6-(*nido*-pentaboran-1-yl)-*nido*-decaborane.

11. Decaborane-Related *conjuncto*-Boranes [B₁₈H₂₂]

Another type of compound worth considering here are the *conjuncto*-boranes [B₁₈H₂₂], in which two decaborane baskets are connected by a common edge. Octadecaborane(22) [B₁₈H₂₂] in the form of a mixture of *syn*- and *anti*-isomers (Figure 45) is formed on the hydrolysis of (H₃O)₂[*trans*-B₂₀H₁₈]·nH₂O and can be separated by fractional crystallization [359]. More recently, a convenient method has been proposed for the synthesis of *anti*-[B₁₈H₂₂] by mild oxidation of (Me₄N)[*nido*-B₉H₁₂] with iodine in toluene, which gives excellent yields (~80%) and thus provides a large-scale and safe route to this important polyborane cluster [360].

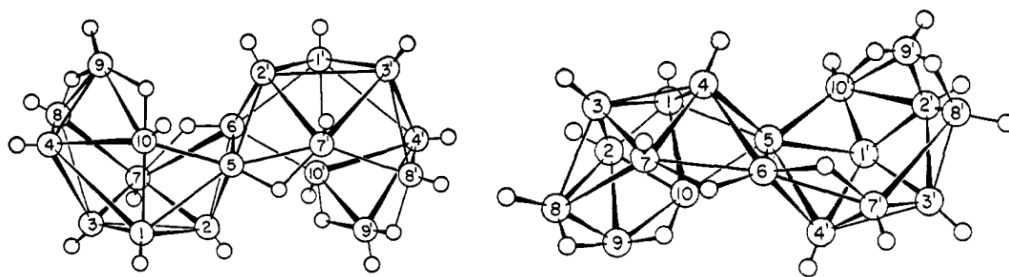


Figure 45. Structures and numbering of atoms in *syn*- (left) and *anti*- (right) isomers of [B₁₈H₂₂]. Reprinted with permission from Ref. [359]. Copyright (1968) the American Chemical Society.

The photophysics of both isomers have been studied by UV–vis spectroscopic techniques and quantum chemical calculations. In an air-saturated hexane solution, *anti*-[B₁₈H₂₂] shows fluorescence with a high quantum yield, $\Phi_F = 0.97$, and singlet oxygen O₂(¹Δ_g) production ($\Phi_\Delta \sim 0.008$). Conversely, the isomer *syn*-[B₁₈H₂₂] shows no measurable fluorescence, instead displaying a much faster, picosecond nonradiative decay of excited singlet states [361]. Due to this, *anti*-[B₁₈H₂₂] can be considered as a potential blue laser material. The photophysical properties of *anti*-[B₁₈H₂₂] can be tuned by the partial substitution of hydrogen atoms with various functional groups. Because of this, combined with its high stability [362–366], *anti*-[B₁₈H₂₂] is attracting increasing research interest, while the *syn*-[B₁₈H₂₂] isomer has received much less attention.

The reaction of *anti*-[B₁₈H₂₂] with chlorine generated in situ from *N*-chlorosuccinimide (NCS) with HCl/dioxane in dichloromethane leads to the 7-chloro derivative *anti*-[7-Cl-B₁₈H₂₁] (Figure 46) [367]. The reaction of *anti*-[B₁₈H₂₂] with AlCl₃ in tetrachloromethane

results in a mixture of the 3,3'- and 3,4'-dichloro derivatives *anti*-[3,3'-Cl₂-B₁₈H₂₀] (Figure 46) and *anti*-[3,4'-Cl₂-B₁₈H₂₀] (Figure 45) together with minor amounts of the other isomeric dichloro derivatives *anti*-[4,4'-Cl₂-B₁₈H₂₀] (Figure 46), *anti*-[3,1'-Cl₂-B₁₈H₂₀] (Figure 46), and *anti*-[7,3'-Cl₂-B₁₈H₂₀], as well as the 3- and 4-chloro derivatives *anti*-[3-Cl-B₁₈H₂₁] and *anti*-[4-Cl-B₁₈H₂₁] and the 3,4,3'- and 3,4,4'-trichloro derivatives *anti*-[3,4,3'-Cl₃-B₁₈H₁₉] and *anti*-[3,4,4'-Cl₃-B₁₈H₁₉], which were separated chromatographically [368].

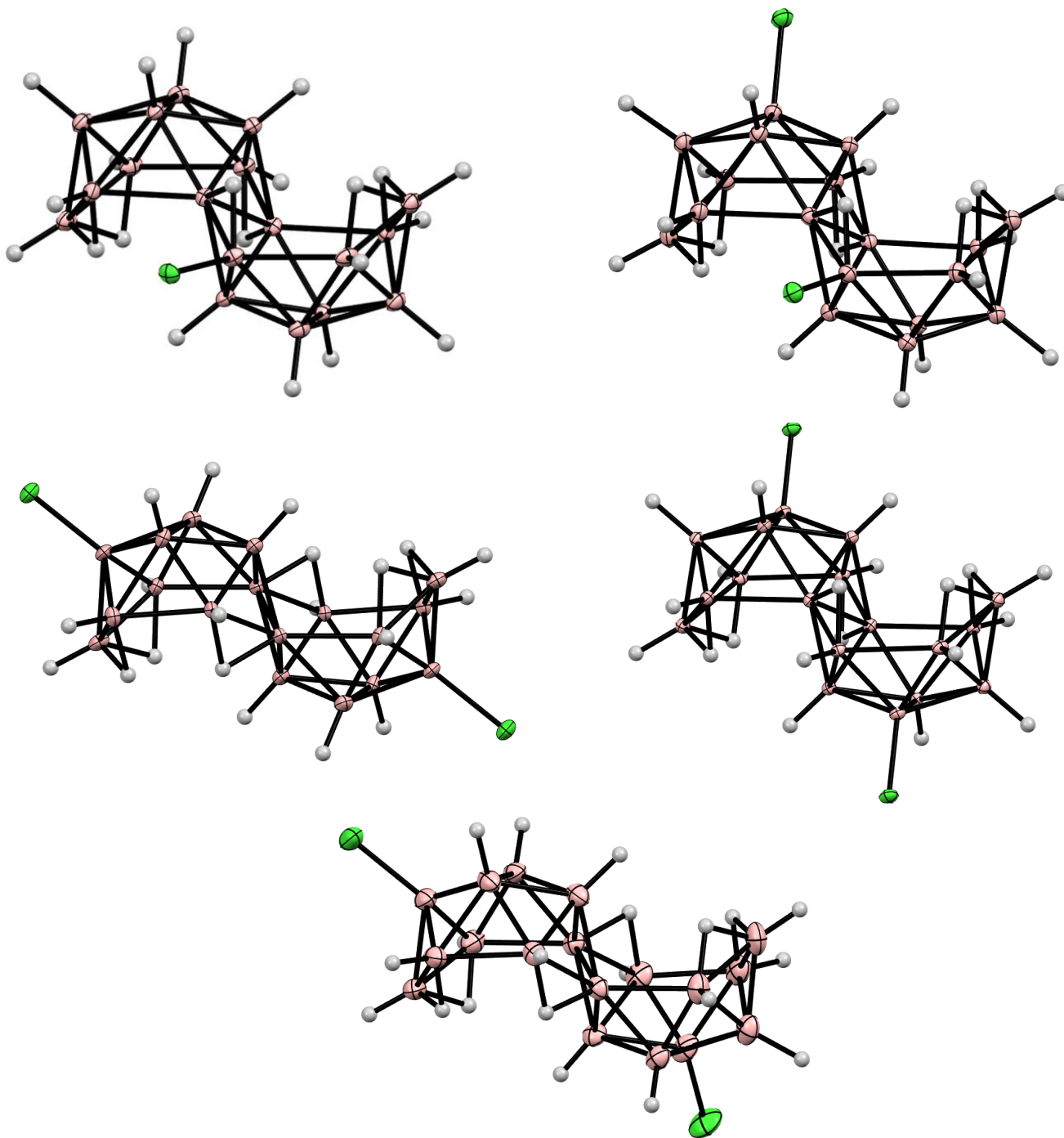


Figure 46. Solid state structures of *anti*-[7-Cl-B₁₈H₂₁] (top left), *anti*-[3,1'-Cl₂-B₁₈H₂₀] (top right), *anti*-[4,4'-Cl₂-B₁₈H₂₀] (middle left), *anti*-[3,3'-Cl₂-B₁₈H₂₀] (middle right), and *anti*-[3,4'-Cl₂-B₁₈H₂₀] (bottom).

The bromination of *anti*-[B₁₈H₂₂] with bromine in dichloromethane in the presence of AlCl₃ leads to the 4-bromo or 4,4'-dibromo derivatives *anti*-[4-Br-B₁₈H₂₁] or *anti*-[4,4'-Br₂-B₁₈H₂₀] depending on the reagent ratio (Figure 47) [369,370].



Figure 47. Solid state structures of *anti*-[4-Br-B₁₈H₂₁] (left) and *anti*-[4,4'-Br₂-B₁₈H₂₀] (right).

The reaction of *anti*-[B₁₈H₂₂] with iodine in ethanol leads to the 4-iodo derivative *anti*-[7-I-B₁₈H₂₁] (Figure 48) [359,371], while the reaction with I₂ or ICl in the presence of AlCl₃ in dichloromethane results in the 4-iodo- and 4,4'-diiodo derivatives *anti*-[4-I₂-B₁₈H₂₁] and *anti*-[4,4'-I₂-B₁₈H₂₀] (Figure 48), depending on the reagent ratio [367,371].

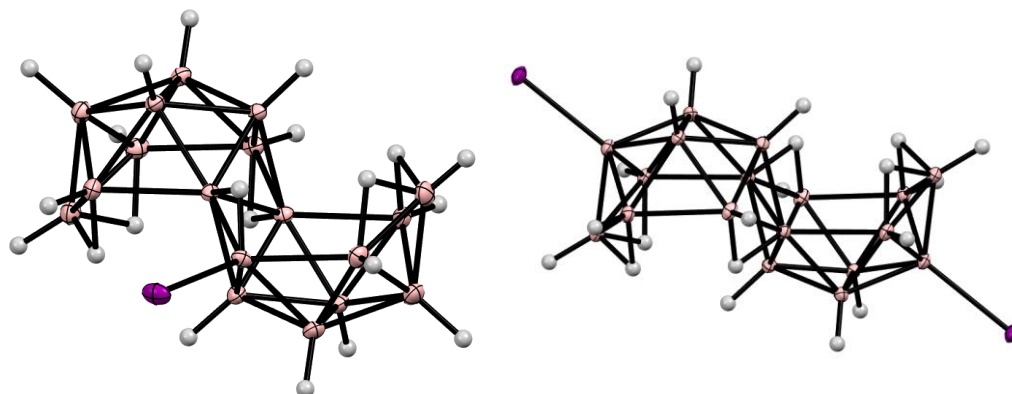


Figure 48. Solid state structures of *anti*-[7-I-B₁₈H₂₁] (left) and *anti*-[4,4'-I₂-B₁₈H₂₀] (right).

The iodine atom in *anti*-[7-I-B₁₈H₂₁] can be substituted by various nucleophiles: the reaction with trifluoroacetamide in toluene in the presence of K₃PO₄ gives the corresponding *N*-boronated amide *anti*-[7-CF₃CONH-B₁₈H₂₁]; the reactions with *t*-BuOK, 4-FC₆H₄OK, and 1-AdSK in toluene or tetrahydrofuran lead to the corresponding (thio)ethers *anti*-[7-RX-B₁₈H₂₁]. The reaction with potassium 2,6-dimethylthiophenolate in toluene results in the corresponding thioether *anti*-[7-(2',6'-Me₂C₆H₃S)-B₁₈H₂₁], while the reaction in tetrahydrofuran produces *anti*-[7-(2',6'-Me₂C₆H₃S(CH₂)₄O)-B₁₈H₂₁] [372]. The Pd-catalyzed reactions of *anti*-[7-I-B₁₈H₂₁] with CF₃CONH₂, *t*-BuOK, and 2,6-Me₂C₆H₃OK in the presence of catalytic amounts of RuPhos Pd G4 and RuPhos in 1,4-dioxane lead to the corresponding derivatives with B-N and B-O bonds *anti*-[7-X-B₁₈H₂₁] [372].

The reaction of *anti*-[B₁₈H₂₂] with neat methyl iodide in the presence of AlCl₃ at room temperature results in the 3,3',4,4'-tetramethyl derivative *anti*-[3,3',4,4'-Me₄-B₁₈H₁₈] (Figure 49) as the main product, together with minor amounts of the 4,4'-dimethyl derivative *anti*-[4,4'-Me₂-B₁₈H₂₀] (Figure 49), the 3,4,4'- and 3,3',4-trimethyl derivatives *anti*-[3,4,4'-Me₃-B₁₈H₁₉] (Figure 47) and *anti*-[3,3',4-Me₃-B₁₈H₁₉], as well as the 1,3,3',4,4'- and 3,3',4,4',8-pentamethyl derivatives *anti*-[1,3,3',4,4'-Me₅-B₁₈H₁₇] and *anti*-[3,3',4,4',8-Me₅-B₁₈H₁₇] and the 1,1',3,3',4,4'-hexamethyl derivative *anti*-[1,1',3,3',4,4'-Me₆-B₁₈H₁₆] [373]. The similar reaction with ethyl iodide gives the 3,3',4,4'-tetraethyl derivative *anti*-[3,3',4,4'-Et₄-B₁₈H₁₈] (Figure 49) [373].

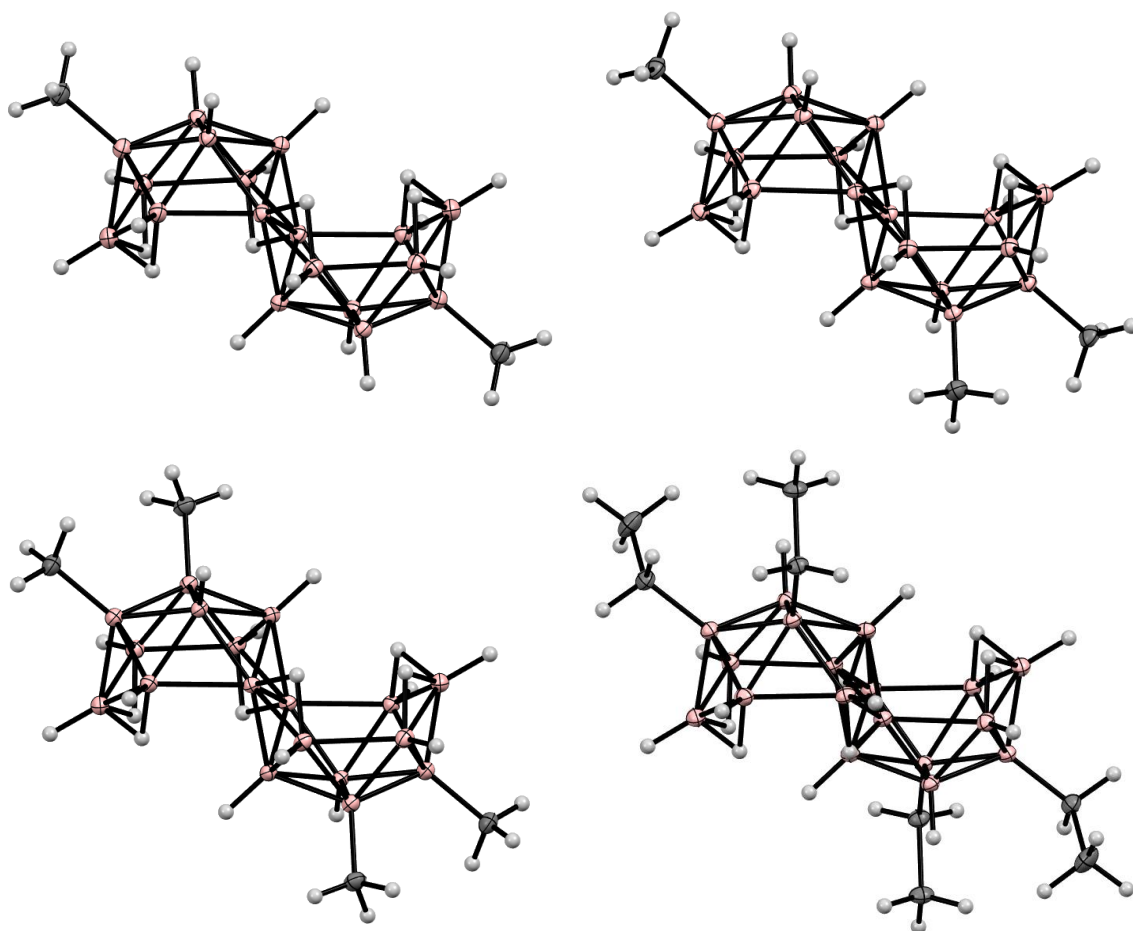


Figure 49. Solid state structures of *anti*-[4,4'-Me₂-B₁₈H₂₀] (**top left**), *anti*-[3,4,4'-Me₃-B₁₈H₁₉] (**top right**), *anti*-[3,3',4,4'-Me₄-B₁₈H₁₈] (**bottom left**), and *anti*-[3,3',4,4'-Et₄-B₁₈H₁₈] (**bottom right**).

The dichloroundecamethyl *anti*-[2,2'-Cl₂-1,1',3,3',4,4',7,7',8,8',10'-Me₁₁-B₁₈H₉], dichlorododecamethyl *anti*-[2,2'-Cl₂-1,1',3,3',4,4',7,7',8,8',10,10'-Me₁₂-B₁₈H₈] (Figure 50), and dichlorotridecamethyl *anti*-[2,2'-Cl₂-1,1',3,3',4,4',7,7',8,8',9,10,10'-Me₁₃-B₁₈H₇] derivatives were obtained by the reaction of *anti*-[B₁₈H₂₂] with methyl iodide in the presence of AlCl₃ in dichloromethane at 55 °C [373,374].

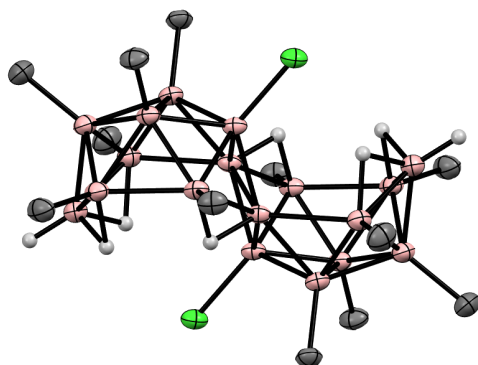


Figure 50. Solid state structure of *anti*-[2,2'-Cl₂-1,1',3,3',4,4',7,7',8,8',10,10'-Me₁₂-B₁₈H₈]. Hydrogen atoms of organic substituents are omitted for clarity.

The reaction of *anti*-[B₁₈H₂₂] with elemental sulfur in the presence of AlCl₃ at 125 °C leads to the 4,4'-dimercapto derivative *anti*-[4,4'-(HS)₂-B₁₈H₂₀] (Figure 51) [375].

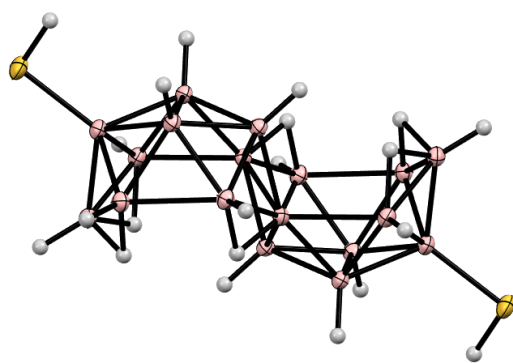


Figure 51. Solid state structure of *anti*-[4,4'-(HS)₂-B₁₈H₂₀].

The reaction of *anti*-[B₁₈H₂₂] with pyridine in refluxing chloroform or benzene unexpectedly results in a two-fold substitution in one of the B₁₀-baskets to form *nido-arachno*-[6',9'-Py₂-B₁₈H₂₀] (Figure 52) together with some amount of *anti*-[8'-Py-B₁₈H₂₁] (Figure 52) and [3',8'-Py₂-B₁₆H₁₈] as the main degradation product. In contrast to the thermochromic fluorescence of *nido-arachno*-[6',9'-Py₂-B₁₈H₂₀] (from 620 nm brick red at room temperature to 585 nm yellow at 8 K), *anti*-[8'-Py-B₁₈H₂₁] exhibits no luminescence [376,377]. The 6',9'-disubstituted derivatives with 4-picoline [377], isoquinoline [378], and 5-hydroxyisoquinoline [379] were prepared in a similar way.

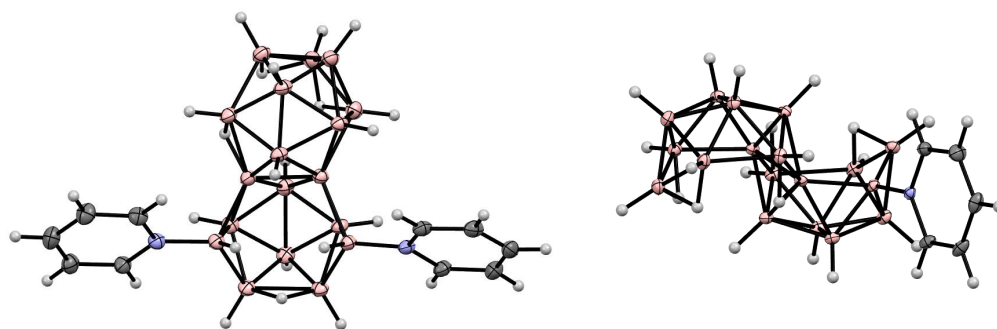


Figure 52. Solid state structures of *nido-arachno*-[6',9'-Py₂-B₁₈H₂₀] (**left**) and *anti*-[8-Py-B₁₈H₂₁] (**right**).

The reaction of *anti*-[B₁₈H₂₂] with methyl isonitrile MeNC in benzene leads to *anti*-[7-((MeNH)C₃N₂HMe₂)-B₁₈H₂₀], in which a reductive trimerization of MeNC gives an unusual imidazole-based carbene, {(MeNH)C₃N₂HMe₂}, that is stabilized by coordination to the macropolyhedral boron cluster (Figure 53) [380].

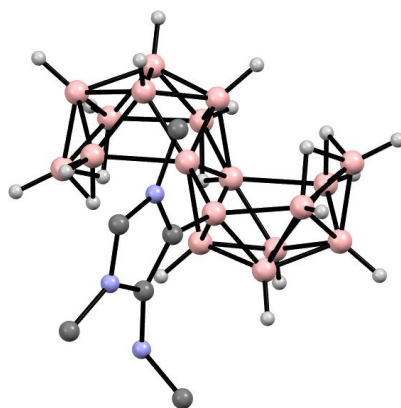


Figure 53. Solid state structure of *anti*-[7-((MeNH)C₃N₂HMe₂)-B₁₈H₂₀]. Hydrogen atoms of organic substituents are omitted for clarity.

The reaction with *tert*-butyl isonitrile in 1,2-dichloroethane results in *anti*-[7- $\{(t\text{-BuNHCH})(t\text{-BuNHC(CN)})\text{CH}_2\}$ -B₁₈H₂₀], in which a reductive oligomerization of *t*-BuNC has given the complex polynitrogen base $\{(t\text{-BuNHCH})(t\text{-BuNHC(CN)})\text{CH}_2\}$ formally as a zwitterionic carbene attached to the macropolyhedral boron cluster (Figure 54) [381].

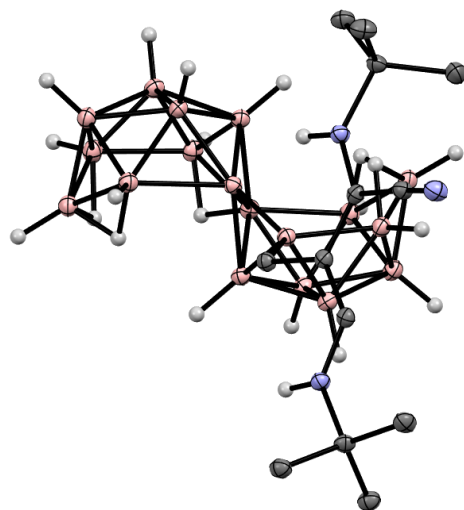


Figure 54. Solid state structure of *anti*-[7- $\{(t\text{-BuNHCH})(t\text{-BuNHC(CN)})\text{CH}_2\}$ -B₁₈H₂₀]. Hydrogen atoms of organic substituents are omitted for clarity.

The synthesis of few substituted derivatives of *syn*-[B₁₈H₂₂] was reported. Heating *syn*-[B₁₈H₂₂] with sulfur in the presence of anhydrous AlCl₃ at 125 °C results in a mixture of the isomeric mercapto derivatives *syn*-[1-HS-B₁₈H₂₁], *syn*-[3-HS-B₁₈H₂₁], and *syn*-[4-HS-B₁₈H₂₁], which were all separated by chromatography on silica (Figure 55) [382].

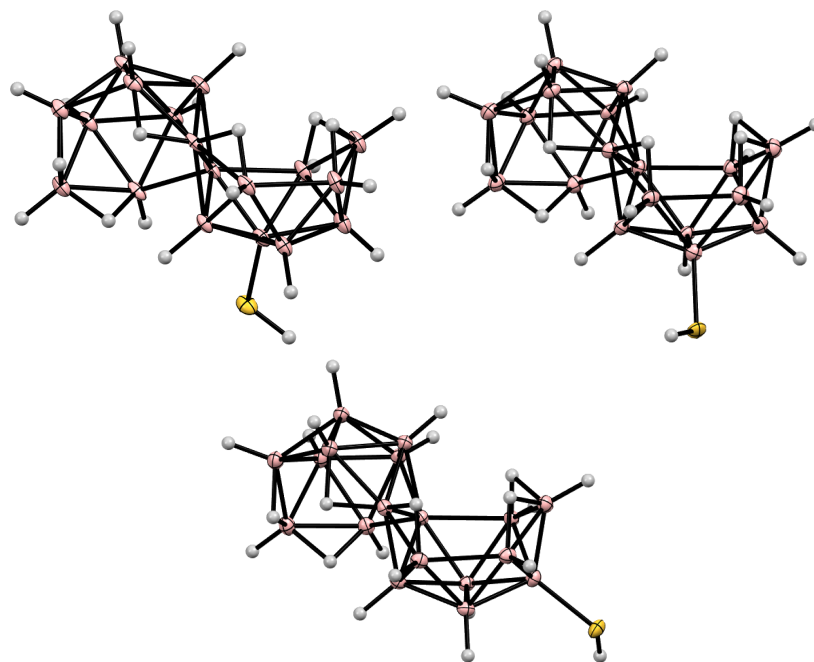


Figure 55. Solid state structures of *syn*-[1-HS-B₁₈H₂₁] (top left), *syn*-[3-HS-B₁₈H₂₁] (top right), and *syn*-[4-HS-B₁₈H₂₁] (bottom).

The 3- and 4-mercapto derivatives of *syn*-[B₁₈H₂₂], *syn*-[3-HS-B₁₈H₂₁], and *syn*-[4-HS-B₁₈H₂₁] were obtained as byproducts of thermolysis of nonathiaborane *arachno*-[SB₈H₁₂]

in boiling cyclohexane [383]. The mercapto derivatives obtained are brightly luminescent under UV irradiation, making these compounds rare examples of a luminescent derivative of *syn*-[B₁₈H₂₂] [382,383].

The deprotonation of *syn*-[B₁₈H₂₂] with NaH in 1,2-dimethoxyethane, followed by the reaction with iodine and dimethylsulfide under reflux, results in the 7-dimethylsulfonium derivative *syn*-[7-Me₂S-B₁₈H₂₀] (Figure 56) [384].

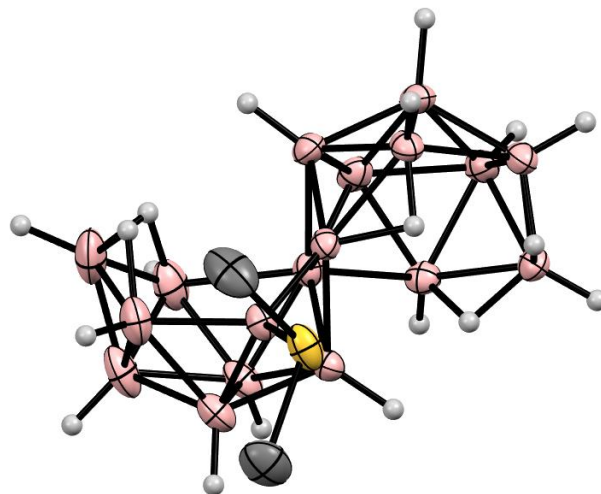


Figure 56. Solid state structure of *syn*-[7-Me₂S-B₁₈H₂₀]. Hydrogen atoms of organic substituents are omitted for clarity.

12. Conclusions

The purpose of this review was to give the most complete picture of the current state of the chemistry of decaborane and its derivatives. After its rapid development on the verge of the 1950s and 1960s, associated with the study of the chemistry of decaborane as a potential component of rocket fuels, the chemistry of decaborane was studied by many research groups. However, no comprehensive review elucidating it in full has appeared for more than 50 years, which certainly hindered the development of this important area of boron cluster chemistry. We would like to hope that this review will be useful both for young researchers just starting their way in boron chemistry and for researchers actively working in this field.

Funding: This work was supported by the Ministry of Science and Higher Education of the Russian Federation (075-03-2023-642).

Data Availability Statement: No new data were created.

Conflicts of Interest: The author declares no conflict of interests.

Sample Availability: Not applicable.

References

1. Grimes, R.N. *Carboranes*, 3rd ed.; Academic Press: London, UK, 2016. [\[CrossRef\]](#)
2. Shmal'ko, A.V.; Sivaev, I.B. Chemistry of carba-*closo*-decaborate anions [CB₉H₁₀][−]. *Russ. J. Inorg. Chem.* **2019**, *64*, 1726–1749. [\[CrossRef\]](#)
3. Sivaev, I.B.; Bregadze, V.I.; Sjöberg, S. Chemistry of *closo*-dodecaborate anion [B₁₂H₁₂]^{2−}: A review. *Collect. Czech. Chem. Commun.* **2002**, *67*, 679–727. [\[CrossRef\]](#)
4. Zhao, X.; Yang, Z.; Chen, H.; Wang, Z.; Zhou, X.; Zhang, H. Progress in three-dimensional aromatic-like *closo*-dodecaborate. *Coord. Chem. Rev.* **2021**, *444*, 214042. [\[CrossRef\]](#)
5. Körbe, S.; Schreiber, P.J.; Michl, J. Chemistry of the carba-*closo*-dodecaborate(−) anion, CB₁₁H₁₂[−]. *Chem. Rev.* **2006**, *106*, 5208–5249. [\[CrossRef\]](#)
6. Douvris, C.; Michl, J. Update 1 of: Chemistry of the carba-*closo*-dodecaborate(−) anion, CB₁₁H₁₂[−]. *Chem. Rev.* **2013**, *113*, R179–R233. [\[CrossRef\]](#)

7. Sivaev, I.B.; Prikaznov, A.V.; Naoufal, D. Fifty years of the *closo*-decaborate anion chemistry. *Collect. Czech. Chem. Commun.* **2010**, *75*, 1149–1199. [\[CrossRef\]](#)
8. Mahfouz, N.; Abi Ghaida, F.; El Hajj, Z.; Diab, M.; Floquet, S.; Mehdi, A.; Naoufal, D. Recent achievements on functionalization within *closo*-decahydrodecaborate $[B_{10}H_{10}]^{2-}$ clusters. *ChemistrySelect* **2022**, *7*, e202200770. [\[CrossRef\]](#)
9. Nakamura, K. Preparation and properties of amorphous boron films deposited by pyrolysis of decaborane in the molecular flow region. *J. Electrochem. Soc.* **1984**, *131*, 2691. [\[CrossRef\]](#)
10. Kim, Y.G.; Dowben, P.A.; Spencer, J.T.; Ramseyer, G.O. Chemical vapor deposition of boron and boron nitride from decaborane(14). *J. Vac. Sci. Technol. A* **1989**, *7*, 2796–2799. [\[CrossRef\]](#)
11. Perkins, F.K.; Rosenberg, R.A.; Lee, S.; Dowben, P.A. Synchrotron-radiation-induced deposition of boron and boron carbide films from boranes and carboranes: Decaborane. *J. Appl. Phys.* **1991**, *69*, 4103–4109. [\[CrossRef\]](#)
12. Saidoh, M.; Ogiwara, N.; Shimada, M.; Arai, T.; Hiratsuka, H.; Koike, T.; Shimizu, M.; Ninomiya, H.; Nakamura, H.; Jimbou, R. Initial boronization of JT-60U tokamak using decaborane. *Jpn. J. Appl. Phys.* **1993**, *32*, 3276–3281. [\[CrossRef\]](#)
13. Kodama, H.; Oyaidzu, M.; Sasaki, M.; Kimura, H.; Morimoto, Y.; Oya, Y.; Matsuyama, M.; Sagara, A.; Noda, N.; Okuno, K. Studies on structural and chemical characterization for boron coating films deposited by PCVD. *J. Nucl. Mater.* **2004**, *329–333*, 889–893. [\[CrossRef\]](#)
14. Bellott, B.J.; Noh, W.; Nuzzo, R.G.; Girolami, G.S. Nanoenergetic materials: Boron nanoparticles from the pyrolysis of decaborane and their functionalisation. *Chem. Commun.* **2009**, 3214–3215. [\[CrossRef\]](#)
15. Ekimov, E.A.; Zibrov, I.P.; Zoteev, A.V. Preparation of boron microcrystals via high-pressure, high-temperature pyrolysis of decaborane, $B_{10}H_{14}$. *Inorg. Mater.* **2011**, *47*, 1194–1198. [\[CrossRef\]](#)
16. Ekimov, E.A.; Lebed, J.B.; Sidorov, V.A.; Lyapin, S.G. High-pressure synthesis of crystalline boron in B-H system. *Sci. Technol. Adv. Mater.* **2011**, *12*, 055009. [\[CrossRef\]](#) [\[PubMed\]](#)
17. Chatterjee, S.; Luo, Z.; Acerce, M.; Yates, D.M.; Johnson, A.T.C.; Sneddon, L.G. Chemical vapor deposition of boron nitride nanosheets on metallic substrates via decaborane/ammonia reactions. *Chem. Mater.* **2011**, *23*, 4414–4416. [\[CrossRef\]](#)
18. Chatterjee, S.; Kim, M.J.; Zakharov, D.N.; Kim, S.M.; Stach, E.A.; Maruyama, B.; Sneddon, L.G. Syntheses of boron nitride nanotubes from borazine and decaborane molecular precursors by catalytic chemical vapor deposition with a floating nickel catalyst. *Chem. Mater.* **2012**, *24*, 2872–2879. [\[CrossRef\]](#)
19. Kher, S.S.; Spencer, J.T. Chemical vapor deposition precursor chemistry. 3. Formation and characterization of crystalline nickel boride thin films from the cluster-assisted deposition of polyhedral borane compounds. *Chem. Mater.* **1992**, *4*, 538–544. [\[CrossRef\]](#)
20. Kher, S.S.; Tan, Y.; Spencer, J.T. Chemical vapor deposition of metal borides. 4. The application of polyhedral boron clusters to the chemical vapor deposition formation of gadolinium boride thin-film materials. *Appl. Organomet. Chem.* **1996**, *10*, 297–304. [\[CrossRef\]](#)
21. Kher, S.S.; Romero, J.V.; Caruso, J.D.; Spencer, J.T. Chemical vapor deposition of metal borides. 6. The formation of neodymium boride thin film materials from polyhedral boron clusters and metal halides by chemical vapor deposition. *Appl. Organomet. Chem.* **2008**, *22*, 300–307. [\[CrossRef\]](#)
22. Tynell, T.; Aizawa, T.; Ohkubo, I.; Nakamura, K.; Mori, T. Deposition of thermoelectric strontium hexaboride thin films by a low pressure CVD method. *J. Cryst. Growth* **2016**, *449*, 10–14. [\[CrossRef\]](#)
23. Guélou, G.; Martirosyan, M.; Ogata, K.; Ohkubo, I.; Kakefuda, Y.; Kawamoto, N.; Kitagawa, Y.; Ueda, J.; Tanabe, S.; Maeda, K.; et al. Rapid deposition and thermoelectric properties of ytterbium boride thin films using hybrid physical chemical vapor deposition. *Materialia* **2018**, *1*, 244–248. [\[CrossRef\]](#)
24. Ohkubo, I.; Aizawa, T.; Nakamura, K.; Mori, T. Control of competing thermodynamics and kinetics in vapor phase thin-film growth of nitrides and borides. *Front. Chem.* **2021**, *9*, 642388. [\[CrossRef\]](#) [\[PubMed\]](#)
25. Zhang, Y.; Peng, Y.; Wan, Q.; Ye, D.; Wang, A.; Zhang, L.; Jiang, W.; Liu, Y.; Li, J.; Zhuang, X.; et al. Fuel cell power source based on decaborane with high energy density and low crossover. *Mater. Today Energy* **2023**, *32*, 101244. [\[CrossRef\]](#)
26. Hawthorne, M.F. Decaborane-14 and its derivatives. In *Advances in Inorganic Chemistry and Radiochemistry*; Academic Press: New York, NY, USA, 1963; Volume 5, pp. 307–347. [\[CrossRef\]](#)
27. Stanko, V.I.; Chapovskii, Y.A.; Brattsev, V.A.; Zakharkin, L.I. The chemistry of decaborane and its derivatives. *Russ. Chem. Rev.* **1965**, *34*, 424–439. [\[CrossRef\]](#)
28. Shore, S.G. *Nido*- and *arachno*-boron hydrides. In *Boron Hydride Chemistry*; Muetterties, E.L., Ed.; Academic Press: New York, NY, USA, 1975; pp. 79–174. [\[CrossRef\]](#)
29. Greenwood, N.N. Boron. In *Comprehensive Inorganic Chemistry*; Pergamon Press: Oxford, UK, 1973; Volume 1, pp. 818–837. [\[CrossRef\]](#)
30. Sivaev, I.B. Molecular boron clusters. In *Comprehensive Inorganic Chemistry*; Elsevier: Amsterdam, The Netherlands, 2023; Volume 1, pp. 740–777. [\[CrossRef\]](#)
31. Stock, A.; Friederici, K.; Priess, O. Borwasserstoffe. III. Feste Borwasserstoffe: Zur Kenntnis des B_2H_6 . *Ber. Dtsch. Chem. Ges.* **1913**, *46*, 3353–3365. [\[CrossRef\]](#)
32. Stock, A.; Pohland, E. Borwasserstoffe. XII. Zur Kenntnis des $B_{10}H_{14}$. *Ber. Dtsch. Chem. Ges.* **1929**, *62*, 90–99. [\[CrossRef\]](#)
33. Stock, A. *Hydrides of Boron and Silicon*; Cornell University Press: Ithaca, NY, USA, 1933.
34. Stock, A. Borwasserstoffe. XI. Strukturformeln der Borhydride. *Ber. Dtsch. Chem. Ges.* **1926**, *59*, 2226–2229. [\[CrossRef\]](#)
35. Huggins, M.L. Boron hydrides. *J. Phys. Chem.* **1922**, *26*, 833–835. [\[CrossRef\]](#)

36. Clark, J.D. *Ignition! An Informal History of Liquid Rocket Propellants*; Rutgers University Press: New Brunswick, NJ, USA, 1972. [CrossRef]
37. *Boron High Energy Fuels: Hearings Before the Committee on Science and Astronautics U.S. House of Representatives. Eighty-Six Congress, First Session*; United States Government Printing Office: Washington, DC, USA, 1959.
38. Goodger, E. Unconventional fuels. *New Sci.* **1957**, 27–29.
39. Siegel, B.; Mack, J.L. The boron hydrides. *J. Chem. Ed.* **1957**, 34, 314–317. [CrossRef]
40. Martin, D.R. The development of borane fuels. *J. Chem. Ed.* **1959**, 36, 208–214. [CrossRef]
41. Gold, J.W.; Militsher, C.; Slauson, D.D. Pentaborane Disposal: Taming the Dragon. Available online: <https://dokumen.tips/documents/pentaborane-taming-the-dragonpdf.html> (accessed on 23 August 2023).
42. Kasper, J.S.; Lucht, C.M.; Harker, D. The structure of the decaborane molecule. *J. Am. Chem. Soc.* **1948**, 70, 881. [CrossRef]
43. Kasper, J.S.; Lucht, C.M.; Harker, M. The crystal structure of decaborane, B₁₀H₁₄. *Acta Cryst.* **1950**, 3, 436–455. [CrossRef]
44. Moore, E.B.; Dickerson, R.E.; Lipscomb, W.N. Least squares refinements of B₁₀H₁₄, B₄H₁₀, and B₅H₁₁. *J. Chem. Phys.* **1957**, 27, 209–211. [CrossRef]
45. Brill, R.; Dietrich, H.; Dierks, H. Distribution of the bonding electrons in decaborane-14. *Angew. Chem. Int. Ed.* **1970**, 9, 524–526. [CrossRef]
46. Brill, R.; Dietrich, H.; Dierks, H. Die Verteilung der Bindungselektronen im Dekaboran-molekül (B₁₀H₁₄). *Acta Cryst. B* **1971**, 27, 2003–2018. [CrossRef]
47. Dietrich, H.; Scheringer, C. Refinement of the molecular charge distribution in decaborane(14). *Acta Cryst. B* **1978**, 34, 54–63. [CrossRef]
48. Tippe, A.; Hamilton, W.C. Neutron diffraction study of decaborane. *Inorg. Chem.* **1969**, 8, 464–470. [CrossRef]
49. Vilkov, L.V.; Mastryukov, V.S.; Akishin, P.A. An electron-diffraction study of the structure of the decaborane molecule in the vapor state. *J. Struct. Chem.* **1964**, 4, 301–304. [CrossRef]
50. Mastryukov, V.S.; Dorofeeva, O.V.; Vilkov, L.V. Reexamination of the electron-diffraction data for the decaborane(14) molecule. *J. Struct. Chem.* **1975**, 16, 110–112. [CrossRef]
51. Eberhardt, W.H.; Crawford, B.; Lipscomb, W.N. The valence structure of the boron hydrides. *J. Chem. Phys.* **1954**, 22, 989–1001. [CrossRef]
52. Lipscomb, W.N. Valence in the boron hydrides. *J. Phys. Chem.* **1957**, 61, 23–27. [CrossRef]
53. Lipscomb, W.N. *Boron Hydrides*; W. A. Benjamin, Inc.: New York, NY, USA, 1963.
54. Moore, E.B.; Lohr, L.L.; Lipscomb, W.N. Molecular orbitals in some boron compounds. *J. Chem. Phys.* **1961**, 35, 1329–1334. [CrossRef]
55. Moore, E.B. Molecular orbitals in B₁₀H₁₄. *J. Chem. Phys.* **1962**, 37, 675–677. [CrossRef]
56. Hoffmann, R.; Lipscomb, W.N. Boron hydrides: LCAO-MO and resonance studies. *J. Chem. Phys.* **1962**, 37, 2872–2883. [CrossRef]
57. Laws, E.A.; Stevens, R.M.; Lipscomb, W.N. Self-consistent field study of decaborane(14). *J. Am. Chem. Soc.* **1972**, 94, 4467–4474. [CrossRef]
58. Lipscomb, W.N. Advances in theoretical studies of boron hydrides and carboranes. In *Boron Hydride Chemistry*; Muetterties, E.L., Ed.; Academic Press: New York, NY, USA, 1975; pp. 39–78. [CrossRef]
59. Kononova, E.G.; Klemenkova, Z.S. The electronic structure of *nido*-B₁₀H₁₄ and [6-Ph-*nido*-6-CB₉H₁₁][−] in terms of Bader's theory (AIM). *J. Mol. Struct.* **2013**, 1036, 311–317. [CrossRef]
60. Shoolery, J.N. The relation of high resolution nuclear magnetic resonance spectra to molecular structures. *Discuss. Faraday Soc.* **1955**, 19, 215–225. [CrossRef]
61. Williams, R.E.; Shapiro, I. Reinterpretation of nuclear magnetic resonance spectra of decaborane. *J. Chem. Phys.* **1958**, 29, 677–678. [CrossRef]
62. Phillips, W.D.; Miller, H.C.; Muetterties, E.L. B¹¹ Magnetic resonance study of boron compounds. *J. Am. Chem. Soc.* **1959**, 81, 4496–4500. [CrossRef]
63. Pilling, R.L.; Tebbe, F.N.; Hawthorne, M.F.; Pier, E.A. Boron-11 nuclear magnetic resonance spectra of two boron hydride derivatives at 60 Mc./sec. *Proc. Chem. Soc.* **1964**, 402–403. [CrossRef]
64. Keller, P.C.; MacLean, D.; Schaeffer, R. Final assignment of B1 (3) N.M.R. resonance of decaborane. *Chem. Commun.* **1965**, 204. [CrossRef]
65. Williams, R.L.; Greenwood, N.N.; Morris, J.H. The nuclear magnetic resonance spectrum of decaborane-14. *Spectrochim. Acta* **1965**, 21, 1579–1587. [CrossRef]
66. Bodner, G.M.; Sneddon, L.G. An assignment of the hydrogen-1 magnetic resonance spectrum of decaborane at 220 MHz. *Inorg. Chem.* **1970**, 9, 1421–1423. [CrossRef]
67. Onak, T.; Marynick, D. Application of a ring current model to decaborane(14). A correlation of proton and boron-11 nuclear magnetic resonance chemical shifts. *Trans. Faraday Soc.* **1970**, 66, 1843–1847. [CrossRef]
68. Greenwood, N.N.; Kennedy, J.D. N.M.R. evidence for a transition between isotropic and anisotropic thermal motion of *nido*-decaborane in an aromatic solvent. *J. Chem. Soc. Chem. Commun.* **1979**, 1099–1101. [CrossRef]
69. Colquhoun, I.J.; McFarlane, W. Heteronuclear two-dimensional nuclear magnetic resonance: Decaborane. *J. Chem. Soc. Dalton Trans.* **1981**, 2014–2016. [CrossRef]

70. Venable, T.L.; Hutton, W.C.; Grimes, R.N. Two-dimensional boron-11-boron-11 nuclear magnetic resonance spectroscopy as a probe of polyhedral structure: Application to boron hydrides, carboranes, metallaboranes, and metallocarboranes. *J. Am. Chem. Soc.* **1984**, *106*, 29–37. [CrossRef]
71. Keller, W.E.; Johnston, H.L. A note on the vibrational frequencies and the entropy of decaborane. *J. Chem. Phys.* **1952**, *20*, 1749–1751. [CrossRef]
72. Hanousek, F.; Štíbr, B.; Heřmánek, S.; Plešek, J. Chemistry of boranes. XXXI. Infrared spectra of decaborane and its deuterio derivatives. *Collect. Czech. Chem. Commun.* **1973**, *38*, 1312–1320. [CrossRef]
73. Pimentel, G.C.; Pitzer, K.S. The ultraviolet absorption and luminescence of decaborane. *J. Chem. Phys.* **1949**, *17*, 882–884. [CrossRef]
74. Pondy, P.R.; Beachell, H.C. Near infrared spectra of diborane, pentaborane, and decaborane. *J. Chem. Phys.* **1956**, *25*, 238–241. [CrossRef]
75. Haaland, A.; Eberhardt, W.H. Electronic spectrum of decaborane. *J. Chem. Phys.* **1962**, *36*, 2386–2392. [CrossRef]
76. Lötze, A.; Olliges, J.; Voigtländer, J. The nuclear quadrupole double resonance spectrum of decaborane. *Chem. Phys. Lett.* **1982**, *93*, 560–563. [CrossRef]
77. Hiyama, Y.; Butler, L.G.; Brown, T.L. Boron-10 and boron-11 nuclear quadrupole resonance spectrum of decaborane[14]. *J. Magn. Res.* **1985**, *65*, 472–480. [CrossRef]
78. Lloyd, D.R.; Lynaugh, N.; Roberts, P.J.; Guest, M.F. Photoelectron studies of boron compounds. Part 5. Higher boron hydrides B_4H_{10} , B_5H_9 and $B_{10}H_{14}$. *J. Chem. Soc. Faraday Trans. 2* **1975**, *71*, 1382–1394. [CrossRef]
79. Hitchcock, A.P.; Wen, A.T.; Lee, S.; Glass, J.A.; Spencer, J.T.; Dowben, P.A. Inner-shell excitation of boranes and carboranes. *J. Phys. Chem.* **1993**, *97*, 8171–8181. [CrossRef]
80. Margrave, J.L. Ionization potentials of B_5H_9 , B_5H_8I , $B_{10}H_{14}$, and $B_{10}H_{13}C_2H_5$ from electron impact studies. *J. Chem. Phys.* **1960**, *32*, 1889. [CrossRef]
81. Kaufman, J.J.; Koski, W.S.; Kuhns, L.J.; Law, R.W. Appearance and ionization potentials of selected fragments from decaborane, $B^{11}_{10}H_{14}^+$. *J. Am. Chem. Soc.* **1962**, *84*, 4198–4205. [CrossRef]
82. Bottei, R.S.; Laubengayer, A.W. The dipole moment and magnetic susceptibility of decaborane. *J. Phys. Chem.* **1962**, *66*, 1449–1451. [CrossRef]
83. Johnson, W.H.; Kilday, M.V.; Prosen, E.J. Heat of formation of decaborane. *J. Res. Natl. Bur. Stand. A Phys. Chem.* **1960**, *64*, 521–525. [CrossRef] [PubMed]
84. Kerr, E.C.; Hallett, N.C.; Johnston, H.L. Low temperature heat capacity of inorganic solids. VI. The heat capacity of decaborane, $B_{10}H_{14}$, from 14 to 305 K. *J. Am. Chem. Soc.* **1951**, *73*, 1117–1119. [CrossRef]
85. Furukawa, G.T.; Park, R.P. Heat capacity, heats of fusion and vaporization, and vapor pressure of decaborane ($B_{10}H_{14}$). *J. Res. Natl. Bur. Stand.* **1955**, *55*, 255–260. [CrossRef]
86. Miller, G.A. The vapor pressure of solid decaborane. *J. Phys. Chem.* **1963**, *67*, 1363–1364. [CrossRef]
87. Nakano, S.; Hemley, R.J.; Gregoryanz, E.A.; Goncharov, A.F.; Mao, H.-K. Pressure-induced transformations of molecular boron hydride. *J. Phys. Condens. Matter* **2002**, *14*, 10453. [CrossRef]
88. Rozendaal, H.M. Clinical observation on the toxicology of boron hydrides. *AMA Arch. Ind. Hyg. Occup. Med.* **1951**, *4*, 257–260. Available online: https://archive.org/details/sim_a-m-a-archives-of-industrial-health_1951-09_4_3/page/256/mode/2up (accessed on 31 July 2023).
89. Krackow, E.H. Toxicity and health hazards of boron hydrides. *AMA Arch. Ind. Hyg. Occup. Med.* **1953**, *8*, 335–339. Available online: https://archive.org/details/sim_a-m-a-archives-of-industrial-health_1953-10_8_4/page/334/mode/2up (accessed on 31 July 2023).
90. Cole, V.V.; Hill, D.L.; Oikemus, A.H. Problems in the study of decaborane and possible therapy of its poisoning. *AMA Arch. Ind. Hyg. Occup. Med.* **1954**, *10*, 158–161. Available online: https://archive.org/details/sim_a-m-a-archives-of-industrial-health_1954-08_10_2/page/158/mode/2up (accessed on 31 July 2023).
91. Lowe, H.; Freeman, G. Boron hydride (borane) intoxication in man. *AMA Arch. Ind. Hyg. Occup. Med.* **1957**, *12*, 523–533. Available online: https://archive.org/details/sim_a-m-a-archives-of-industrial-health_1957-12_16_6/page/522/mode/2up (accessed on 31 July 2023). [CrossRef]
92. Cordasco, E.M.; Cooper, R.W.; Murphy, J.V.; Anderson, C. Pulmonary aspects of some toxic experimental space fuels. *Dis. Chest* **1962**, *41*, 68–72. [CrossRef]
93. Merritt, J.H. Pharmacology and toxicology of propellant fuels: Boron hydrides. *Aeromed. Rev.* **1966**, *3*, 1–11.
94. Svirbely, J.L. Acute toxicity studies of decaborane and pentaborane by inhalation. *AMA Arch. Ind. Hyg. Occup. Med.* **1954**, *10*, 298–304. Available online: https://archive.org/details/sim_a-m-a-archives-of-industrial-health_1954-10_10_4/page/298/mode/2up (accessed on 31 July 2023).
95. Svirbely, J.L. Subacute toxicity of decaborane and pentaborane vapors. *AMA Arch. Ind. Hyg. Occup. Med.* **1954**, *10*, 305–311. Available online: https://archive.org/details/sim_a-m-a-archives-of-industrial-health_1954-10_10_4/page/304/mode/2up (accessed on 31 July 2023).
96. Svirbely, J.L. Toxicity tests of decaborane for laboratory animals. I. Acute toxicity studies. *AMA Arch. Ind. Hyg. Occup. Med.* **1955**, *11*, 132–137. Available online: https://archive.org/details/sim_a-m-a-archives-of-industrial-health_1955-02_11_2/page/132/mode/2up (accessed on 31 July 2023).

97. Svirbely, J.L. Toxicity tests of decaborane for laboratory animals. I. Effect of repeated doses. *AMA Arch. Ind. Hyg. Occup. Med.* **1955**, *11*, 138–141. Available online: https://archive.org/details/sim_a-m-a-archives-of-industrial-health_1955-02_11_2/page/138/mode/2up (accessed on 31 July 2023).
98. Walton, R.P.; Richardson, J.A.; Brodie, O.J. Cardiovascular actions of decaborane. *J. Pharmacol. Exp. Ther.* **1955**, *114*, 367–378.
99. Lamberti, J.M. Review of the toxicological properties of pentaborane, diborane, decaborane, and boric acid. *NASA Tech. Rep.* **1956**, NACA-RM-E56H13a. Available online: <https://ntrs.nasa.gov/api/citations/19930090289/downloads/19930090289.pdf> (accessed on 31 July 2023).
100. Roush, G. The toxicology of the boranes. *J. Occup. Med.* **1959**, *1*, 46–52. Available online: <https://www.jstor.org/stable/44999044> (accessed on 31 July 2023). [CrossRef]
101. Fabre, R.; Chary, R.; Bocquet, P.; Jayot, R. Etat actuel de la toxicologie des hydrides de bore. *Arch. Mal. Prof. Med. Trav. Secur. Soc.* **1959**, *20*, 701–712.
102. Miller, D.F.; Tamas, A.; Robinson, L.; Merriweather, E. Observations on experimental boron hydride exposures. *Toxicol. Appl. Pharmacol.* **1960**, *2*, 430–440. [CrossRef]
103. Miller, D.F.; Tamas, A.A.; Robinson, L.; Merriweather, E. Cumulative effects of borane toxicity as revealed by a clinical test. *Tech. Rep. Aerospace Med. Res. Lab.* **1960**, WADD-60-604. Available online: <https://web.archive.org/web/20181030113902/http://www.dtic.mil/dtic/tr/fulltext/u2/247355.pdf> (accessed on 31 July 2023).
104. Delgado, J.M. Effects of decaborane on brain activity. *Tech. Rep. Aerospace Med. Res. Lab.* **1963**, AMRL-TDR-63-41. Available online: <https://web.archive.org/web/20180726163136/http://www.dtic.mil/dtic/tr/fulltext/u2/411769.pdf> (accessed on 31 July 2023).
105. Delgado, J.M.R.; Back, K.C.; Tamas, A.A. The effect of boranes on the monkey brain. *Arch. Int. Pharmacodyn. Thérap.* **1963**, *141*, 262–270.
106. Lalli, G. Sulla tossicità di alcuni propellenti per missile. *Ann. Geophys.* **1963**, *16*, 385–406. [CrossRef]
107. Merritt, J.A. Methylene blue in the treatment of decaborane toxicity. *Arch. Environ. Health* **1965**, *10*, 452–454. [CrossRef]
108. Reynolds, H.H.; Back, K.C. Effect of decaborane injection on operant behavior of monkeys. *Toxicol. Appl. Pharmacol.* **1966**, *8*, 197–209. [CrossRef]
109. Fairchild, M.D.; Sterman, M.B.; McRae, G.L. The effects of decaborane on cerebral electrical activity and locomotor behavior in the cat. *Tech. Rep. Aerosp. Med. Res. Lab.* **1972**, AMRL-TR-72-80. Available online: <https://web.archive.org/web/20180724164936/http://www.dtic.mil/dtic/tr/fulltext/u2/756526.pdf> (accessed on 31 July 2023).
110. Tadepalli, A.S.; Buckley, J.P. Cardiac and peripheral vascular effects of decaborane. *Toxicol. Appl. Pharmacol.* **1974**, *29*, 210–222. [CrossRef]
111. Dekaboran. *The MAK-Collection for Occupational Health and Safety*; Greim, G., Ed.; Wiley-VCH Verlag: Berlin, Germany, 2002; Volume 1. [CrossRef]
112. Merritt, J.H.; Schultz, E.J.; Wykes, A.A. Effect of decaborane on the norepinephrine content of rat brain. *Biochem. Pharmacol.* **1964**, *13*, 1364–1366. [CrossRef]
113. Oliverio, A. Release of cardiac noradrenaline by decaborane in the heart-lung preparation of guinea pig. *Biochem. Pharmacol.* **1965**, *14*, 1689–1692. [CrossRef]
114. von Euler, U.S.; Lishajko, F. Stereospecific catecholamine uptake in rabbit hearts depleted by decaborane. *Int. J. Neuropharmacol.* **1965**, *4*, 273–280. [CrossRef]
115. von Euler, U.S.; Lishajko, F. Catecholamine depletion and uptake in adrenergic nerve vesicles and in rabbit organs after decaborane. *Acta Physiol. Scand.* **1965**, *65*, 324–330. [CrossRef]
116. Byodeman, S.; von Euler, U.S. Neurotransmitter deficiency and reloading in noradrenaline depleted rabbits. *Acta Physiol. Scand.* **1966**, *66*, 134–140. [CrossRef]
117. Merritt, J.H.; Schultz, E.J. The effect of decaborane on the biosynthesis and metabolism of norepinephrine in the rat brain. *Life Sci.* **1966**, *5*, 27–32. [CrossRef]
118. Johnson, D.G. The effect of cold exposure on the catecholamine excretion of rats treated with decaborane. *Acta Physiol. Scand.* **1966**, *68*, 129–133. [CrossRef]
119. Merritt, J.H.; Sulkowski, T.S. Inhibition of aromatic L-amino acid decarboxylation by decaborane. *Biochem. Pharmacol.* **1967**, *16*, 369–373. [CrossRef]
120. Bhattacharya, I.C. Uptake of noradrenaline in the isolated perfused rat heart after depletion with decaborane. *Acta Physiol. Scand.* **1968**, *73*, 128–138. [CrossRef]
121. Medina, M.A.; Landez, J.H.; Foster, L.L. Inhibition of tissue histamine formation by decaborane. *J. Pharmacol. Exp. Ther.* **1969**, *169*, 132–137. Available online: <https://jpet.aspetjournals.org/content/169/1/132> (accessed on 31 July 2023).
122. Scott, W.N.; Landez, J.H.; Cole, H.D. Effects of boranes upon tissues of the rat. I. Aspartate aminotransferase and lactic dehydrogenase. *Proc. Soc. Exp. Biol. Med.* **1970**, *134*, 348–352. [CrossRef]
123. Kory, P.; Scott, W.N. Effects of boranes upon tissues of the rat. II. Tissue amino acid content in rats on a normal diet. *Proc. Soc. Exp. Biol. Med.* **1970**, *135*, 629–632. [CrossRef]
124. Landez, J.H.; Scott, W.N. Effects of boranes upon tissues of the rat. III. Tissue amino acids in rats on a pyridoxine-deficient diet. *Proc. Soc. Exp. Biol. Med.* **1971**, *136*, 1389–1393. [CrossRef]
125. Malmfors, T.; von Euler, U.S. Depletion and repletion of noradrenaline in adrenergic nerves of the rat after decaborane treatment. *Experientia* **1971**, *27*, 417–419. [CrossRef]

126. Shahab, L.; Lishajko, F.; von Euler, U.S. Differentiated storage mechanisms for noradrenaline and dopamine in the rabbit heart. *Neuropharmacology* **1971**, *10*, 765–769. [CrossRef]
127. Menon, M.; Clark, W.G.; Aures, D. Effect of tremorine, oxotremorine and decaborane on brain histamine levels in rats. *Pharmacol. Res. Commun.* **1971**, *3*, 345–350. [CrossRef]
128. Schayer, R.W.; Reilly, M.A. Effect of decaborane on histamine formation in mice. *J. Pharmacol. Exp. Ther.* **1971**, *177*, 177–180. Available online: <https://jpet.aspetjournals.org/content/177/1/177> (accessed on 31 July 2023).
129. Naeger, L.L.; Leibman, K.C. Mechanisms of decaborane toxicity. *Toxicol. Appl. Pharmacol.* **1972**, *22*, 517–527. [CrossRef]
130. Valerino, D.M.; Soliman, M.R.I.; Aurori, K.C.; Tripp, S.L.; Wykes, A.A.; Vesell, E.S. Studies on the interaction of several boron hydrides with liver microsomal enzymes. *Toxicol. Appl. Pharmacol.* **1974**, *29*, 358–366. [CrossRef]
131. Merritt, J.A.; Meyer, H.C.; Greenberg, R.I.; Tanton, G.A. The production of decaborane-14 from diborane by laser induced chemistry. *Propellants Explos. Pyrotech.* **1979**, *4*, 78–82. [CrossRef]
132. Dunks, G.B.; Palmer Ordóñez, K. A one-step synthesis of $B_{11}H_{14}^-$ ion from $NaBH_4$. *Inorg. Chem.* **1978**, *17*, 1514–1516. [CrossRef]
133. Dunks, G.B.; Palmer Ordóñez, K. A simplified preparation of $B_{10}H_{14}$ from $NaBH_4$. *Inorg. Chem.* **1978**, *17*, 2555–2556. [CrossRef]
134. Dunks, G.B.; Barker, K.; Hedaya, E.; Hefner, C.; Palmer-Ordóñez, K.; Remec, P. Simplified synthesis of $B_{10}H_{14}$ from $NaBH_4$ via $B_{11}H_{14}^-$ ion. *Inorg. Chem.* **1981**, *20*, 1692–1697. [CrossRef]
135. Belov, P.P.; Storozhenko, P.A.; Voloshina, N.S.; Kuznetsova, M.G. Synthesis of decaborane by the reaction of sodium undecaborate with mild organic oxidants. *Russ. J. Appl. Chem.* **2018**, *90*, 1804–1809. [CrossRef]
136. Voloshina, N.S.; Belov, P.P.; Storozhenko, P.A.; Shebashova, N.M.; Kozlova, E.E.; Egorova, N.V.; Kuznetsova, M.G.; Gurkova, E.L. Specific features of oxidation of sodium tetradecahydroundecaborate to decaborane with manganese dioxide. *Russ. J. Appl. Chem.* **2020**, *93*, 807–812. [CrossRef]
137. Mongeot, H.; Atchekzai, H.R. Opening of the $B_{10}H_{10}^{2-}$ cage to give $B_{10}H_{14}$. *Z. Naturforsch. B* **1981**, *36*, 313–314. [CrossRef]
138. Guter, G.A.; Schaeffer, G.W. The strong acid behavior of decaborane. *J. Am. Chem. Soc.* **1956**, *78*, 3546. [CrossRef]
139. Normant, H.J. Unit cells and space groups for two etherates of sodium tridecahydrodecaborate(1-). *Acta Cryst.* **1959**, *12*, 695. [CrossRef]
140. Greenwood, N.N.; Sharrocks, D.N. Decaborane anions and the synthesis of polyhedral borane complexes of mercury(II) and cobalt(II). *J. Chem. Soc. A* **1969**, 2334–2338. [CrossRef]
141. Hawthorne, M.F.; Pitochelli, A.R.; Strahm, R.D.; Miller, J.J. The preparation and characterization of salts which contain the $B_{10}H_{13}$ anion. *J. Am. Chem. Soc.* **1960**, *82*, 1825–1829. [CrossRef]
142. Hawthorne, M.F. The reaction of phosphine methylenes with boron hydrides. *J. Am. Chem. Soc.* **1958**, *80*, 3480–3481. [CrossRef]
143. Onak, T.; Rosendo, H.; Siwapinyoyos, G.; Kubo, R.; Liauw, L. Reaction of 1,8-bis(dimethylamino)naphthalene, a highly basic and weakly nucleophilic amine, with several polyboranes and with boron trifluoride. *Inorg. Chem.* **1979**, *18*, 2943–2945. [CrossRef]
144. Pérez, S.; Sanz Miguel, P.J.; Macías, R. Decaborane anion tautomerism: Ion pairing and proton transfer control. *Dalton Trans.* **2018**, *47*, 5850–5859. [CrossRef] [PubMed]
145. Heřmánek, S.; Plotová, H.; Plešek, J. On the acidity characteristics of decaborane(14) and its benzyl derivatives in organic solvent-water systems. *Collect. Czech. Chem. Commun.* **1975**, *40*, 3593–3601. [CrossRef]
146. McCrary, P.D.; Barber, P.S.; Kelley, S.P.; Rogers, R.D. Nonaborane and decaborane cluster anions can enhance the ignition delay in hypergolic ionic liquids and induce hypergolicity in molecular solvents. *Inorg. Chem.* **2014**, *53*, 4770–4776. [CrossRef] [PubMed]
147. Sneddon, L.G.; Huffman, J.C.; Schaeffer, R.O.; Streib, W.E. Structure of the $B_{10}H_{13}^-$ ion. *J. Chem. Soc. Chem. Commun.* **1972**, 474–475. [CrossRef]
148. Wynd, A.J.; Welch, A.J. Structure of $[PhCH_2NMe_3]^+[B_{10}H_{13}]^-$. *Acta Cryst. C* **1989**, *45*, 615–617. [CrossRef]
149. Siedle, A.R.; Bodner, G.M.; Todd, L.J. Studies in boron hydrides—V: Assignment of the ^{11}B NMR spectrum of the tridecahydro decaborate(1-) ion. *J. Inorg. Nucl. Chem.* **1971**, *33*, 3671–3676. [CrossRef]
150. Wilks, P.H.; Carter, J.C. Preparation and properties of sodium decaboranate(12,2-). *J. Am. Chem. Soc.* **1966**, *88*, 3441. [CrossRef]
151. Bridges, A.N.; Gaines, D.F. The dianion of *nido*-decaborane(14), *nido*-dodecahydrodecaborate(2-), $[B_{10}H_{12}^{2-}]$, and its solution behavior. *Inorg. Chem.* **1995**, *34*, 4523–4524. [CrossRef]
152. Hofmann, M.; von Ragué Schleyer, P. Structures of *arachno*- and *hypho*- B_{10} clusters and stability of their possible Lewis base adducts ($[B_{10}H_{12}]^{2-}$, $[B_{10}H_{12} \cdot L]^{2-}$, $[B_{10}H_{12} \cdot 2L]^{2-}$, $[B_{10}H_{13}]^-$, $[B_{10}H_{13} \cdot L]^-$, $[B_{10}H_{12} \cdot 2L]$). An *ab initio*/IGLO/NMR investigation. *Inorg. Chem.* **1998**, *37*, 5557–5565. [CrossRef]
153. Muettterties, E.L. Chemistry of boranes. VI. Preparation and structure of $B_{10}H_{14}^{2-}$. *Inorg. Chem.* **1963**, *2*, 647–648. [CrossRef]
154. Kendall, D.S.; Lipscomb, W.N. Crystal structure of tetramethylammonium tetradecahydrodecaborate. Structure of the $B_{10}H_{14}^{2-}$ ion. *Inorg. Chem.* **1973**, *12*, 546–551. [CrossRef]
155. Lipscomb, W.N.; Wiersema, R.J.; Hawthorne, M.F. Structural ambiguity of the $B_{10}H_{14}^{2-}$ ion. *Inorg. Chem.* **1972**, *11*, 651–652. [CrossRef]
156. Schaeffer, R.; Tebbe, F. Formation of $B_{10}H_{15}^-$ as an intermediate in borohydride attack on decaborane-14. *Inorg. Chem.* **1964**, *3*, 1638–1640. [CrossRef]
157. Rietz, R.R.; Siedle, A.R.; Schaeffer, R.O.; Todd, L.J. High-resolution nuclear magnetic resonance study of the pentadecahydro-decaborate(1-) ion. *Inorg. Chem.* **1973**, *12*, 2100–2102. [CrossRef]
158. Zahkarkin, L.I.; Stanko, V.I.; Chapovskii, Y.A. Reactions of acetals and ortho-ethers with decaborane and diacetonitrile decaborane. *Bull. Acad. Sci. USSR Div. Chem. Sci.* **1962**, *11*, 1048–1049. [CrossRef]

159. Lee, S.H.; Park, Y.J.; Yoon, C.M. Reductive etherification of aromatic aldehydes with decaborane. *Tetrahedron Lett.* **1999**, *40*, 6049–6050. [CrossRef]
160. Funke, U.; Jiay, H.; Fischer, S.; Scheunemann, M.; Steinbach, J. One-step reductive etherification of 4-[¹⁸F]fluoro-benzaldehyde with decaborane. *J. Label Compd. Radiopharm.* **2006**, *49*, 745–755. [CrossRef]
161. Park, E.S.; Lee, J.H.; Kim, S.J.; Yoon, C.M. One-pot reductive amination of acetals with aromatic amines using decaborane (B₁₀H₁₄) in methanol. *Synth. Commun.* **2003**, *33*, 3387–3396. [CrossRef]
162. Toyosuke, T.; Tsuneo, M.; Katsunori, K.; Yuichi, I. The reaction of decaborane with carbonyl compounds. *Bull. Chem. Soc. Jpn.* **1978**, *51*, 1259–1260. [CrossRef]
163. Bae, J.W.; Lee, S.H.; Jung, Y.J.; Yoon, C.-O.M.; Yoon, C.M. Reduction of ketones to alcohols using a decaborane/pyrrolidine/cerium(III) chloride system in methanol. *Tetrahedron Lett.* **2001**, *42*, 2137–2139. [CrossRef]
164. Lee, S.H.; Nam, M.H.; Cho, M.Y.; Yoo, B.W.; Rhee, H.J.; Yoon, C.M. Chemoselective reduction of aldehydes using decaborane in aqueous solution. *Synth. Commun.* **2006**, *36*, 2469–2474. [CrossRef]
165. Lee, S.H.; Jung, Y.J.; Cho, Y.J.; Yoon, C.-O.M.; Hwang, H.-J.; Yoon, C.M. Dehalogenation of α -halocarbonyls using decaborane as a transfer hydrogen agent in methanol. *Synth. Commun.* **2001**, *31*, 2251–2254. [CrossRef]
166. Lee, S.H.; Park, J.Y.; Yoon, C.M. Hydrogenation of alkenes or alkynes using decaborane in methanol. *Tetrahedron Lett.* **2000**, *41*, 887–889. [CrossRef]
167. Hawthorne, M.F.; Miller, J.J. Deuterium exchange of decaborane with deuterium oxide and deuterium chloride. *J. Am. Chem. Soc.* **1958**, *80*, 754. [CrossRef]
168. Miller, J.J.; Hawthorne, M.F. The course of base-catalyzed hydrogen exchange in decaborane. *J. Am. Chem. Soc.* **1959**, *81*, 4501–4503. [CrossRef]
169. Dupont, J.A.; Hawthorne, M.F. The nature of the electrophilic deuterium exchange reaction of decaborane with deuterium chloride. *J. Am. Chem. Soc.* **1962**, *84*, 1804–1808. [CrossRef]
170. Dupont, J.A.; Hawthorne, M.F. Deuterium exchange of decaborane with deuterium chloride under electrophilic conditions. *J. Am. Chem. Soc.* **1959**, *81*, 4998–4999. [CrossRef]
171. Dopke, J.A.; Gaines, D.F. Deuteration of decaborane(14) via exchange with deuterated aromatic solvents. *Inorg. Chem.* **1999**, *38*, 4896–4897. [CrossRef]
172. Gaines, D.F.; Beall, H. Hydrogen–deuterium exchange in decaborane(14): Mechanistic studies. *Inorg. Chem.* **2000**, *39*, 1812–1813. [CrossRef] [PubMed]
173. Hillman, M. The chemistry of decaborane. Iodination studies. *J. Am. Chem. Soc.* **1960**, *82*, 1096–1099. [CrossRef]
174. Sprecher, R.F.; Aufderheide, B.E.; Luther, G.W., III; Carter, J.C. Boron-11 nuclear magnetic resonance chemical shift assignments for monohalogenated decaborane(14) isomers. *J. Am. Chem. Soc.* **1974**, *96*, 4404–4410. [CrossRef]
175. Stuchlik, J. Gas chromatographic separation of 1- and 2-halogenodecaboranes. *J. Chromatogr. A* **1973**, *81*, 142–143. [CrossRef]
176. Schaeffer, R.; Shoolery, J.N.; Jones, R. Structures of halogen substituted boranes. *J. Am. Chem. Soc.* **1958**, *80*, 2670–2673. [CrossRef]
177. Williams, R.E.; Onak, T.P. Boron-11 nuclear magnetic resonance spectra (32.1 Mc.) of alkylated derivatives of dicarbahexaborane(8) and 1-iododecaborane(14). *J. Am. Chem. Soc.* **1964**, *86*, 3159–3160. [CrossRef]
178. Hillman, M. The chemistry of decaborane. II. Iodination in solvent. *J. Inorg. Nucl. Chem.* **1960**, *12*, 384–385. [CrossRef]
179. Wallbridge, M.H.G.; Williams, J.; Williams, R.L. Boron hydride derivatives. Part XI. Iodination of decaborane. *J. Chem. Soc. A* **1967**, 132–133. [CrossRef]
180. Safronov, A.V.; Sevryugina, Y.V.; Jalisatgi, S.S.; Kennedy, R.D.; Barnes, C.L.; Hawthorne, M.F. Unfairly forgotten member of the iodicborane family: Synthesis and structural characterization of 8-iodo-1,2-dicarba-closo-dodecaborane, its precursors, and derivatives. *Inorg. Chem.* **2012**, *51*, 2629–2637. [CrossRef] [PubMed]
181. Sequeira, A.; Hamilton, W.C. Crystal and molecular structure of monoiododecaborane. *Inorg. Chem.* **1967**, *6*, 1281–1286. [CrossRef]
182. Schaeffer, R. The molecular structure of B₁₀H₁₂I₂. *J. Am. Chem. Soc.* **1957**, *79*, 2726–2728. [CrossRef]
183. Plešek, J.; Štíbr, B.; Heřmánek, S. Chemistry of boranes. VI. The reaction of bis-dialkylsulphido-dodecahydrodecaboranes with hydrohalogens. General preparation of 6- (or 5-) halogentridecahydrodecaboranes. *Collect. Czech. Chem. Commun.* **1966**, *31*, 4744–4745. [CrossRef]
184. Sedmera, P.; Hanousek, F.; Samek, Z. Chemistry of boranes. XIII. Determination of structure of some halogenedecaboranes and oxido-bis-tridecahydrodecaborane by means of ¹¹B NMR and IR spectra. *Collect. Czech. Chem. Commun.* **1968**, *33*, 2169–2175. [CrossRef]
185. Štíbr, B.; Plešek, J.; Heřmánek, S. Chemistry of boranes. XV. Synthesis, properties, reactions and mechanism of formation of 5(6)-halogenotridecahydrodecaboranes. *Collect. Czech. Chem. Commun.* **1969**, *34*, 194–205. [CrossRef]
186. Ewing, W.C.; Carroll, P.J.; Sneddon, L.G. Crystallographic characterizations and new high-yield synthetic routes for the complete series of 6-X-B₁₀H₁₃ halodecaboranes (X = F, Cl, Br, I) via superacid-induced cage-opening reactions of closo-B₁₀H₁₀²⁻. *Inorg. Chem.* **2008**, *47*, 8580–8582. [CrossRef]
187. Ewing, W.C.; Carroll, P.J.; Sneddon, L.G. Efficient Syntheses of 5-X-B₁₀H₁₃ halodecaboranes via the photochemical (X = I) and/or base-catalyzed (X = Cl, Br, I) isomerization reactions of 6-X-B₁₀H₁₃. *Inorg. Chem.* **2010**, *49*, 1983–1994. [CrossRef] [PubMed]
188. Zakharkin, L.I.; Kalinin, V.N. Halogenation of decaborane in the presence of aluminum chloride. *Zh. Obshch. Khim.* **1966**, *36*, 2160–2162.

189. Bonnetot, B.; Miele, P.; Naoufal, D.; Mongeot, H. The interaction of the $[B_{10}H_{10}]^{2-}$ cage with Lewis acids and the formation of decaborane derivatives by cage-opening reactions. *Collect. Czech. Chem. Commun.* **1997**, *62*, 1273–1278. [\[CrossRef\]](#)
190. Stuchlík, J.; Heřmánek, S.; Plešek, J.; Štíbr, B. Chemistry of boranes. XVIII. A preparative separation of halogenodecaboranes. The isolation of 1-, 2-, 5-, and 6-bromotridecahydrodecaboranes. *Collect. Czech. Chem. Commun.* **1970**, *35*, 339–343. [\[CrossRef\]](#)
191. Dupont, T.J.; Loffredo, R.E.; Haltiwanger, R.C.; Turner, C.A.; Norman, A.D. Oxidative cleavage of dimethylstanna-undecaborane: Preparation and structural characterization of 5,10-dibromodecaborane(14). *Inorg. Chem.* **1978**, *17*, 2062–2067. [\[CrossRef\]](#)
192. Hillman, M.; Mangold, D.J. Chlorodecaborane. *Inorg. Chem.* **1965**, *4*, 1356–1357. [\[CrossRef\]](#)
193. Williams, R.E.; Pier, E. Chlorodecaboranes identified as 1-ClB₁₀H₁₃ and 2-ClB₁₀H₁₃ by 64.2-Mc. ¹¹B nuclear magnetic resonance spectra. *Inorg. Chem.* **1965**, *4*, 1357–1358. [\[CrossRef\]](#)
194. Mongeot, H.; Atchekzai, J.; Bonnetot, B.; Colombier, M. Preparation du 6-B₁₀H₁₃Cl a partir de melanges AlCl₃-(Et₄N)₂B₁₀H₁₀. *Bull. Soc. Chim. Fr.* **1987**, 75–77.
195. Bonnetot, B.; Aboukhassib, A.; Mongeot, H. Study of the interaction of AlCl₃ with the B₁₀H₁₀²⁻ cage in the solid state. *Inorg. Chim. Acta* **1989**, *156*, 183–187. [\[CrossRef\]](#)
196. Hawthorne, M.F.; Miller, J.J. The alkoxylation of decaborane. *J. Am. Chem. Soc.* **1960**, *82*, 500. [\[CrossRef\]](#)
197. Norman, A.D.; Rosell, S.L. Evidence of terminal ethoxy group substitution in ethoxydecaborane(14). *Inorg. Chem.* **1969**, *8*, 2818–2820. [\[CrossRef\]](#)
198. Loffredo, R.E.; Drullinger, L.F.; Slater, J.A.; Turner, C.A.; Norman, A.D. Preparation and properties of 6-ethoxy-, 6-phenyl-, and 6-trimethylsiloxydecaborane(14). *Inorg. Chem.* **1976**, *15*, 478–480. [\[CrossRef\]](#)
199. Beachell, H.C.; Schar, W.C. The reaction of decaborane with substituted alcohols. *J. Am. Chem. Soc.* **1958**, *80*, 2943–2945. [\[CrossRef\]](#)
200. Amberger, E.; Leidl, P. Synthese von (CH₃)₃SiB₁₀H₁₃. *J. Organomet. Chem.* **1969**, *18*, 345–347. [\[CrossRef\]](#)
201. Ewing, W.C.; Carroll, P.J.; Sneddon, L.G. Syntheses and surprising regioselectivity of 5- and 6-substituted decaboranyl ethers via the nucleophilic attack of alcohols on 6- and 5-halodecaboranes. *Inorg. Chem.* **2011**, *50*, 4054–4064. [\[CrossRef\]](#)
202. Hawthorne, M.F.; Mavunkal, I.J.; Knobler, C.B. Electrophilic reactions of protonated *closo*-B₁₀H₁₀²⁻ with arenes, alkane C-H bonds, and triflate ion forming aryl, alkyl, and triflate *nido*-6-X-B₁₀H₁₃ derivatives. *J. Am. Chem. Soc.* **1992**, *114*, 4427–4429. [\[CrossRef\]](#)
203. Bondarev, O.; Sevryugina, Y.V.; Jalisatgi, S.S.; Hawthorne, M.F. Acid-induced opening of [*closo*-B₁₀H₁₀]²⁻ as a new route to 6-Substituted *nido*-B₁₀H₁₃ decaboranes and related carboranes. *Inorg. Chem.* **2012**, *51*, 9935–9942. [\[CrossRef\]](#)
204. Berkeley, E.R.; Ewing, W.C.; Carroll, P.J.; Sneddon, L.G. Synthesis, structural characterization, and reactivity studies of 5-CF₃SO₃-B₁₀H₁₃. *Inorg. Chem.* **2014**, *53*, 5348–5358. [\[CrossRef\]](#)
205. Wang, Y.; Han, H.; Kang, J.-X.; Peng, J.; Lu, X.; Cao, H.-J.; Liu, Z.; Chen, X. Silylium ion-mediated cage-opening functionalization of *closo*-B₁₀H₁₀²⁻ salts. *Chem. Commun.* **2022**, *58*, 11933–11936. [\[CrossRef\]](#) [\[PubMed\]](#)
206. Naoufal, D.; Kodeih, M.; Cornu, D.; Miele, P. New method of synthesis of 6-hydroxy-*nido*-decaborane 6-(OH)B₁₀H₁₃ by cage opening of *closo*-[B₁₀H₁₀]²⁻. *J. Organomet. Chem.* **2005**, *690*, 2787–2789. [\[CrossRef\]](#)
207. Greenwood, N.N.; Hails, M.J.; Kennedy, J.D.; McDonald, W.S. Reactions of 6,6'-bis(*nido*-decaboranyl) oxide and 6-hydroxy-*nido*-decaborane with dihalogenobis(phosphine) complexes of nickel, palladium, and platinum, and some related chemistry; nuclear magnetic resonance investigations and the crystal and molecular structures of bis(dimethylphosphine)-di-μ-(2,3,4-η³-*nido*-hexaboranyl)-diplatinum(Pt-Pt), [Pt₂(μ-η³-B₆H₉)₂(PMe₂Ph)₂], and of 2,4-dichloro-1,1-bis(dimethylphenylphosphine)-*closo*-1-nickeladecaborane, [(PhMe₂P)₂NiB₉H₇Cl₂]. *J. Chem. Soc. Dalton Trans.* **1985**, 953–972. [\[CrossRef\]](#)
208. Štíbr, B.; Plešek, J.; Hanousek, F.; Heřmánek, S. Chemistry of boranes. XXIII. Reaction of 6,9-bis(dialkylsulfido)-dodecahydrodecaboranes with mercuric salts. *Collect. Czech. Chem. Commun.* **1971**, *36*, 1794–1799. [\[CrossRef\]](#)
209. Kelley, S.P.; Rachiero, G.P.; Titi, H.M.; Rogers, R.D. New reactions for old ions: Cage rearrangements, hydrolysis, and two-electron reduction of *nido*-decaborane in neat 1-ethyl-3-methylimidazolium acetate. *ACS Omega* **2018**, *3*, 8491–8496. [\[CrossRef\]](#) [\[PubMed\]](#)
210. Plešek, J.; Heřmánek, S.; Štíbr, B. Chemistry of boranes. VIII. Synthesis and reactions of 6,6'-oxido-bis-tridecahydrodecaborane. *Collect. Czech. Chem. Commun.* **1968**, *33*, 691–698. [\[CrossRef\]](#)
211. Kennedy, J.D.; Greenwood, N.N. A proton and boron-11 NMR study of icosaborane oxide, B₂₀H₁₆O. *Inorg. Chim. Acta* **1980**, *38*, 93–96. [\[CrossRef\]](#)
212. Greenwood, N.N.; McDonald, W.S.; Spalding, T.R. Crystal and molecular structure of 6,6'-bis(*nido*-decaboranyl) oxide (B₁₀H₁₃)₂O. *J. Chem. Soc. Dalton Trans.* **1980**, 1251–1252. [\[CrossRef\]](#)
213. Bonnetot, B.; Tangi, A.; Colombier, M.; Mongeot, H. Dehydration of (H₃O)₂B₁₀H₁₀: An improved preparation of icosaborane oxide, (B₁₀H₁₃)₂O. *Inorg. Chim. Acta* **1985**, *105*, L15–L16. [\[CrossRef\]](#)
214. Pace, R.J.; Williams, J.; Williams, R.L. Boron hydride derivatives. Part VII. The characterisation of some decaborane derivatives of the type, B₁₀H₁₂, 2M. *J. Chem. Soc.* **1961**, 2196–2204. [\[CrossRef\]](#)
215. Knoth, W.H.; Muetterties, E.L. Chemistry of boranes. II: Decaborane derivatives based on the B₁₀H₁₂ structural unit. *J. Inorg. Nucl. Chem.* **1961**, *20*, 66–72. [\[CrossRef\]](#)
216. Fein, M.M.; Green, J.; Bobinski, J.; Cohen, M.S. Reaction products from decaborane and amides. *Inorg. Chem.* **1965**, *4*, 583–584. [\[CrossRef\]](#)
217. Cragg, R.H.; Fortuin, M.S.; Greenwood, N.N. Complexes of decaborane. Part I. Ultraviolet spectra of some bis-(ligand) complexes containing phosphorus and sulphur. *J. Chem. Soc. A* **1970**, 1817–1821. [\[CrossRef\]](#)
218. Janoušek, Z.; Plešek, J.; Plzák, Z. Open cage boranes and heteroborane thiols: Syntheses, structures, and some properties. *Collect. Czech. Chem. Commun.* **1979**, *44*, 2904–2907.

219. Bould, J.; Macháček, J.; Londesborough, M.G.S.; Macías, R.; Kennedy, J.D.; Bastl, Z.; Rupper, P.; Baše, T. Decaborane thiols as building blocks for self-assembled monolayers on metal surfaces. *Inorg. Chem.* **2012**, *51*, 1685–1694. [CrossRef]
220. Zakharkin, L.I.; Stanko, V.I.; Okhlobystin, O.Y. Reaction of decaborane and pentaborane with mercaptans and sulfides. *Bull. Acad. Sci. USSR Div. Chem. Sci.* **1961**, *10*, 1942–1943. [CrossRef]
221. Hawthorne, M.F.; Pilling, R.L.; Grimes, R.N. The mechanism of $B_{10}H_{10}^{-2}$ formation from $B_{10}H_{12}(\text{ligand})_2$ species. *J. Am. Chem. Soc.* **1967**, *89*, 1067–1074. [CrossRef]
222. Beall, H.; Gaines, D.F. Reactions of 6,9-bis(dimethyl sulfide)-decaborane(14), 6,9- $[(CH_3)_2S]_2B_{10}H_{12}$: Mechanistic considerations. *Inorg. Chem.* **1998**, *37*, 1420–1422. [CrossRef]
223. Sands, D.E.; Zalkin, A. The crystal structure of $B_{10}H_{12}[S(CH_3)_2]_2$. *Acta Cryst.* **1962**, *15*, 410–417. [CrossRef]
224. Yumatov, V.D.; Murakhtanov, V.V.; Volkov, V.V.; Il'inchik, E.A.; Volkov, O.V. Comparative study of electronic structure of 6,9-bis(dimethyl sulfide)-*arachno*-decaborane(12) $B_{10}H_{12}[S(CH_3)_2]_2$ in a series of sulfide derivatives by the X-ray emission method. *Russ. J. Inorg. Chem.* **1998**, *43*, 1557–1561.
225. Yumatov, V.D.; Il'inchik, E.A.; Mazalov, L.N.; Volkov, O.V.; Volkov, V.V. X-Ray and X-ray photoelectron spectroscopy studies of the electronic structure of borane derivatives. *J. Struct. Chem.* **2001**, *42*, 281–295. [CrossRef]
226. Il'inchik, E.A.; Volkov, V.V.; Mazalov, L.N. X-ray photoelectron spectroscopy of boron compounds. *J. Struct. Chem.* **2005**, *46*, 523–534. [CrossRef]
227. Volkov, V.V.; Ikorskii, V.N.; Dunaev, S.T. Diamagnetism of compounds of the $B_{10}H_{12}L_2$ series. *Bull. Acad. Sci. USSR Div. Chem. Sci.* **1988**, *37*, 845–848. [CrossRef]
228. Zakharkin, L.I.; Stanko, V.I.; Klimova, A.I. Exchange reactions of decaborane complexes of the type $B_{10}H_{12}[X]_2$. *Bull. Acad. Sci. USSR Div. Chem. Sci.* **1964**, *13*, 857–858. [CrossRef]
229. Graybill, B.M.; Hawthorne, M.F. The nature of the colored 6,9-bis-pyridine decaborane molecule, $B_{10}H_{12}Py_2$. *J. Am. Chem. Soc.* **1961**, *83*, 2673–2676. [CrossRef]
230. Marshall, M.D.; Hunt, R.M.; Hefferan, G.T.; Adams, R.M.; Makhlof, J.M. Opening the $B_{10}H_{10}^{-2}$ -cage to produce $B_{10}H_{12}(Et_2S)_2$. *J. Am. Chem. Soc.* **1967**, *89*, 3361–3362. [CrossRef]
231. Guillevis, G.; Dazord, J.; Mongeot, H.; Cueilleron, J. Improved conversion of potassium tetrahydroborate into bis(dialkylsulfide)-decaborane(12), $B_{10}H_{12}(R_2S)_2$, via bis(tetraethylammonium) decahydrodecaborate, $(Et_4N)_2B_{10}H_{10}$. *J. Chem. Res. (S)* **1978**, 402.
232. Wang, G.-C.; Lu, Y.-X.; Huang, X.-Y.; Dai, L.-X. A new method for the synthesis of bis(diethylsulfide)decaborane. *Acta Chim. Sin.* **1981**, *39*, 251–254. Available online: http://sioc-journal.cn/Jwk_hxxb/EN/Y1981/V39/I3/251 (accessed on 31 July 2023).
233. Heying, T.L.; Naar-Colin, C. Some chemistry of substituted decaboranes. *Inorg. Chem.* **1964**, *3*, 282–285. [CrossRef]
234. Ahmad, R.; Crook, J.E.; Greenwood, N.N.; Kennedy, J.D. Synthesis, reactions, and nuclear magnetic resonance studies of some substituted *arachno*-decaborane and *arachno*-nonaborane derivatives, and the isolation of novel polyhedral diplatinaboranes. Crystal and molecular structure of $[Pt_2(PMe_2Ph)_2(\eta^3-B_2H_5)(\eta^3-B_6H_9)]$. *J. Chem. Soc. Dalton Trans.* **1986**, 2433–2442. [CrossRef]
235. V. Petříček, V.; Cisařova, I.; Subrtova, V. Structure of $\sigma(+)$ -5-bromo-6,9-bis(dimethylsulphido)-*nido*-decaborane(12), $C_4H_{23}B_{10}BrS_2$, determined with a twinned crystal. *Acta Cryst. C* **1983**, *39*, 1070–1072. [CrossRef]
236. Bould, J.; Dörfler, U.; Thornton-Pett, M.; Kennedy, J.D. A rearrangement of the 10-boron *nido*/*arachno* decaboranyl cluster. *Inorg. Chem. Commun.* **2001**, *4*, 544–546. [CrossRef]
237. Bridges, A.N.; Powell, D.R.; Dopke, J.A.; Desper, J.M.; Gaines, D.F. Monoalkyldecaborane(14) syntheses via nucleophilic alkylation and hydroboration. *Inorg. Chem.* **1998**, *37*, 503–509. [CrossRef]
238. Bould, J.; Dörfler, U.; Rath, N.P.; Barton, L.; Kilner, C.A.; Londesborough, M.G.S.; Ormsby, D.L.; Kennedy, J.D. Macropolyhedral boron-containing cluster chemistry. A synthetic approach via the auto-fusion of $[6,9-(SMe_2)_2\text{-}arachno\text{-}B_{10}H_{12}]$. *Dalton Trans.* **2006**, 3752–3765. [CrossRef]
239. Beachell, H.C.; Hoffman, D.E. The reaction of decaborane with amines and related compounds. *J. Am. Chem. Soc.* **1962**, *84*, 180–182. [CrossRef]
240. Schaeffer, R. A new type of substituted borane. *J. Am. Chem. Soc.* **1957**, *79*, 1006–1007. [CrossRef]
241. van der Maas Reddy, J.; Lipscomb, W.N. Molecular structure of $B_{10}H_{12}(CH_3CN)_2$. *J. Am. Chem. Soc.* **1959**, *81*, 754. [CrossRef]
242. van der Maas Reddy, J.; Lipscomb, W.N. Molecular structure of $B_{10}H_{12}(CH_3CN)_2$. *J. Chem. Phys.* **1959**, *31*, 610–616. [CrossRef]
243. Mebs, S.; Kalinowski, R.; Grabowsky, S.; Förster, D.; Kickbusch, R.; Justus, E.; Morgenroth, W.; Paulmann, C.; Luger, P.; Gabel, D.; et al. Real-space indicators for chemical bonding. Experimental and theoretical electron density studies of four deltahedral boranes. *Inorg. Chem.* **2011**, *50*, 90–103. [CrossRef] [PubMed]
244. Beall, H. Icosahedral carboranes. XVII. Simplified preparation of *o*-carborane. *Inorg. Chem.* **1972**, *11*, 637–638. [CrossRef]
245. Hawthorne, M.F.; Pitochelli, A.R. Displacement reactions on the $B_{10}H_{12}$ unit. *J. Am. Chem. Soc.* **1958**, *80*, 6685. [CrossRef]
246. Hawthorne, M.F.; Pitochelli, A.R. The reactions of bis-acetonitrile decaborane with amines. *J. Am. Chem. Soc.* **1959**, *81*, 5519. [CrossRef]
247. Fein, M.M.; Bobinski, J.; Paustian, J.E.; Grafstein, D.; Cohen, M.S. Reaction of decaborane and its derivatives. II. Addition reactions of 6,9-bis(acetonitrile)decaborane with hydrazine. *Inorg. Chem.* **1965**, *4*, 422. [CrossRef]
248. Froehner, G.; Challis, K.; Gagnon, K.; Getman, T.D.; Luck, R.L. A re-investigation of the reactions of amines and alcohols with 6,9-bis(acetonitrile)decaborane. *Synth. React. Inorg. Metal-Org. Nano-Metal Chem.* **2007**, *36*, 777–785. [CrossRef]
249. Stogniy, M.Y.; Erokhina, S.A.; Sivaev, I.B.; Bregadze, V.I. Nitrilium derivatives of polyhedral boron compounds (boranes, carboranes, metallacarboranes): Synthesis and reactivity. *Phosphorus Sulfur Silicon Relat. Elem.* **2019**, *194*, 983–988. [CrossRef]

250. Zhdanov, A.P.; Nelyubin, A.V.; Klyukin, I.N.; Selivanov, N.A.; Bortnikov, E.O.; Grigoriev, M.S.; Zhizhin, K.Y.; Kuznetsov, N.T. Nucleophilic addition reaction of secondary amines to acetonitrilium *closo*-decaborate $[2-B_{10}H_9NCCH_3]^-$. *Russ. J. Inorg. Chem.* **2019**, *64*, 841–846. [CrossRef]
251. Stogniy, M.Y.; Erokhina, S.A.; Suponitsky, K.Y.; Anisimov, A.A.; Godovikov, I.A.; Sivaev, I.B.; Bregadze, V.I. Synthesis of novel carboranyl amidines. *J. Organomet. Chem.* **2020**, *909*, 121111. [CrossRef]
252. Bogdanova, E.V.; Stogniy, M.Y.; Chekulaeva, L.A.; Anisimov, A.A.; Suponitsky, K.Y.; Sivaev, I.B.; Grin, M.A.; Mironov, A.F.; Bregadze, V.I. Synthesis and reactivity of propionitrilium derivatives of cobalt and iron bis(dicarbollides). *New J. Chem.* **2020**, *44*, 15836–15848. [CrossRef]
253. El Anwar, S.; Růžicková, Z.; Bovol, D.; Fojt, L.; Grüner, B. Tetrazole ring substitution at carbon and boron sites of the cobalt bis(dicarbollide) ion available via dipolar cycloadditions. *Inorg. Chem.* **2020**, *59*, 17430–17442. [CrossRef] [PubMed]
254. Bogdanova, E.V.; Stogniy, M.Y.; Suponitsky, K.Y.; Sivaev, I.B.; Bregadze, V.I. Synthesis of boronated amidines by addition of amines to nitrilium derivative of cobalt bis(dicarbollide). *Molecules* **2021**, *26*, 6544. [CrossRef] [PubMed]
255. Voinova, V.V.; Selivanov, N.A.; Plyushchenko, I.V.; Vokuev, M.F.; Bykov, A.Y.; Klyukin, I.N.; Novikov, A.S.; Zhdanov, A.P.; Grigoriev, M.S.; Rodin, I.A.; et al. Fused 1,2-diboraoxazoles based on *closo*-decaborate anion—Novel members of diboroheterocycle class. *Molecules* **2021**, *26*, 248. [CrossRef] [PubMed]
256. Stogniy, M.Y.; Erokhina, S.A.; Suponitsky, K.Y.; Markov, V.Y.; Sivaev, I.B. Synthesis and crystal structures of nickel(II) and palladium(II) complexes with *o*-carboranyl amidine ligands. *Dalton Trans.* **2021**, *50*, 4967–4975. [CrossRef]
257. Nelyubin, A.V.; Selivanov, N.A.; Bykov, A.Y.; Klyukin, I.N.; Novikov, A.S.; Zhdanov, A.P.; Karpechenko, N.Y.; Grigoriev, M.S.; Zhizhin, K.Y.; Kuznetsov, N.T. Primary amine nucleophilic addition to nitrilium *closo*-dodecaborate $[B_{12}H_{11}NCCH_3]^-$: A simple and effective route to the new BNCT drug design. *Int. J. Mol. Sci.* **2021**, *22*, 13391. [CrossRef]
258. Laskova, J.; Ananiev, I.; Kosenko, I.; Serdyukov, A.; Stogniy, M.; Sivaev, I.; Grin, M.; Semioshkin, A.; Bregadze, V.I. Nucleophilic addition reactions to nitrilium derivatives $[B_{12}H_{11}NCCH_3]^-$ and $[B_{12}H_{11}NCCH_2CH_3]^-$. Synthesis and structures of *closo*-dodecaborate-based iminols, amides and amidines. *Dalton Trans.* **2022**, *51*, 3051–3059. [CrossRef]
259. Williams, J.; Williams, R.L.; Wright, J.C. Boron hydride derivatives. Part IX. The reaction of decaborane with ammonia. *J. Chem. Soc.* **1963**, 5816–5824. [CrossRef]
260. Rozenberg, A.S.; Neehiporenko, G.N.; Alekseev, A.P. Decomposition of nitrogen-hydrogen complexes of decaborane(12). 1. The kinetics of the thermal decomposition of decaborane(12) diammoniate. *Bull. Acad. Sci. USSR Div. Chem. Sci.* **1978**, *27*, 284–287. [CrossRef]
261. Baidina, I.A.; Podberezskaya, N.V.; Alekseev, V.I.; Volkov, V.V.; Borisov, S.V. Crystal structure of 6,9-bis-aminododecahydro-*nido*-decaborane $B_{10}H_{12}(NH_3)_2$. *J. Struct. Chem.* **1978**, *19*, 476–479. [CrossRef]
262. Polyanskaya, T.M.; Volkov, V.V. Crystal and molecular structure of 6,9-bis(trimethylamino)-*nido*-decaborane(12) $B_{10}H_{12}[N(CH_3)_3]_2$. *J. Struct. Chem.* **1989**, *30*, 629–634. [CrossRef]
263. Baidina, I.A.; Podberezskaya, N.V.; Volkov, V.V.; Borisov, S.V. Crystal structure of 6,9-bis-(triethylamino)-*nido*-decaborane $B_{10}H_{12}[(C_2H_5)_3N]_2$. *J. Struct. Chem.* **1978**, *19*, 479–482. [CrossRef]
264. Volkov, V.V.; Il'inchik, E.A.; Khudorozhko, G.F.; Yumatov, V.D.; Mazalov, L.N. Comparative study of $B_{10}H_{12}(NH_3)_2$ and $B_{10}H_{12}(NEt_3)_2$. *Bull. Acad. Sci. USSR Div. Chem. Sci.* **1985**, *34*, 2079–2085. [CrossRef]
265. Rozenberg, A.S. Decomposition of nitrogen-hydrogen complexes of decaborane(12). 2. An IR study of the mechanism of decomposition of decaborane(12) diammoniate. *Bull. Acad. Sci. USSR Div. Chem. Sci.* **1978**, *27*, 287–290. [CrossRef]
266. Isaenko, L.I.; Myakishev, K.G.; Posnaya, I.S.; Volkov, V.V. About the thermal stability of several derivatives of boron hydrides. *Izv. Sib. Otd. Akad. Nauk SSSR Ser. Khim.* **1982**, 73–78.
267. Graybill, B.M.; Pitochelli, A.R.; Hawthorne, M.F. The preparation and reactions of $B_{10}H_{13}(\text{Ligand})$ anions. *Inorg. Chem.* **1962**, *1*, 622–626. [CrossRef]
268. Cendrowski-Guillaume, S.M.; O'Loughlin, J.L.; Pelczer, I.; Spencer, J.T. Reactivity of decaborane(14) with pyridine: Synthesis and characterization of the first 6,6-substituted isomer of *nido*- $B_{10}H_{14}$, 6,6-(C_5H_5N) $_2B_{10}H_{12}$, and application of ^{11}B - ^{11}B double-quantum NMR spectroscopy. *Inorg. Chem.* **1995**, *34*, 3935–3941. [CrossRef]
269. Bould, J.; Laromaine, A.; Bullen, N.J.; Viñas, C.; Thornton-Pett, M.; Sillanpää, R.; Kivekäs, R.; Kennedy, J.D.; Teixidor, F. Borane reaction chemistry. Alkyne insertion reactions into boron-containing clusters. Products from the thermolysis of $[6,9-(2-HC\equiv C-C_5H_4N)_2\text{-arachno-}B_{10}H_{12}]$. *Dalton Trans.* **2008**, 1552–1563. [CrossRef]
270. Volkov, V.V.; Myakishev, K.G.; Potapova, O.G.; Polyanskaya, T.M.; Dunaev, S.T.; Il'inchik, E.A.; Baidina, I.A.; Hudorozhko, G.F. Synthesis and physico-chemical study of 6,9-bis-pyridino-*nido*-decaborane(14). *Izv. Sib. Otd. Akad. Nauk SSSR Ser. Khim.* **1988**, *3*, 20–27.
271. Il'inchik, E.A.; Volkov, V.V.; Dunaev, S.T. Structural effects in the electron absorption and luminescence spectra of decaborane(14) derivatives $B_{10}H_{12}L_2$. *J. Struct. Chem.* **1996**, *37*, 51–57. [CrossRef]
272. Volkov, V.V.; Il'inchik, E.A.; Volkov, O.V.; Yuryeva, O.P. The luminescence of cluster derivatives of boron hydrides, and some applied aspects. *Chem. Sustain. Develop.* **2000**, *8*, 185–191. Available online: https://sibran.ru/upload/iblock/fed/the_luminescence_of_cluster_derivatives_of_boron_hydrides_and_some_applied_aspects.PDF (accessed on 31 July 2023).
273. Volkov, V.V.; Il'inchik, E.A.; Yur'eva, O.P.; Volkov, O.V. Luminescence of the derivatives of boranes and adducts of decaborane(14) of the $B_{10}H_{12}[Py(X)]_2$ type. *J. Appl. Spectr.* **2000**, *67*, 864–870. [CrossRef]

274. Volkov, V.V.; Myakishev, K.G.; Dunaev, S.T. Thermal transformations of $B_{10}H_{12}(NH_3)_2$, $B_{10}H_{12}(C_5H_5N)_2$, and $B_{10}H_{12}(C_9H_7N)_2$. *Bull. Acad. Sci. USSR Div. Chem. Sci.* **1988**, *37*, 2234–2236. [\[CrossRef\]](#)
275. Polyanskaya, T.M.; Volkov, V.V.; Andrianov, V.I.; Il'inchik, E.A. Structures of two modifications of 6,9-bis-pyridine-nido-decaborane(12). *Bull. Acad. Sci. USSR Div. Chem. Sci.* **1989**, *38*, 1751–1754. [\[CrossRef\]](#)
276. Londesborough, M.G.S.; Price, C.; Thornton-Pett, M.; Clegg, W.; Kennedy, J.D. Two potential pyridine-borane oligomer and polymer building blocks. Structural characterisation of $[NC_5H_4 \cdot C_5H_4N \cdot B_{10}H_{12} \cdot NC_5H_4 \cdot C_5H_4N]$ and $[Me_2S \cdot B_{10}H_{12} \cdot NC_4H_4N \cdot B_{10}H_{12} \cdot SMe_2]$ by conventional and synchrotron X-ray methods. *Inorg. Chem. Commun.* **1999**, *2*, 298–300. [\[CrossRef\]](#)
277. Genady, A.R.; Fayed, T.A.; Gabel, D. Synthesis, characterization, and spectrophotometric studies of novel fluorescent *arachno* decaborane and nonaborane clusters containing aza-distyrylbenzene derivatives. *J. Organomet. Chem.* **2008**, *693*, 1065–1072. [\[CrossRef\]](#)
278. Hawthorne, M.F.; Pilling, R.L.; Vasavada, R.C. The mechanism of ligand exchange with $B_{10}H_{12}(\text{ligand})_2$ species. *J. Am. Chem. Soc.* **1967**, *89*, 1075–1078. [\[CrossRef\]](#)
279. Rachiero, G.P.; Titi, H.M.; Rogers, R.D. Versatility and remarkable hypergolicity of *exo*-6, *exo*-9 imidazole-substituted *nido*-decaborane. *Chem. Commun.* **2017**, *53*, 7736–7739. [\[CrossRef\]](#)
280. Fetter, N.R. Reaction of decaborane with 2-isopropyl- and 2-methyl-5-(2-chloroethyl) tetrazole. *Chem. Ind.* **1959**, 1548.
281. Kendall, D.S.; Lipscomb, W.N. Molecular structure and two crystal structures of 6-isothiocyanadecaborane, $6-B_{10}H_{13}NCS$. *Inorg. Chem.* **1973**, *12*, 2915–2919. [\[CrossRef\]](#)
282. Müller, J.; Paetzold, P.; Boese, R. The reaction of decaborane with hydrazoic acid: A novel access to azaboranes. *Heteroat. Chem.* **1990**, *1*, 461–465. [\[CrossRef\]](#)
283. Il'inchik, E.A.; Dunaev, S.T.; Myakishev, K.G.; Asanov, I.P. On solvation and thermal transformations of $B_{10}H_{12}(PPh_3)_2$. *Zh. Neorg. Khim.* **1994**, *39*, 1071–1074.
284. Polyanskaya, T.M.; Yumatov, V.D.; Volkov, V.V. Molecular and electronic structure of 6,9-(PPh_3)₂-*arachno*- $B_{10}H_{12}$. *Dokl. Chem.* **2003**, *390*, 144–147. [\[CrossRef\]](#)
285. Fontaine, X.L.R.; Kennedy, J.D. Identification of the *endo,exo* isomer of 6,9-(PM_2Ph)₂-*arachno*- $B_{10}H_{12}$ by nuclear magnetic resonance spectroscopy. *J. Chem. Soc. Dalton Trans.* **1987**, 1573–1575. [\[CrossRef\]](#)
286. Dörfler, U.; McGrath, T.D.; Cooke, P.A.; Kennedy, J.D.; Thornton-Pett, M. *exo,endo* and *exo,exo* isomers of 6,9-(PM_2Ph)₂-*arachno*- $B_{10}H_{12}$ and its halogenated derivatives. Molecular structures of *exo,endo*- and *exo,exo*-6,9-(PM_2Ph)₂-*arachno*- $B_{10}H_{12}$ and *exo*-6,*endo*-9-(PM_2Ph)₂-2-Br-*arachno*- $B_{10}H_{11}$. *J. Chem. Soc. Dalton Trans.* **1997**, 4739–4746. [\[CrossRef\]](#)
287. Zakharkin, L.I.; Stanko, V.I. Complexes of decaborane with organic phosphorus and arsenic compounds. *Bull. Acad. Sci. USSR Div. Chem. Sci.* **1961**, *10*, 1936–1937. [\[CrossRef\]](#)
288. Polak, R.J.; Heying, T.L. The preparation of phosphite and phosphinite decaboranes. *J. Org. Chem.* **1962**, *27*, 1483–1484. [\[CrossRef\]](#)
289. Stanko, V.I.; Klimova, A.I.; Zakharkin, L.I. Complexes of decaborane with trialkyl-, triaryl-, trialkyltrithiophosphites and trialkyl-, trialkyltrithioarsenites. *Bull. Acad. Sci. USSR Div. Chem. Sci.* **1962**, *11*, 856–857. [\[CrossRef\]](#)
290. Schroeder, H.; Reiner, J.R.; Heying, T.L. Chemistry of decaborane-phosphorus compounds. I. Nucleophilic substitutions of bis-(chlorodiphenylphosphine)-decaborane. *Inorg. Chem.* **1962**, *1*, 618–621. [\[CrossRef\]](#)
291. Schroeder, H.; Reiner, J.R.; Knowles, T.A. Chemistry of decaborane-phosphorus compounds. III. Decaborane-14-phosphine polymers. *Inorg. Chem.* **1963**, *2*, 393–396. [\[CrossRef\]](#)
292. Seyferth, D.; Rees, W.S.; Haggerty, J.S.; Lightfoot, A. Preparation of boron-containing ceramic materials by pyrolysis of the decaborane(14)-derived $[B_{10}H_{12} \cdot Ph_2POPPh_2]_x$ polymer. *Chem. Mater.* **1989**, *1*, 45–52. [\[CrossRef\]](#)
293. Packirisamy, S. Decaborane(14)-based polymers. *Progr. Polym. Sci.* **1996**, *21*, 707–773. [\[CrossRef\]](#)
294. Donaghy, K.J.; Carroll, P.J.; Sneddon, L.G. Reactions of 1,1'-bis(diphenylphosphino)ferrocene with boranes, thiaboranes, and carboranes. *Inorg. Chem.* **1997**, *36*, 547–553. [\[CrossRef\]](#)
295. Schroeder, H. Chemistry of decaborane-phosphorus compounds. II. Synthesis and reactions of diphenylphosphinododecaborane-14. *Inorg. Chem.* **1963**, *2*, 390–393. [\[CrossRef\]](#)
296. Friedman, L.B.; Perry, S.L. Crystal and molecular structure of 5,6- μ -diphenylphosphino-decaborane(14). *Inorg. Chem.* **1973**, *12*, 288–293. [\[CrossRef\]](#)
297. Muettetries, E.L.; Aftandilian, V.D. Chemistry of boranes. IV. Phosphine derivatives of $B_{10}H_{14}$ and B_9H_{15} . *Inorg. Chem.* **1962**, *1*, 731–734. [\[CrossRef\]](#)
298. Thornton-Pett, M.; Beckett, M.A.; Kennedy, J.D. Polyhedral phosphaborane chemistry: Crystal and molecular structure of the diphenylphosphido-bridged *arachno*-decaboranyl cluster compound $[PMePh_3][6,9-\mu-(PPh_2)B_{10}H_{12}]$. *J. Chem. Soc. Dalton Trans.* **1986**, 303–308. [\[CrossRef\]](#)
299. Miller, R.W.; Spencer, J.T. Small heteroborane cluster systems. 7. Reaction of phosphalkyne *t*-BuCP with bis-(acetonitrile) decaborane(12). A new synthetic route to a large phosphaborane cluster compound. *Polyhedron* **1996**, *15*, 3151–3155. [\[CrossRef\]](#)
300. Miller, R.W.; Spencer, J.T. Small heteroborane cluster systems. 8. Preparation of phosphaborane clusters from the reaction of polyhedral boranes with low-coordinate phosphorus compounds: Reaction chemistry of phosphalkynes with decaborane(14). *Organometallics* **1996**, *15*, 4293–4300. [\[CrossRef\]](#)
301. Williams, R.L.; Dunstan, I.; Blay, N.J. Boron hydride derivatives. Part IV. Friedel–Crafts methylation of decaborane. *J. Chem. Soc.* **1960**, 5006. [\[CrossRef\]](#)

302. Obenland, C.O.; Newberry, J.R.; Schreiner, W.L.; Bartoszek, E.J. Friedel-Crafts methylation of decaborane. *Ind. Eng. Chem. Prod. Res. Dev.* **1965**, *4*, 281–283. [\[CrossRef\]](#)
303. Polak, R.J.; Goodspeed, N.C. Catalyst study in methylation of decaborane. *Ind. Eng. Chem. Prod. Res. Dev.* **1965**, *4*, 158–160. [\[CrossRef\]](#)
304. Holub, J.; Růžicka, A.; Růžicková, Z.; Fanfrlík, J.; Hnyk, D.; Štíbr, B. Electrophilic methylation of decaborane(14): Selective synthesis of tetramethylated and heptamethylated decaboranes and their conjugated bases. *Inorg. Chem.* **2020**, *59*, 10540–10547. [\[CrossRef\]](#) [\[PubMed\]](#)
305. Blay, N.J.; Dunstan, I.; Williams, R.L. Boron hydride derivatives. Part III. Electrophilic substitution in pentaborane and decaborane. *J. Chem. Soc.* **1960**, 430–433. [\[CrossRef\]](#)
306. Cueilleron, J.; Guillot, P. Preparation de quelques composés du decaborane. *Bull. Chim. Fr.* **1960**, 2044–2052.
307. Perloff, A. The crystal structure of 1-ethyldecaborane. *Acta Cryst.* **1964**, *17*, 332–338. [\[CrossRef\]](#)
308. Dunstan, I.; Williams, R.L.; Blay, N.J. Boron hydride derivatives. Part V. Nucleophilic substitution in decaborane. *J. Chem. Soc.* **1960**, 5012–5015. [\[CrossRef\]](#)
309. Dunstan, I.; Blay, N.J.; Williams, R.L. Boron hydride derivatives. Part VI. Decaborane Grignard reagent. *J. Chem. Soc.* **1960**, 5016–5019. [\[CrossRef\]](#)
310. Gallagher, J.; Siegel, B. Grignard synthesis of alkyl decaboranes. *J. Am. Chem. Soc.* **1959**, *81*, 504. [\[CrossRef\]](#)
311. Siegel, B.; Mack, J.L.; Lowe, J.U.; Gallagher, J. Decaborane Grignard reagents. *J. Am. Chem. Soc.* **1958**, *80*, 4523–4526. [\[CrossRef\]](#)
312. Palchak, R.J.F.; Norman, J.H.; Williams, R.E. Decaborane, “6-benzyl” $B_{10}H_{13}$ chemistry. *J. Am. Chem. Soc.* **1961**, *83*, 3380–3384. [\[CrossRef\]](#)
313. Gaines, D.F.; Bridges, A.N. New routes to monoalkyl decaborane(14) derivatives. *Organometallics* **1993**, *12*, 2015–2016. [\[CrossRef\]](#)
314. Tolpin, E.I.; Mizusawa, E.; Becker, D.S.; Venzel, J. Synthesis and chemistry of 9-cyclohexyl-5(7)-(dimethyl sulfide)-nido-decaborane(11), $B_{10}H_{11}C_6H_{11}S(CH_3)_2$. *Inorg. Chem.* **1980**, *19*, 1182–1187. [\[CrossRef\]](#)
315. Millan, M.D.; Davis, J.H. Hydroboration of (1R)-(+)- α -pinene and (1S)-(–)- β -pinene with $B_{10}H_{12}(SMe_2)_2$: A straightforward approach to the preparation of optically active 6-(alkyl)-nido- $B_{10}H_{13}$ derivatives. *Tetrahedron Asymmetry* **1998**, *9*, 709–712. [\[CrossRef\]](#)
316. Mizusawa, E.; Rudnick, S.E.; Eriks, K. The crystal and molecular structure of 9-cyclohexyl-5(7)-(dimethyl sulfide)-nido-decaborane(11), $B_{10}H_{11}C_6H_{11}S(CH_3)_2$. *Inorg. Chem.* **1980**, *19*, 1188–1191. [\[CrossRef\]](#)
317. Kusari, U.; Li, Y.; Bradley, M.G.; Sneddon, L.G. Polyborane reactions in ionic liquids: New efficient routes to functionalized decaborane and o-carborane clusters. *J. Am. Chem. Soc.* **2004**, *126*, 8662–8663. [\[CrossRef\]](#) [\[PubMed\]](#)
318. Kusari, U.; Carroll, P.J.; Sneddon, L.G. Ionic-liquid-promoted decaborane olefin-hydroboration: A new efficient route to 6-R- $B_{10}H_{13}$ derivatives. *Inorg. Chem.* **2008**, *47*, 9203–9215. [\[CrossRef\]](#)
319. Yu, X.-H.; Cao, K.; Huang, Y.; Yang, J.; Li, J.; Chang, G. Platinum catalyzed sequential hydroboration of decaborane: A facile approach to poly(alkenyldecaborane) with decaborane in the mainchain. *Chem. Commun.* **2014**, *50*, 4585–4587. [\[CrossRef\]](#)
320. Boggio, P.; Toppino, A.; Geninatti Cich, S.; Alberti, D.; Marabello, D.; Medana, C.; Prandi, C.; Venturello, P.; Aime, S.; Deagostino, A. The hydroboration reaction as a key for a straightforward synthesis of new MRI-NCT agents. *Org. Biomol. Chem.* **2015**, *13*, 3288–3297. [\[CrossRef\]](#)
321. Naoufal, D.; Laila, Z.; Yazbeck, O.; Hamad, H.; Ibrahim, G.; Aoun, R.; Safa, A.; El Jamal, M. Kanj Synthesis, characterization and mechanism of formation of 6-substituted nido- $B_{10}H_{13}$ decaboranes by the opening reaction of closo-decahydrodecaborate $[B_{10}H_{10}]^{2-}$ cage. *Main Group Chem.* **2013**, *12*, 39–48. [\[CrossRef\]](#)
322. Pender, M.J.; Wideman, T.; Carroll, P.J.; Sneddon, L.G. Transition metal promoted reactions of boron hydrides. 15. Titanium-catalyzed decaborane–olefin hydroborations: One-step, high-yield syntheses of monoalkyldecaboranes. *J. Am. Chem. Soc.* **1998**, *120*, 9108–9109. [\[CrossRef\]](#)
323. Pender, M.J.; Carroll, P.J.; Sneddon, L.G. Transition-metal-promoted reactions of boron hydrides. 17. Titanium-catalyzed decaborane–olefin hydroborations. *J. Am. Chem. Soc.* **2001**, *123*, 12222–12231. [\[CrossRef\]](#) [\[PubMed\]](#)
324. Wei, X.; Carroll, P.J.; Sneddon, L.G. New routes to organodecaborane polymers via ruthenium-catalyzed ring-opening metathesis polymerization. *Organometallics* **2004**, *23*, 163–165. [\[CrossRef\]](#)
325. Wei, X.; Carroll, P.J.; Sneddon, L.G. Ruthenium-catalyzed ring-opening polymerization syntheses of poly(organodecaboranes): New single-source boron-carbide precursors. *Chem. Mater.* **2006**, *18*, 1113–1123. [\[CrossRef\]](#)
326. Pender, M.J.; Forsthoefel, K.M.; Sneddon, L.G. Molecular and polymeric precursors to boron carbide nanofibers, nanocylinders, and nanoporous ceramics. *Pure Appl. Chem.* **2003**, *75*, 1287–1294. [\[CrossRef\]](#)
327. Pender, M.J.; Sneddon, L.G. An efficient template synthesis of aligned boron carbide nanofibers using a single-source molecular precursor. *Chem. Mater.* **2000**, *12*, 280–283. [\[CrossRef\]](#)
328. Li, J.; Yang, H.; Liang, Y.; Chen, J.; Xie, M.; Zhou, L.; Xiong, Q.; Li, W. Ruthenium-catalyzed cascade ring-opening polymerization/hydroboration for the synthesis of low cross-linking poly(6-norbornenyldecaborane) and its thermal property. *Adv. Mater. Res.* **2014**, *1035*, 288–291.
329. Zhang, X.; Li, J.; Cao, K.; Yi, Y.; Yang, J.; Li, B. Synthesis and characterization of B-C polymer hollow microspheres from a new organodecaborane preceramic polymer. *RSC Adv.* **2015**, *5*, 86214–86218. [\[CrossRef\]](#)
330. Wang, J.; Gou, Y.; Jian, K.; Huang, J.; Wang, H. Boron carbide ceramic hollow microspheres prepared from poly(6- $CH_2=CH(CH_2)_4-B_{10}H_{13}$) precursor. *Mater. Design* **2016**, *109*, 408–414. [\[CrossRef\]](#)

331. Wang, J.; Gou, Y.; Zhang, Q.; Jian, K.; Chen, Z.; Wang, H. Linear organodecaborane block copolymer as a single-source precursor for porous boron carbide ceramics. *J. Eur. Ceram. Soc.* **2017**, *37*, 1937–1943. [\[CrossRef\]](#)
332. Li, J.; Cao, K.; Li, J.; Liu, M.; Zhang, S.; Yang, J.; Zhang, Z.; Li, B. Synthesis and ceramic conversion of a new organodecaborane preceramic polymer with high-ceramic-yield. *Molecules* **2018**, *23*, 2461. [\[CrossRef\]](#)
333. Mazighi, K.; Carroll, P.J.; Sneddon, L.G. Transition metal promoted reactions of boron hydrides. 13. Platinum catalyzed synthesis of 6,9-dialkyldecaboranes. *Inorg. Chem.* **1993**, *32*, 1963–1969. [\[CrossRef\]](#)
334. Chatterjee, S.; Carroll, P.J.; Sneddon, L.G. Metal-catalyzed decaborane-alkyne hydroboration reactions: Efficient routes to alkenyldecaboranes. *Inorg. Chem.* **2010**, *49*, 3095–3097. [\[CrossRef\]](#) [\[PubMed\]](#)
335. Chatterjee, S.; Carroll, P.J.; Sneddon, L.G. Iridium and ruthenium catalyzed syntheses, hydroborations, and metathesis reactions of alkenyl-decaboranes. *Inorg. Chem.* **2013**, *52*, 9119–9130. [\[CrossRef\]](#) [\[PubMed\]](#)
336. Ernest, R.L.; Quintana, W.; Rosen, R.; Carroll, P.J.; Sneddon, L.G. Reactions of decaborane(14) with silylated acetylenes. Synthesis of the new monocarbon carborane 9-Me₂S-7-[(Me₃Si)₂CH]CB₁₀H₁₁. *Organometallics* **1987**, *6*, 80–88. [\[CrossRef\]](#)
337. Burgos-Adorno, G.; Carroll, P.J.; Quintana, W. Synthesis and characterization of a new alkenyldecaborane and alkenyl monocarbon carboranes. *Inorg. Chem.* **1996**, *35*, 2568–2575. [\[CrossRef\]](#)
338. Meyer, F.; Paetzold, P.; Englert, U. Reaktion von Decaboran mit dem Phosphaalkin PCtBu. *Chem. Ber.* **1994**, *127*, 93–95. [\[CrossRef\]](#)
339. Bould, J.; Lonsborough, M.G.S.; Ormsby, D.L.; MacBride, J.A.H.; Wade, K.; Kilner, C.A.; Clegg, W.; Teat, S.J.; Thornton-Pett, M.; Greatrex, R.; et al. Macropolyhedral boron-containing cluster chemistry: Models for intermediates en route to globular and discoidal megaloborane assemblies. Structures of [*nido*-B₁₀H₁₂(*nido*-B₅H₈)₂] and [(CH₂CH₂C₅H₄N)-*arachno*-B₁₀H₁₀(NC₅H₄-*closo*-C₂B₁₀H₁₀)] as determined by synchrotron X-ray diffraction analysis. *J. Organomet. Chem.* **2002**, *657*, 256–261. [\[CrossRef\]](#)
340. Kim, S.; Treacy, J.W.; Nelson, Y.A.; Gonzalez, J.A.M.; Gembicky, M.; Houk, K.N.; Spokoyny, A.M. Arene C–H borylation strategy enabled by a non-classical boron cluster-based electrophile. *Nat. Commun.* **2023**, *14*, 1671. [\[CrossRef\]](#)
341. Demel, J.; Kloda, M.; Lang, K.; Škoch, K.; Hynek, J.; Opravil, A.; Novotný, M.; Bould, J.; Ehn, M.; Lonsborough, M.G.S. Direct Phenylation of *nido*-B₁₀H₁₄. *J. Org. Chem.* **2022**, *87*, 10034–10043. [\[CrossRef\]](#)
342. Bůžek, D.; Škoch, K.; Ondrušová, S.; Kloda, M.; Bovol, D.; Mahun, A.; Kobera, L.; Lang, K.; Lonsborough, M.G.S.; Demel, J. “Activated Borane”—A porous borane cluster network as an effective adsorbent for removing organic pollutants. *Chem. Eur. J.* **2022**, *28*, e202201885. [\[CrossRef\]](#)
343. Wille, A.E.; Su, K.; Carroll, P.J.; Sneddon, L.G. New synthetic routes to azacarborane clusters: Nitrile insertion reactions of *nido*-5,6-C₂B₈H₁₁[−] and *nido*-B₁₀H₁₃[−]. *J. Am. Chem. Soc.* **1996**, *118*, 6407–6421. [\[CrossRef\]](#)
344. Baše, K.; Alcock, N.W.; Howarth, O.W.; Powell, H.R.; Harrison, A.T.; Wallbridge, M.G.H. The structure of the *arachno*-[B₁₀H₁₃C≡N]^{2−} anion: An example of *endo* substitution in the decaborane(14) framework. *J. Chem. Soc. Chem. Commun.* **1988**, 341–342. [\[CrossRef\]](#)
345. Orlova, A.M.; Sivaev, I.B.; Lagun, V.L.; Katser, S.B.; Solntsev, K.A.; Kuznetsov, N.T. Synthesis and structure of Pb(Bipy)₂(6-B₁₀H₁₃CN). *Koord. Khim.* **1996**, *22*, 119–124.
346. Sivaev, I.B. Chemistry of 11-vertex polyhedral boron hydrides (Review). *Russ. J. Inorg. Chem.* **2019**, *64*, 955–976. [\[CrossRef\]](#)
347. Geisberger, G.; Linti, G.; Nöth, H. Beiträge zur Chemie des Bors. 213. Reaktionen eines Amino-imino-borans mit Triboran(7) und Decaboran(14). *Chem. Ber.* **1992**, *125*, 2691–2699. [\[CrossRef\]](#)
348. Bridges, A.N.; Liu, J.; Kultyshev, R.G.; Gaines, D.F.; Shore, S.G. Partial insertion of the 9-BBN unit into the *nido*-B₁₀ framework: Preparation and structural characterization of (9-BBN)B₁₀H₁₃ and [(9-BBN)B₁₀H₁₂][−]. *Inorg. Chem.* **1998**, *37*, 3276–3283. [\[CrossRef\]](#)
349. Greenwood, N.N.; Kennedy, J.D.; Taylorson, D. Mass spectroscopic evidence for icosaborane(26). *J. Phys. Chem.* **1978**, *82*, 623–625. [\[CrossRef\]](#)
350. Greenwood, N.N.; Kennedy, J.D.; Spalding, T.R.; Taylorson, D. Isomers of icosaborane(26): Some synthetic routes and preliminary characterisations in the bis(*nido*-decaboranyl) system. *J. Chem. Soc. Dalton Trans.* **1979**, 840–846. [\[CrossRef\]](#)
351. Boocock, S.K.; Cheek, Y.M.; Greenwood, N.N.; Kennedy, J.D. A new route to isomers of icosaborane(26), B₂₀H₂₆. The use of 115.5-MHz ¹¹B and ¹¹B-¹H nuclear magnetic resonance spectroscopy for the comparison and characterisation of separated isomers and the identification of three further icosaboranes as 1,2′-, 2,5′-, and 5,5′(or 5,7′)-(B₁₀H₁₃)₂. *J. Chem. Soc. Dalton Trans.* **1981**, 1430–1437. [\[CrossRef\]](#)
352. Brown, G.M.; Pinson, J.W.; Ingram, L.L. Crystal and molecular structure of 1,5′-bidecaboran(14)yl: A new borane from γ irradiation of decaborane(14). *Inorg. Chem.* **1979**, *18*, 1951–1956. [\[CrossRef\]](#)
353. Bould, J.; Clegg, W.; Kennedy, J.D.; Teat, S.J. Isomeric icosaboranes B₂₀H₂₆: The synchrotron structure of 1,1′-bis(*nido*-decaboranyl). *Acta Cryst. C* **2001**, *57*, 779–780. [\[CrossRef\]](#)
354. Barrett, S.A.; Greenwood, N.N.; Kennedy, J.D.; Thornton-Pett, M. The chemistry of isomers of icosaborane(26): Crystal and molecular structure of 1,2′-bi(*nido*-decaboranyl). *Polyhedron* **1985**, *4*, 1981–1984. [\[CrossRef\]](#)
355. Greenwood, N.N.; Kennedy, J.D.; McDonald, W.S.; Staves, J.; Taylorson, D. Isomers of B₂₀H₂₆: Structural characterisation by X-ray diffraction of 2,2′-bi(*nido*-decaboranyl). *J. Chem. Soc. Chem. Commun.* **1979**, 17–18. [\[CrossRef\]](#)
356. Boocock, S.K.; Greenwood, N.N.; Kennedy, J.D.; McDonald, W.S.; Staves, J. The chemistry of isomeric icosaboranes, B₂₀H₂₆. Molecular structures and physical characterization of 2,2′-bi(*nido*-decaboranyl) and 2,6′-bi(*nido*-decaboranyl). *J. Chem. Soc. Dalton Trans.* **1980**, 790–796. [\[CrossRef\]](#)
357. Boocock, S.K.; Greenwood, N.N.; Kennedy, J.D.; Taylorson, D. Isomers of B₂₀H₂₆: Elucidation of the structure of 6,6′-bi(*nido*-decaboranyl) by ¹¹B-¹H and ¹H-¹¹B n.m.r. spectroscopy. *J. Chem. Soc. Chem. Commun.* **1979**, 16–17. [\[CrossRef\]](#)

358. Bould, J.; Dörfler, U.; Clegg, W.; Teat, S.J.; Thornton-Pett, M.; Kennedy, J.D. Triple linking of the decaboranyl cluster. Structure of $[(\text{SMe}_2)_2\text{B}_{10}\text{H}_{10}(\text{B}_{10}\text{H}_{13})_2]$ as determined by synchrotron X-ray diffraction analysis. *Chem. Commun.* **2001**, 1788–1789. [\[CrossRef\]](#)
359. Olsen, F.P.; Vasavada, R.C.; Hawthorne, M.F. The chemistry of $n\text{-B}_{18}\text{H}_{22}$ and $i\text{-B}_{18}\text{H}_{22}$. *J. Am. Chem. Soc.* **1968**, *90*, 3946–3951. [\[CrossRef\]](#)
360. Li, Y.; Sneddon, L.G. Improved synthetic route to $n\text{-B}_{18}\text{H}_{22}$. *Inorg. Chem.* **2006**, *45*, 470–471. [\[CrossRef\]](#)
361. Londesborough, M.G.S.; Hnyk, D.; Bould, J.; Bould, J.; Serrano-Andres, L.; Sauri, V.; Oliva, J.M.; Kubat, P.; Polivka, T.; Lang, K. Distinct photophysics of the isomers of $\text{B}_{18}\text{H}_{22}$ explained. *Inorg. Chem.* **2012**, *51*, 1471–1479. [\[CrossRef\]](#)
362. Londesborough, M.G.S.; Dolanský, J.; Braborec, J.; Cerdán, L. Interaction of $anti\text{-B}_{18}\text{H}_{22}$ with light. In *Handbook of Boron Science with Applications in Organometallics, Catalysis, Materials and Medicine*; Hosmane, N.S., Eagling, R., Eds.; World Scientific Publishing: London, UK, 2019; Volume 3, pp. 115–136. [\[CrossRef\]](#)
363. Cerdan, L.; Frances-Monerris, A.; Roca-Sanjuan, D.; Bould, J.; Dolandky, J.; Fuciman, M.; Londesborough, M.G.S. Unveiling the role of upper excited electronic states in the photochemistry and laser performance of $anti\text{-B}_{18}\text{H}_{22}$. *J. Mater. Chem. C* **2020**, *8*, 12806–12818. [\[CrossRef\]](#)
364. Tan, C.; Zhang, B.; Chen, J.; Zhang, L.; Huang, X.; Meng, H. Study of hydrolysis kinetic of new laser material [$anti\text{-B}_{18}\text{H}_{22}$]. *Russ. J. Inorg. Chem.* **2019**, *64*, 1359–1364. [\[CrossRef\]](#)
365. Ševčík, J.; Urbanek, P.; Hanulíková, B.; Čapkova, T.; Urbanek, M.; Antoš, J.; Londesborough, M.G.S.; Bould, J.; Ghasemi, B.; Petřkovský, L.; et al. The photostability of novel boron hydride blue emitters in solution and polystyrene matrix. *Materials* **2021**, *14*, 589. [\[CrossRef\]](#) [\[PubMed\]](#)
366. Čapkova, T.; Hanulíková, B.; Ševčík, J.; Urbanek, P.; Antos, J.; Urbanek, M.; Kuritka, I. Incorporation of the new $anti\text{-octadecaborane}$ laser dyes into thin polymer films: A temperature-dependent photoluminescence and infrared spectroscopy study. *Int. J. Mol. Sci.* **2022**, *23*, 8832. [\[CrossRef\]](#) [\[PubMed\]](#)
367. Anderson, K.P.; Rheingold, A.L.; Djurovich, P.I.; Soman, O.; Spokoyny, A.M. Synthesis and luminescence of monohalogenated $\text{B}_{18}\text{H}_{22}$ clusters. *Polyhedron* **2022**, *227*, 116099. [\[CrossRef\]](#)
368. Ehn, M.; Bovol, D.; Bould, J.; Strnad, V.; Litecká, M.; Lang, K.; Kirakci, K.; Clegg, W.; Waddell, P.G.; Londesborough, M.G.S. A window into the workings of $anti\text{-B}_{18}\text{H}_{22}$ luminescence—Blue-fluorescent isomeric pair $3,3'\text{-Cl}_2\text{-B}_{18}\text{H}_{20}$ and $3,4'\text{-Cl}_2\text{-B}_{18}\text{H}_{20}$ (and others). *Molecules* **2023**, *28*, 4505. [\[CrossRef\]](#)
369. Anderson, K.P.; Waddington, M.A.; Balaich, G.J.; Stauber, J.M.; Bernier, N.A.; Caram, J.R.; Djurovich, P.I.; Spokoyny, A.M. A molecular boron cluster-based chromophore with dual emission. *Dalton Trans.* **2020**, *49*, 16245–16251. [\[CrossRef\]](#) [\[PubMed\]](#)
370. Anderson, K.P.; Hua, A.S.; Plumley, J.B.; Ready, A.D.; Rheingold, A.L.; Peng, T.L.; Djurovich, I.; Kerestes, C.; Snyder, N.A.; Andrews, A.; et al. Benchmarking the dynamic luminescence properties and UV stability of $\text{B}_{18}\text{H}_{22}$ -based materials. *Dalton Trans.* **2022**, *51*, 9223–9228. [\[CrossRef\]](#)
371. Londesborough, M.G.S.; Dolansky, J.; Bould, J.; Braborec, J.; Kirakci, K.; Lang, K.; Cisařova, I.; Kubat, P.; Roca-Sanjuan, D.; Frances-Monerris, A.; et al. Effect of iodination on the photophysics of the laser borane $anti\text{-B}_{18}\text{H}_{22}$: Generation of efficient photosensitizers of oxygen. *Inorg. Chem.* **2019**, *58*, 10248–10259. [\[CrossRef\]](#)
372. Anderson, K.P.; Djurovich, P.I.; Rubio, V.P.; Liang, A.; Spokoyny, A.M. Metal-catalyzed and metal-free nucleophilic substitution of $7\text{-I-B}_{18}\text{H}_{21}$. *Inorg. Chem.* **2022**, *61*, 15051–15057. [\[CrossRef\]](#)
373. Bould, J.; Lang, K.; Kirakci, K.; Cerdan, L.; Roca-Sanjuan, D.; Frances-Monerris, A.; Clegg, W.; Waddell, P.G.; Fuciman, M.; Polivka, T.; et al. A series of ultra-efficient blue borane fluorophores. *Inorg. Chem.* **2020**, *59*, 17058–17070. [\[CrossRef\]](#)
374. Londesborough, M.G.S.; Lang, K.; Clegg, W.; Waddell, P.G.; Bould, J. Swollen polyhedral volume of the $anti\text{-B}_{18}\text{H}_{22}$ cluster via extensive methylation: $Anti\text{-B}_{18}\text{H}_8\text{Cl}_2\text{Me}_{12}$. *Inorg. Chem.* **2020**, *59*, 2651–2654. [\[CrossRef\]](#)
375. Sauri, V.; Oliva, J.M.; Hnyk, D.; Bould, J.; Braborec, J.; Merchan, M.; Kubat, P.; Cisařova, I.; Lang, K.; Londesborough, M.G.S. Tuning the Photophysical Properties of $anti\text{-B}_{18}\text{H}_{22}$: Efficient intersystem crossing between excited singlet and triplet states in new $4,4'\text{-(HS)}_2\text{-anti-B}_{18}\text{H}_{20}$. *Inorg. Chem.* **2013**, *52*, 9266–9274. [\[CrossRef\]](#)
376. Londesborough, M.G.S.; Dolansky, J.; Cerdan, L.; Lang, K.; Jelinek, T.; Oliva, J.M.; Hnyk, D.; Roca-Sanjuan, D.; Frances-Monerris, A.; Martinčík, J.; et al. Thermochromic fluorescence from $\text{B}_{18}\text{H}_{20}(\text{NC}_5\text{H}_5)_2$: An inorganic–organic composite luminescent compound with an unusual molecular geometry. *Adv. Opt. Mater.* **2017**, *5*, 1600694. [\[CrossRef\]](#)
377. Londesborough, M.G.S.; Dolansky, J.; Jelinek, T.; Kennedy, J.D.; Cisařova, I.; Kennedy, R.D.; Roca-Sanjuan, D.; Frances-Monerris, A.; Lang, K.; Clegg, W. Substitution of the laser borane $anti\text{-B}_{18}\text{H}_{22}$ with pyridine: A structural and photophysical study of some unusually structured macropolyhedral boron hydrides. *Dalton Trans.* **2018**, *47*, 1709–1725. [\[CrossRef\]](#) [\[PubMed\]](#)
378. Chen, J.; Xiong, L.; Zhang, L.; Huang, X.; Meng, H.; Tan, C. Synthesis, aggregation-induced emission of a new $anti\text{-B}_{18}\text{H}_{22}$ -isoquinoline hybrid. *Chem. Phys. Lett.* **2020**, *747*, 137328. [\[CrossRef\]](#)
379. Xiong, L.; Zheng, Y.; Wang, H.; Yan, J.; Huang, X.; Meng, H.; Tan, C. A novel AIEE active $anti\text{-B}_{18}\text{H}_{22}$ derivative-based Cu^{2+} and Fe^{3+} fluorescence off-on-off sensor. *Methods Appl. Fluoresc.* **2022**, *10*, 035004. [\[CrossRef\]](#)
380. Jelinek, T.; Kennedy, J.D.; Štibr, B.; Thornton-Pett, M. Macropolyhedral boron-containing cluster chemistry. A reductive trimerisation of MeNC to give an imidazole-based carbene stabilized by coordination to boron in an eighteen-vertex cluster compound. *J. Chem. Soc. Chem. Commun.* **1994**, 1999–2000. [\[CrossRef\]](#)
381. Jelinek, T.; Kilner, C.A.; Štibr, B.; Thornton-Pett, M.; Kennedy, J.D. Macropolyhedral borane reaction chemistry: Reductive oligomerisation of $^{\text{ter}}\text{BuNC}$ by $anti\text{-B}_{18}\text{H}_{22}$ to give the boron-coordinated $\{(^{\text{ter}}\text{BuNHCH})(^{\text{ter}}\text{BuNHC}(\text{CN}))\text{CH}_2\}$ carbene residue. *Inorg. Chem. Commun.* **2005**, *8*, 491–494. [\[CrossRef\]](#)

382. Patel, D.K.; Sooraj, B.S.; Kirakci, K.; Macháček, J.; Kučeráková, M.; Bould, J.; Dušek, M.; Frey, M.; Neumann, C.; Ghosh, S.; et al. Macropolyhedral *syn*-B₁₈H₂₂, the “forgotten” isomer. *J. Am. Chem. Soc.* **2023**, *145*, 17975–17986. [[CrossRef](#)] [[PubMed](#)]
383. Ehn, M.; Litecká, M.; Londesborough, M.G.S. Unexpected minor products from the thermal auto-fusion of *arachno*-SB₈H₁₂: Luminescent 4-(HS)-*syn*-B₁₈H₂₁ and 3-(HS)-*syn*-B₁₈H₂₁. *Inorg. Chem. Commun.* **2023**, *155*, 111021. [[CrossRef](#)]
384. Jelínek, T.; Grüner, B.; Císařová, I.; Štíbr, B.; Kennedy, J.D. Macropolyhedral boron-containing cluster chemistry: The reaction of *syn*-B₁₈H₂₂ with SMe₂ and I₂ in monoglyme: Structure of [7-(SMe₂)-*syn*-B₁₈H₂₀]. *Inorg. Chem. Commun.* **2007**, *10*, 125–128. [[CrossRef](#)]

Disclaimer/Publisher’s Note: The statements, opinions and data contained in all publications are solely those of the individual author(s) and contributor(s) and not of MDPI and/or the editor(s). MDPI and/or the editor(s) disclaim responsibility for any injury to people or property resulting from any ideas, methods, instructions or products referred to in the content.